# Evaluation of Hydrodynamic Characteristics of an Integrated Multi-Environment Wastewater Treatment System

Farnaz Behzadian

A thesis in

Department of Building, Civil and Environmental Engineering

Presented in Partial Fulfillment of the Requirements

For the Degree of Master of Applied Science at Concordia University

Montreal, Quebec, Canada

March 2010

*Your file Votre référence*
*ISBN:* 978-0-494-67102-3
*Our file Notre référence*
*ISBN:* 978-0-494-67102-3

# ABSTRACT


## Evaluation of Hydrodynamic Characteristics of an Integrated Multi-Environment Wastewater Treatment System

Farnaz Behzadian

A new integrated multi-environment wastewater treatment technology has been developed for high-rate removal of organic carbonaceous compounds and inorganic contaminants, notably nitrogen and phosphorus, as well as suspended solids. This technology uses two separate but interlinked reactors containing four zones with different environmental conditions of aerobic, microaerophilic, anoxic and anaerobic for biological treatment as well as two clarification zones and a filtration unit for efficient separation of solids from liquid. The first reactor of the treatment system is designed based on the concept of airlift reactors. The influence of operating and process parameters such as the hydraulic retention time (HRT) and superficial gas velocity ($U_G$) on the hydrodynamic characteristics of the first reactor was examined. The liquid circulation velocity, gas hold-up and overall volumetric oxygen transfer coefficient increase with the increase of superficial gas velocity, while the mean circulation time decreases with the increase of air flow rate. The theoretical analysis of time dependent changes in the volume of mixed liquor demonstrated that liquid circulates from 363 to 1686 times between the three zones of aerobic, microaerophilic and anoxic before 99% of the bioreactor's content is replaced by the added wastewater. At air flow rates higher than 30 L/min, the mixing performance of the first reactor resembles the patterns observed in continuous stirred tank reactors (CSTRs). Using the openings with the size of

½" between the riser and downcomer at air flow rates of 15-30 L/min provide higher mass transfer coefficient and better zone generation, suggesting an improved treatment performance of the system.

*Dedicated to*

*My dearest mother and brother for their love, support, encouragement and inspiration they have given me in all steps of my life.*

# ACKNOWLEDGMENTS

I would like to take the opportunity to thank Dr. Laleh Yerushalmi, and Prof. Catherine Mulligan for their extreme help and support during this project. Without their help finishing this work would be impossible.

I would like to thank Dr. Mahmood Alimahmoodi for his great assistance, guidance and cooperation in this research.

Also, I would like to acknowledge the financial support provided by Concordia University and Programme de soutien à l'innovation en agroalimentaire of the Ministère de l'Agriculture, des Pêcheries et de l'Alimentation du Québec for this research.

# TABLE OF CONTENTS

## Contents

# LIST OF TABLES

# LIST OF FIGURES

# LIST OF SYMBOLS AND ABBREVIATIONS

| | | | |
|---|---|---|---|
| $A_b$ | Free area of the liquid flow ($m^2$) | $h_{dis}$ | Height of dispersion (m) |
| $A_d$ | Cross sectional area of downcomer ($m^2$) | k | Specific rate of liquid discharge (1/h) |
| $A_r$ | Cross sectional area of riser ($m^2$) | $K_B$ | Friction loss coefficient at the bottom of reactor(dimensionless) |
| $a_L$ | Gas-liquid interfacial area per unit liquid volume ($m^2/m^3$) | $k_L$ | True mass transfer coefficient (m/s) |
| BNR | Biological Nutrient Removal | $k_La_L$ | Overall volumetric mass transfer coefficient(1/s) |
| C* | Saturation concentration of oxygen in the liquid (mmol/L) | $L_d$ | Distance between two electrodes in downcomer (m) |
| $C_L$ | Concentration of oxygen in the liquid at a given time (mmol/L) | $\dot{m}_a$ | Mass flow rate of air (kg/s) |
| CSTR | Continuous Stirred Tank Reactors | $\dot{m}_w$ | Mass flow rate of water(kg/s) |
| DO | Dissolved Oxygen | N.O. C | Number of liquid circulations |
| $d_B$ | Sauter mean bubble diameter (m) | ORP | Oxidation-Reduction Potential |
| FBR | Fluidized Bed Reactors | PFR | Plug Flow Reactors |
| g | Gravitational acceleration ($m/s^2$) | $Q_a$ | Circulating liquid flow rate in the aerobic zone (L/min) |
| HRT | Hydraulic Retention Time (h) | $Q_{air}$ | Air Flow rate from diffusers (L/min) |
| $HRT_a$ | Instantaneous hydraulic retention time in aerobic zone (s) | $Q_b$ | Flow rate of liquid that exits through the anoxic zone (L/min) |
| $HRT_m$ | Inst. hydraulic retention time in microaerophilic zone (s) | $Q_{cir}$ | Volumetric liquid circulation flow rate (L/min) |
| $HRT_x$ | Instantaneous hydraulic retention time in anoxic zone (s) | $Q_e$ | Flow rate of liquid that exits through the clarifier (L/min) |
| $h_L$ | Unaerated height of liquid in the reactor (m) | $Q_G$ | Gas flow rate (L/min) |
| $h_D$ | Aerated height of liquid in the reactor (m) | $Q_i$ | Flow rate of raw wastewater (L/d) |

| | | | |
|---|---|---|---|
| $Q_m$ | Circulating liquid flow rate in the microaerophilic zone (L/min) | $V_R$ | Overall volume of reactor (L) |
| $Q_r$ | Flow rate of the recycled liquid between two reactors (L/min) | $V_r$ | Volume of riser (L) |
| $Q_x$ | Circulating liquid flow rate in the anoxic zone (L/min) | $V_x$ | Volume of anoxic zone (L) |
| RTD | Residence Time Distribution | VFA | Volatile Fatty Acids |
| SRT | Solid Retention Time | $x_C$ | Circulation path (m) |
| $t_C$ | Mean circulation time (s) | $Y_i$ | Initial volume of mixed liquor inside the reactor (L) |
| $t_d$ | Mean residence time of liquid in downcomer (s) | $Y_r$ | Volume of mixed liquor inside the reactor at time t (L) |
| $t_m$ | Mean residence time (h) | $Y_w$ | Volume of waste water inside the reactor at time t (L) |
| $U_G$ | Superficial gas velocity (m/s) | $\alpha$ | Coefficient of correlation |
| $U_L$ | Superficial liquid velocity (m/s) | $\beta$ | Exponent of correlation |
| $U_{LC}$ | Mean liquid circulation velocity (m/s) | $\omega$ | Coefficient of correlation |
| $U_{Ld}$ | Superficial liquid velocity in downcomer (m/s) | $\nu$ | Exponent of correlation |
| $U_{Lr}$ | Superficial liquid velocity in riser (m/s) | $\varepsilon$ | Overall gas hold up (dimensionless) |
| $V_a$ | Volume of aerobic zone (L) | $\varepsilon_r$ | Gas hold up in riser (dimensionless) |
| $V_d$ | Volume of downcomer (L) | $\varepsilon_d$ | Gas hold up in downcomer (dimensionless) |
| $V_G$ | Volume of gas (L) | $\sigma^2_t$ | Variance ($h^2$) |
| $V_{Li}$ | Volume of liquid (L) | $\sigma^2$ | Dimensionless variance |
| $V_{Ld}$ | Linear liquid velocity in downcomer (m/s) | $\rho_a$ | Density of air ($kg/m^3$) |
| $V_{Lr}$ | Linear liquid velocity in riser (m/s) | $\rho_w$ | Density of water ($kg/m^3$) |
| $V_m$ | Volume of microaerophilic zone (L) | | |

# CHAPTER 1: INTRODUCTION AND OBJECTIVES

## 1.1 Introduction

The treatment of wastewater requires the removal of organic and inorganic contaminants, usually present in solid or dissolved form, before its discharge into the receiving waters. The organic contaminants include proteins, lipids and polysaccharides while the inorganic contaminants include nutrients, particularly nitrogen and phosphorus. Conventional treatment technologies commonly use biological processes for the treatment of municipal or industrial wastewaters around the world. These

processes use indigenous microorganisms such as bacteria to consume the contaminants as their food and energy source and produce an effluent that conforms to environmental standards and can be discharged to the receiving waters. As a result of microbial growth and propagation during the treatment process, wastewater treatment plants produce large amounts of solids or sludge, which mostly consist of dead or settled bacteria/microorganisms and must be treated and disposed of by various processes. The reduction of sludge during wastewater treatment operations has become a serious environmental concern. These concerns are particularly urgent when treating high organic load wastewaters such as those originating from animal farms and agricultural activities that result in the generation of substantial amounts of biological solids when using traditional treatment technologies (Ahn et al., 2002, Liu 2003, Wei et al., 2003). The wastewaters of agricultural activities or animal farms also carry a very high concentration of inorganic material, i.e. nitrogen and phosphorus that must be removed during the treatment process as required by stringent environmental standards. The discharge limits for nitrogen and phosphorus are becoming increasingly severe throughout Canada and the industrialized world due to the health hazards of these nutrients, their contribution to algal blooms and the depletion of oxygen in lakes and rivers which threatens aquatic life (de-Bashan and Bashan, 2004). The removal of nutrients, especially from the high organic load and nutrient-rich wastewaters of agricultural activities cannot be adequately accomplished by existing technologies and thus it has become a serious challenge to the wastewater treatment market.

Most existing technologies for wastewater treatment in the Canadian and international markets were originally designed for secondary treatment, i.e. removal of organic carbonaceous compounds and solid-liquid separation, and not the removal of nutrients. These treatment systems generally include suspended-growth systems such as activated sludge and sequencing batch reactor (SBR), or attached-growth systems such as trickling filter, rotating biological contactors (RBC), and fluidized-bed reactors (FBR), or a combination of these processes. Suspended-growth systems offer good mixing and high mass transfer rates. However, they often produce a large amount of biological sludge, and show difficulties in maintaining an adequate solid retention time (SRT) or retaining different groups of microbial cells, especially the slow growing nitrifiers that are needed for nitrification and nitrogen removal process. Fixed-film or attached-growth systems provide better solid-liquid separation, a more stable operation, and produce lower amounts of sludge. However, these systems suffer from mass-transfer limitations inherent in fixed-film processes, and occasional clogging, especially during the treatment of high organic-load wastewaters. Well-known international companies such as Paques and Biothane use technologies that are based on a combination of fixed-film and suspended growth processes and operate under aerobic and anaerobic conditions. They include BIOPAQ® IC, UASB, high-rate activated sludge and sequencing batch reactors, and CIRCOX® (Frijters et al. 1997, Zhang et al. 2007). These technologies mostly remove organic biodegradable contaminants and do not provide nutrient removal, while CIRCOX® only removes nitrogen, not phosphorus, does not stabilize sludge and has a limited capacity for solid-liquid separation.

In order to provide a complete treatment of wastewater, including the removal of nutrients in addition to the carbonaceous compounds and suspended solids, treatment systems require the presence of multiplicity of vessels or zones in order to create aerobic, anoxic and anaerobic conditions that are needed for the biological nitrogen and phosphorus removal processes.

Conventional wastewater treatment technologies commonly use additional aerated, anoxic or anaerobic units in series, along with various internal recycle streams to achieve the required removal of nutrients and to meet stringent discharge criteria. These systems are known as the anoxic/oxic (A/O) or anaerobic/anoxic/oxic (A2/O) treatment systems. They provide adequate treatment; however, they have a complicated design that contains a multiplicity of anaerobic/anoxic/aerobic reactors, unit operations and recycle streams. They also have a very large footprint and elaborate control strategies (Im et al. 2001, Choi et al 2005). Particularly, they usually produce a large amount of biological solids (sludge).

The technology proposed in this project addresses the limitations and weaknesses of existing technologies. It has a unique design for the removal of organic contaminants as well as inorganic nutrients and should reduce the generation of biological sludge by preventing its excessive production during the treatment process, directly addressing environmental concerns during wastewater treatment operations. The technology uses two interlinked vessels (reactors) containing four biological zones with different environmental conditions of aerobic, microaerophilic, anoxic and anaerobic. The

presence of these environmental conditions which are defined based on their respective concentrations of dissolved oxygen (DO) and oxidation-reduction potential (ORP), support the growth and proliferation of a diversified group of suspended as well as fixed-film microorganisms and ensure the removal of organic contaminating compounds as well as the polluting inorganic nutrients. The schematic diagram of the treatment system is presented in Figure 1.

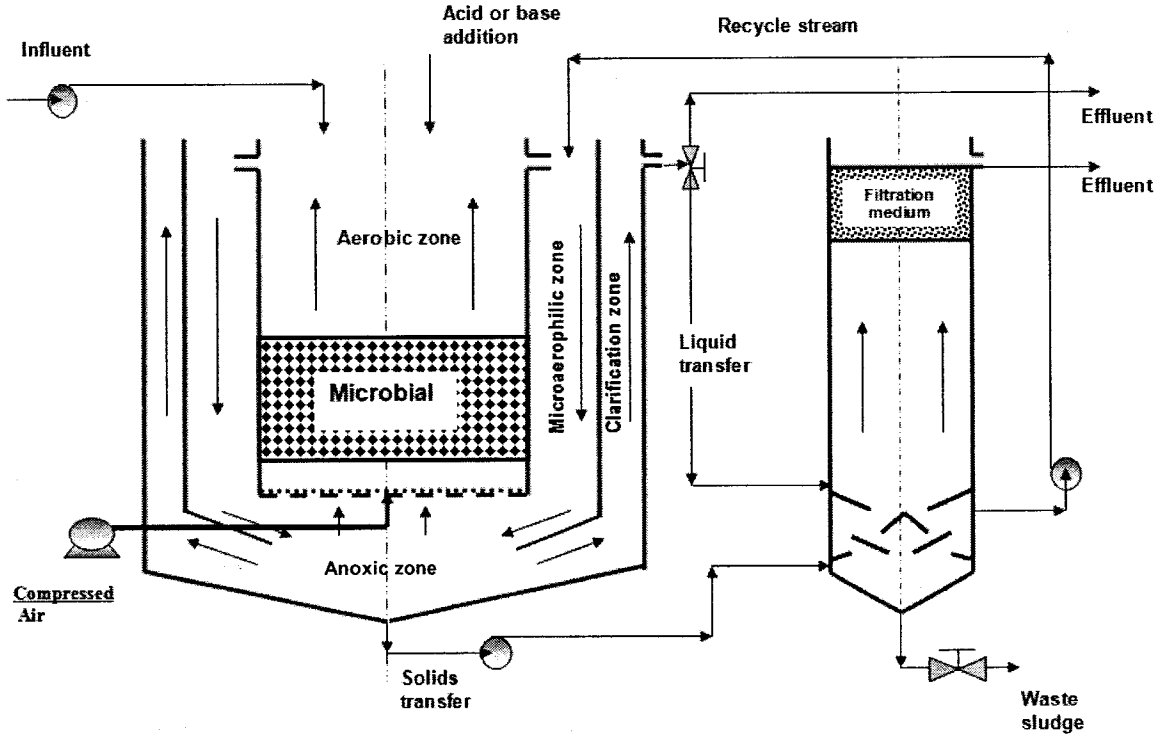


Figure 1: Schematic diagram of the new multi-environment wastewater treatment system

## 1.2 Objectives of this study

### 1.2.1 Main Objective:

The main objective of this project was the hydrodynamic characterization of a new multi-environment treatment technology for the treatment of wastewater and contaminated groundwater. The fabricated reactors that constitute the treatment system were installed in the Environmental Engineering Laboratories of Concordia University. The examined hydrodynamic parameters include gas hold up (ε), mean liquid circulation time, liquid circulation velocity, linear and superficial liquid velocities in riser and downcomer, overall volumetric oxygen transfer coefficient ($k_La_L$), residence time distribution (RTD), and liquid displacement.

### 1.2.2 Detailed Objectives:

The detailed objectives of this project are as follows:

1- Development of a monitoring and control system for the continuous acquisition and storage of process parameters including dissolved oxygen (DO) concentration, oxidation-reduction potential (ORP), pH, air flow rate, and liquid flow rate.

2- Determination of hydrodynamic properties of the first reactor of the treatment system including gas hold up (ε), mean circulation time, mean liquid circulation velocity, linear and superficial liquid velocities in riser and downcomer, oxygen transfer coefficient ($k_La_L$), residence time distribution (RTD), and liquid displacement as a

function of the operating conditions such as hydraulic retention time (HRT) and superficial gas velocity ($U_G$).

3- Determination of the impact of hydrodynamic parameters, identified above, on the liquid flow pattern and the generation of various zones, as well as residence time distribution (RTD) and mean residence time ($t_m$) in the first reactor of the treatment system.

4- Development of a mathematical model to describe time-dependent changes in the mixed liquor volume inside the first reactor and the dependence of number of liquid circulations between the zones on the influent flow rate as well as the instantaneous hydraulic retention time in the aerobic zone.

5- Establishment of the optimum operating conditions of the reactor for the generation of zones with different environmental conditions inside the first reactor of the treatment system.

6- Evaluation of the impact of microbial support on selected hydrodynamic parameters.

This research project has been presented in the following chapters:

- Chapter 1; outlines a brief introduction on conventional wastewater treatment technologies and the advantages of the studied technology.
- Chapter 2; describes the details of the developed technology as well as the definition of most important operating and hydrodynamic characteristics of the treatment system.

- Chapter 3; presents mathematical analysis for the estimation of selected hydrodynamic parameters.
- Chapter 4; presents the experimental set up and the applied methodology for the measurement and evaluation of different hydrodynamic parameters as a function of operating and process parameters.
- Chapter 5; presents the experimental results of this research as well as comparison with analytical estimations based on the developed mathematical models and literature-cited experimental results.
- Chapter 6; presents the conclusive remarks based on the obtained experimental results and recommendations for optimized performance and operating conditions of the new wastewater treatment system.

# CHAPTER 2: LITERATURE REVIEW

## 2.1 Background

The treatment of wastewater and contaminated groundwater requires the removal of organic and inorganic contaminants, usually present in solid and/or dissolved form, before their discharge into the receiving waters. The organic contaminants include sources of COD/BOD such as proteins, lipids and polysaccharides as well as hazardous compounds such as aromatic and aliphatic hydrocarbons. The nitrogenous and phosphorus compounds, which are among the most undesirable inorganic contaminants

of wastewater and contaminated groundwater, also need to be removed during the treatment process.

During biological treatment processes, organic substances are removed since these substances serve as the source of carbon in the microbial metabolism. Nitrogen and phosphorus are also consumed by microorganisms as essential nutrients to support microbial growth during assimilatory processes, while excess amounts of nitrogenous compounds is removed during dissimilatory microbial nitrogen metabolism where they are transformed to molecular nitrogen and released into the atmosphere. The remaining phosphorus may be removed by the "luxury phosphorus uptake" process where special groups of microorganisms accumulate phosphorus and store it as poly-phosphorus compounds, thus removing it from the system during sludge disposal. Removal of nitrogen and phosphorous is enforced by environment agencies because of contribution of these inorganic compounds to the eutrophication phenomenon.

Most previous biological treatment technologies, using either suspended-growth or attached-growth processes, were mainly concerned about the removal of carbonaceous compounds and separation of sludge from liquid, but they were not very efficient in the removal of nutrients mainly nitrogenous and phosphorus compounds from wastewaters. This is due to the fact that the removal of these inorganic compounds requires special environments with different levels of dissolved oxygen concentration and oxidation-reduction potential.

In order to meet stringent discharge criteria including nitrogen and phosphorus removal, wastewater treatment plants usually upgrade their performance by using add-on technologies such as biological nutrient removal (BNR) systems. The theories of biological nitrogen and phosphorus removal mechanisms demonstrate that nitrogen removal needs the presence of aerobic and anoxic environments, while the removal of phosphorus demands the presence of anaerobic and aerobic environments in the treatment system.

Conventional wastewater treatment technologies, originally developed for the removal of carbonaceous compounds (BOD) and suspended solids, accommodate nutrient removal by providing additional aerated, anoxic or anaerobic units in series, along with various internal recycle streams to achieve the required removal of nitrogen and/or phosphorus. These modifications have increased the complexity of the treatment systems and complicated their proper design and optimization.

Nitrification, the first step in the biological nitrogen removal mechanism that involves the conversion of ammonia nitrogen to nitrate nitrogen, requires an aerobic environment and is achieved in all aerobic reactors if the right operating conditions such as the liquid pH, carbonate concentration, and sludge retention time exist. Denitrification, i.e. the transformation of nitrate nitrogen to molecular nitrogen, can be accomplished by the addition of an anoxic activated sludge reactor or fixed-film system. In these combined processes, the wastewater or contaminated groundwater is commonly fed into the anoxic denitrification reactor. The effluent from the anoxic

reactor is then fed into the aerobic reactor. A sufficient retention time in the aerobic reactor is needed to ensure a complete oxidation of carbonaceous compounds as well as adequate growth and proliferation of slow-growing nitrifiers to carry out the nitrification process and convert ammonia-nitrogen to nitrate-nitrogen. In order to achieve phosphorus removal as well as nitrogen removal, the incorporation of an additional anaerobic zone in the treatment system is necessary. Several systems have been developed along with these design elements. One of the most successful systems is the five-stage Bardenpho process (WEF 2006) that is quite renowned and has widespread applications (Figure 2).

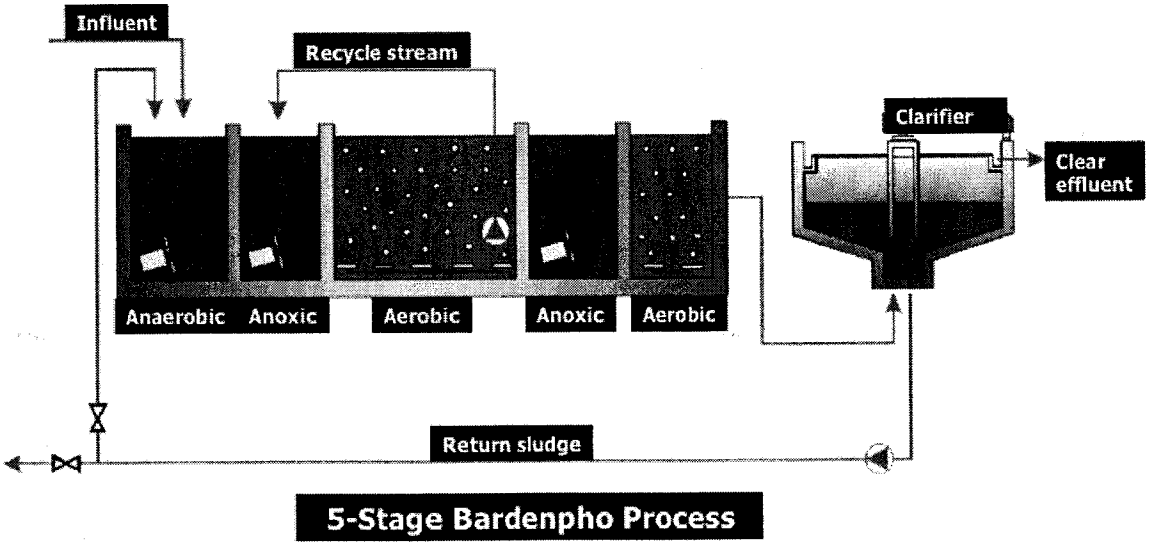


Figure 2. Schematic diagram of the 5-stage Bardenpho process (WEF 2006)

In the Bardenpho system, there are one anaerobic, two aerobic and two anoxic zones. In this process, the untreated wastewater is first added to the anaerobic zone where soluble phosphorus is released and VFAs are uptaken by the phosphorus accumulating microorganisms (PAOs). The effluent of the anaerobic tank is fed into the anoxic zone for the reduction of nitrate and its conversion to nitrogen. The effluent of the anoxic zone flows to the aerobic zone for BOD removal and nitrification. The separation of solids and liquid takes place in a clarifier. Two recycle streams are present in this process: one from the clarifier to the anaerobic zone to return a portion of the separated sludge, and the second one from the aerobic to the anoxic zone carrying nitrate for the denitrification process. In this configuration, a more complete removal of nitrogen is achieved due to the existence of two aerobic and two anoxic zones. Moreover, the anaerobic zone will not receive nitrate in the recycle stream, thus a better phosphorus removal process can also take place. The five-stage Bardenpho process has a high nutrient removal capacity and can remove high concentrations of nitrogen and phosphorus from wastewater and contaminated groundwater. However, this technology uses six vessels to perform the treatment. The process uses a large footprint, produces a great amount of sludge and requires high maintenance because of the number of pumps, air compressors and other equipment needed.

Several wastewater and groundwater treatment technologies for the removal of organic carbon and nutrients are described in the patent literature. Most prior art technologies suffer from complicated designs, high maintenance requirements or large footprints as

well as a limited capacity to address the treatment of groundwater or landfill leachate contaminated with a mixture of contaminating compounds of organic and inorganic nature. Examples of such contamination include mixtures of hydrocarbons (e.g. diesel fuel, jet fuel or gasoline) with nitrate and phosphorus, commonly resulting from the combined agricultural and airport or military activities. These kinds of contaminations require the simultaneous presence of diversified groups of microorganisms as well as different environmental conditions including different levels of dissolved oxygen concentration and redox potential for their complete treatment. Provisions have to be made for adequate biomass growth and maintenance of all different microbial groups, effective solid-liquid separation, sludge stabilization, and proper optimization and control of environmental conditions in the multiple zones of the treatment system.

Despite the foregoing advancements in the prior art, there nonetheless exists a broad and long felt need for a process that more effectively treats wastewater and removes undesirable nitrogen and phosphorous nutrients from wastewater. There is also the need for performing such an effective process in a system that is more compact, self-contained, easy to maintain, easy to operate, widely applicable, less cumbersome mechanically, and more cost-effective than traditional processes and systems. The present technology has been designed to address those long felt needs and provide solutions to various problems recognized by the prior art.

Among the various designs used in aerobic treatment systems, airlift reactors have attracted the attention of several researchers due to their unique hydrodynamic

characteristics and their capacity for combining different biological environments as well as separation and clarification units in a single vessel. Several design configurations of airlift reactors have been suggested to improve the reactor performance during nitrification/denitrification (Bakker et al. 1996; van Benthum 1999a, 1999b) and simultaneous COD, nitrogen and phosphorous removal (Kreuk et al., 2005). The technology examined in this dissertation is a new multi-environment treatment system that uses two interlinked reactors. The first reactor operates according to the principles of airlift reactors. However, it contains certain design modifications implemented to improve treatment performance of the system while making it different from conventional airlift reactors. The detailed design of the technology is explained extensively in the next section.

## 2.2 Description of the technology:

The examined treatment system uses two separate but interlinked reactors for the biological treatment and solid-liquid separation processes. The first reactor contains an aerobic zone, a microaerophilic zone and an anoxic zone plus a clarification zone. The second reactor contains an anaerobic zone, a solid-liquid separation zone and a filtration unit. Figure 3 illustrates the set up of the multi-environment treatment technology installed in the Environmental Engineering Laboratories of Concordia University.

The aerobic zone located in the center of the first reactor operates according to the principles of airlift reactors. It contains air diffusers at the bottom of the zone for the introduction of air into this zone.

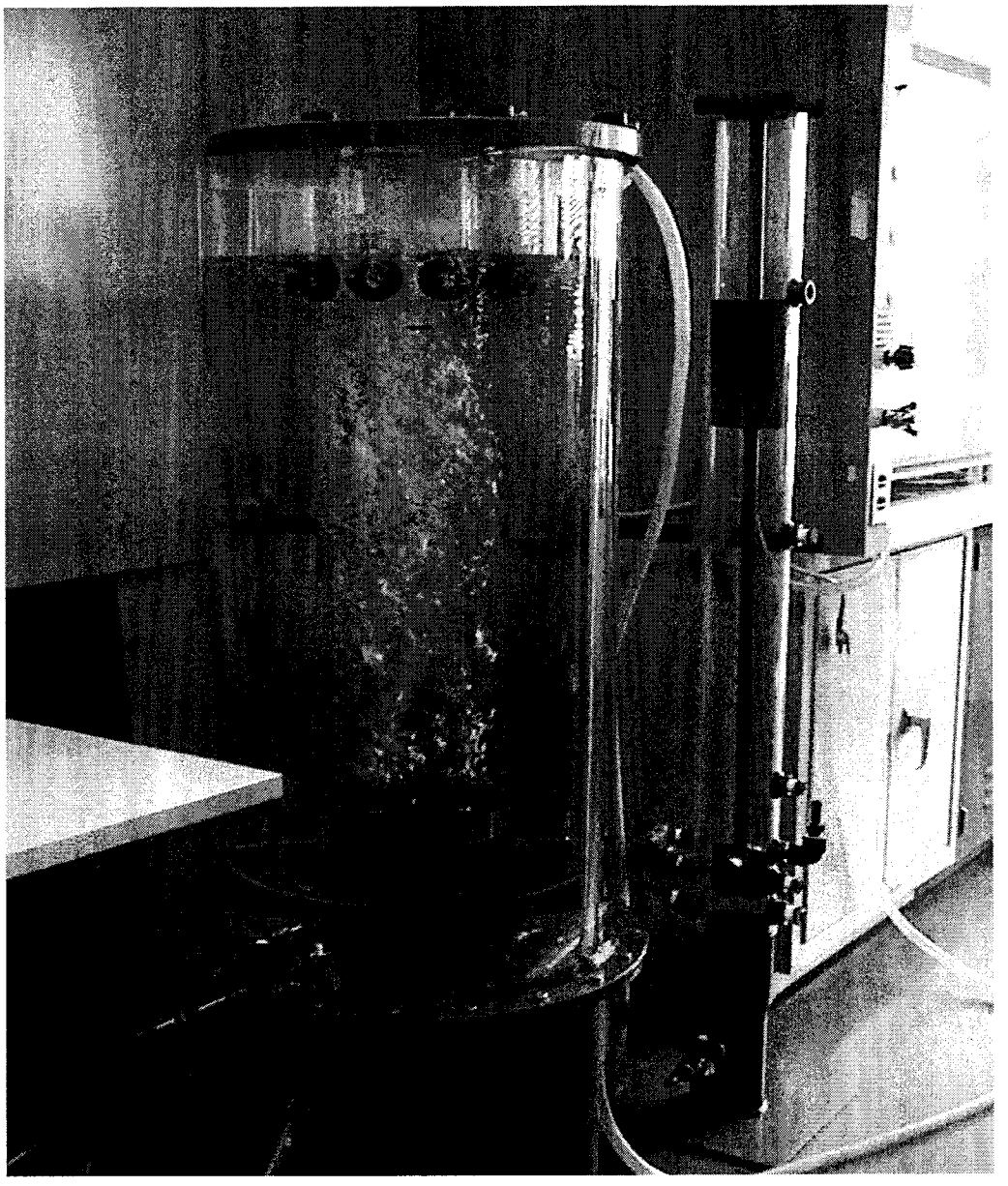

Figure 3. Laboratory set up of the new multi-environment wastewater treatment system

The air bubbles mix the liquid and its content of microorganisms, and provide oxygen for the aerobic biological processes that take place in this zone. Aeration also produces circulation of liquid between the aerobic zone and its adjacent microaerophilic and anoxic zones that are located at the sides and under the aerobic zone, respectively. This tends to reduce, compared to the prior art, the number of pumps and recycles streams in the treatment system of the present technology. During the treatment operations, the aerobic zone contains suspended microorganisms of heterotrophic and autotrophic groups that grow inside the circulating liquid, known as mixed liquor. There is also a microbial support installed in the middle of aerobic zone, above the diffusers in order to support the attachment of microbial biomass and the formation of microbial biofilm, as shown in Figure 4. Thus, the aerobic zone contains both suspended-growth and attached-growth microbial biomass. Most of the organic carbonaceous contaminants are removed in this zone. The nitrification process, a part of the biological nitrogen removal process, also takes place in the aerobic zone. The microaerophilic and anoxic zones are employed for the denitrification processes to transform the nitrogenous compounds into nitrogen gas and to completely remove nitrogen. The anaerobic zone in the second reactor along with the aerobic, microaerophilic and anoxic zones of the first reactor are employed for the removal of phosphorus compounds.

The influent wastewater is introduced into the treatment system from the top of the aerobic zone. The compressed air is introduced in the treatment system through air diffusers located at the bottom of the aerobic zone.

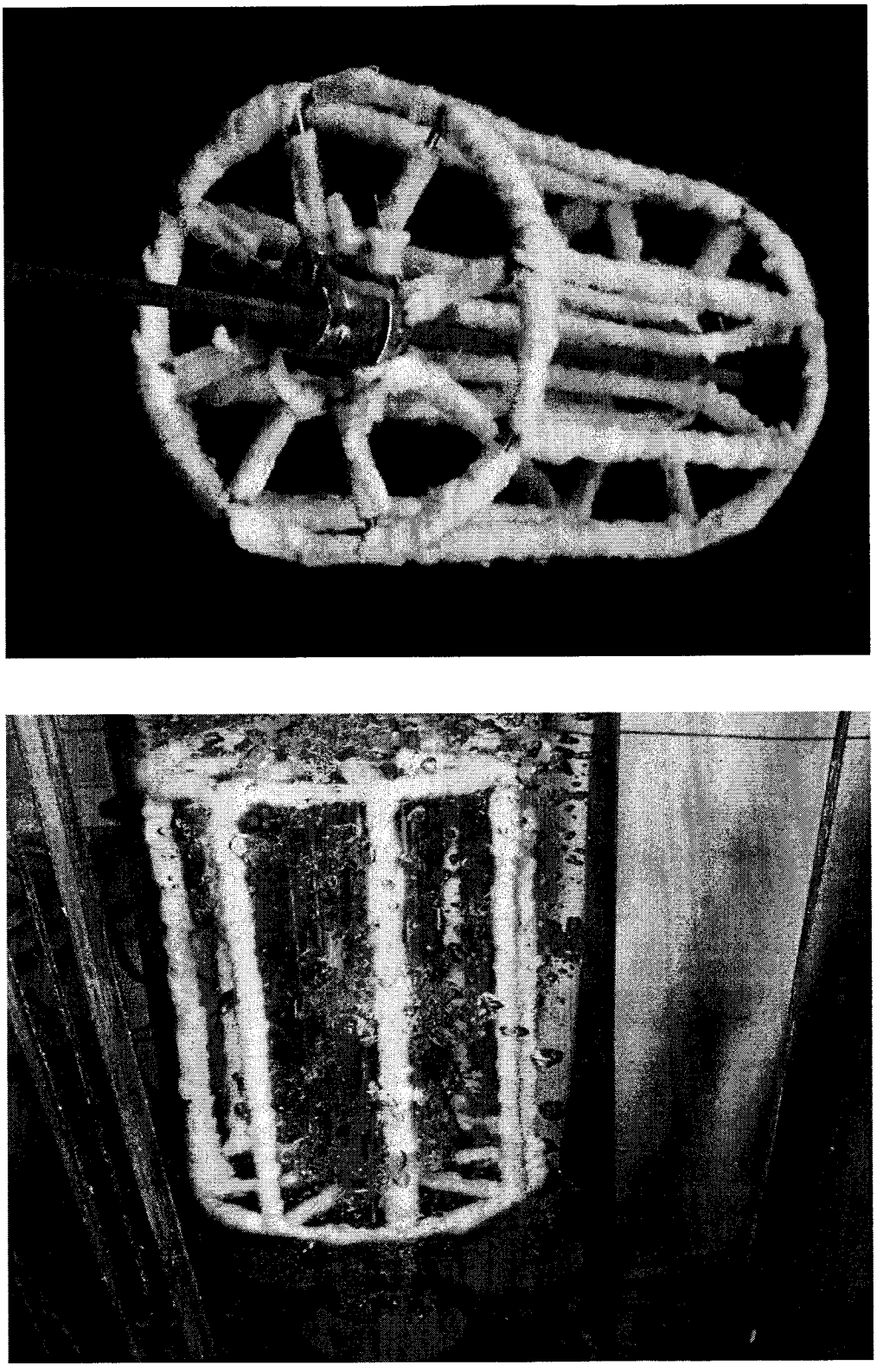

Figure 4. Microbial support inside the aerobic zone of the first reactor of the treatment system

The upward flow of liquid in the aerobic zone carries the suspended solids and flows towards the adjacent microaerophilic zone through eight openings located at the top of the cylindrical partition wall separating the aerobic zone from the microaerophilic zone (Figure 5).

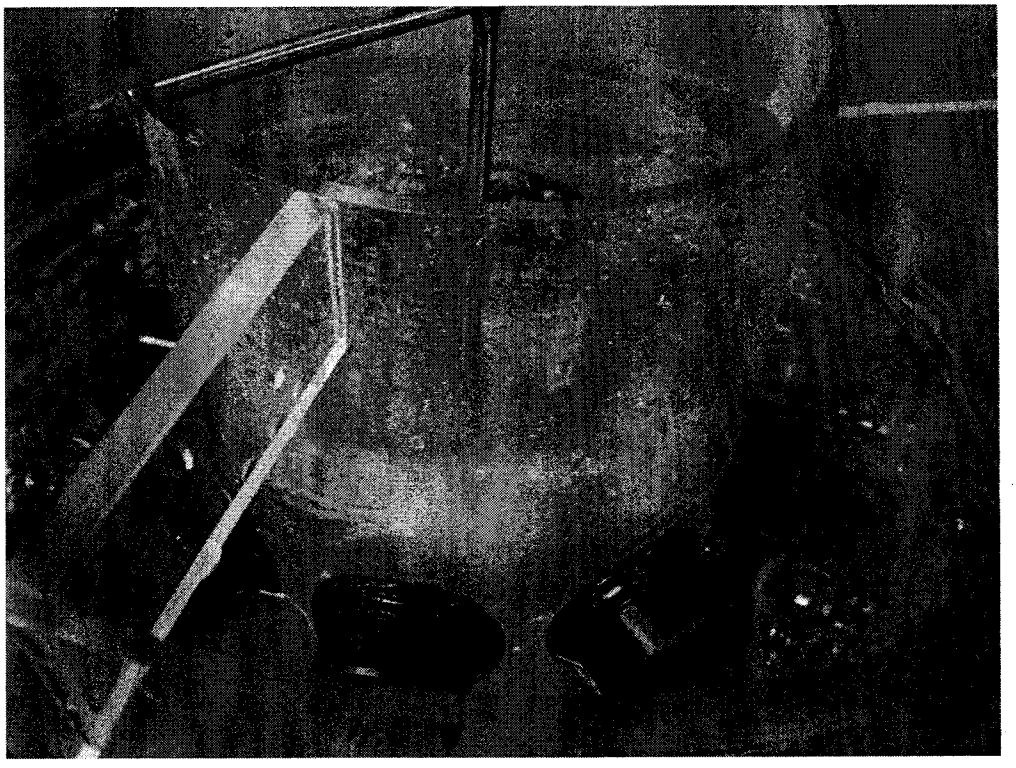

Figure 5. Eight Openings for the passage of flow from the aerobic zone to microaerophili zone

The mixture of liquid and suspended solids including dispersed microorganisms, bioflocs or other solid organic, inorganic or inert material, known as the mixed liquor, flows downward in the microaerophilic zone and passes through the anoxic zone that is located at the bottom of the first reactor and under the aerobic zone. The clarification

zone is disposed concentrically relative to the microaerophilic zone and separated therefrom by a cylindrical wall leaving channels for the passage of liquid at the bottom of the wall.

The compressed air entering from the bottom of aerobic zone creates a pressure difference across the air diffusers and directs the flow of mixed liquor towards the aerobic zone, thus creating a continuously circulating liquid between the aerobic, microaerophilic and anoxic zones. The flow pattern of mixed liquor in the anoxic zone is further controlled by the design of half cone that is attached to the dividing wall between the microaerophilic zone and clarification zone. This arrangement directs the mixed liquor towards the centrally-located aerobic zone while reducing fluid turbulence at the entrance of the clarification. The resulting circulation exposes the contaminating compounds in the mixed liquor to three different environments, i.e. aerobic, microaerophilic and anoxic during each cycle, ensuring a high biodegradation rate of organic material as well as nitrification and denitrification and phosphorus removal by a diverse group of microorganisms.

The solids are separated from the liquid in two clarification zones. The first zone is adjacent to the microaerophilic zone while the second zone is physically separated from the first clarification zone and acts as a back-up clarifier in the event of biological upset or whenever the quality of effluent emerging from the first tank does not conform to the treatment criteria. While the mixed liquor continuously circulates between the three zones of the treatment system in the first reactor, a fraction of liquid freely flows

towards the clarification zone that is adjacent to the microaerophilic zone and leaves the system in accordance with the laws of continuity since there is no liquid accumulation in the system. As the liquid flows upward in the first clarification zone, the solid material flows downward and precipitates to the bottom of the anoxic zone. The effluent emerging from the first clarification zone may be assessed by turbidity probes that are placed in the effluent line to determine its turbidity. In the event of a poor quality of effluent, it can be directed towards the second clarification (solid-liquid separation) unit (zone) that is housed in the second reactor. Here, the remaining solid material will precipitate to the anaerobic zone while liquid flows towards the exit port of the system. The liquid passes through a filtration unit located at the top of the second reactor to retain the fine suspended solids and the remaining colloidal material, ensuring the emergence of a relatively clear effluent from the treatment system. The filtration unit contains packing material such as activated carbon, peat moss or sand.

## 2.3 Hydrodynamic studies

The significant hydrodynamic parameters of the treatment system and the methods of their measurement will be described in the next chapters. The hydrodynamic studies include the evaluation of hydrodynamic characteristics of the treatment system in response to the variations of operating conditions and process parameters. In this study, the impact of gas flow rate and instantaneous HRT, controlled by the size and number of the openings between the aerobic and microaerophilic zones, on gas hold up ($\varepsilon$), mean

circulation time ($t_C$), mean liquid circulation velocity ($U_{LC}$), linear and superficial liquid velocities in different zones, overall volumetric oxygen transfer coefficient ($k_La_L$), and liquid displacement inside the reactor was investigated. The mixing properties and residence time distribution of the treatment system in response to different air flow rates, as well as the relationship between selected hydrodynamic parameters were also evaluated.

### 2.3.1 Hydraulic retention time

The Hydraulic Retention Time (HRT) is a measure of the average length of time that a soluble compound remains in a reactor. The hydraulic retention time or liquid phase mean residence time is commonly calculated from the following equation:

$$HRT = \frac{V_{Li}}{Q_i} \qquad (2.1)$$

### 2.3.2 Superficial gas velocity

Superficial gas velocity is the average velocity of gas sparged into the riser column and it is calculated by dividing the gas flow rate ($Q_G$) by the riser cross sectional area ($A_r$):

$$U_G = \frac{Q_G}{A_r} \qquad (2.2)$$

The impact of this important operating parameter on the individual hydrodynamic parameters of the treatment system has been evaluated and will be presented in the following chapters.

### 2.3.3 Gas hold up (ε)

The volume fraction of gas-phase in gas-liquid dispersion is known as the gas hold-up or the gas void fraction. The overall gas holdup is defined as:

$$\varepsilon = \frac{V_G}{V_G + V_{Li}} \qquad (2.3)$$

Where $V_G$ and $V_{Li}$ are the gas and liquid volumes in the reactor, respectively (Chisti 1989).

Gas holdup in an airlift reactor is an important parameter because of its impact on liquid circulation velocity, liquid mixing, gas residence time and gas-liquid interfacial area which affects mass transfer coefficient.

In airlift reactors, the individual riser and downcomer gas hold ups, $\varepsilon_r$ and $\varepsilon_d$, respectively, are related to the overall gas hold up (Chisti 1989):

$$\varepsilon = \frac{\varepsilon_r A_r + \varepsilon_d A_d}{A_r + A_d} \qquad (2.4)$$

### 2.3.4 Mean circulation time ($t_C$) and mean liquid circulation velocity ($U_{Lc}$):

The driving force for the circulation of liquid in airlift reactors is the difference in the bulk densities of liquid in the riser and downcomer (de Nevers 1968, Freedman and

Davidson 1969, Chisti 1989) that is caused by differences in gas hold-up in the riser and downcomer. The fluid continuously flows upwards in the riser and downwards in the downcomer. The average time required for one complete circulation between the riser and downcomer is called mean circulation time. By dividing the circulation path ($x_C$) to mean circulation time ($t_C$), mean liquid circulation velocity ($U_{Lc}$) can be obtained (Blenke 1979, Chisti 1989) :

$$U_{LC} = \frac{x_C}{t_C} \qquad (2.5)$$

### 2.3.5 Linear and superficial liquid velocities in riser and downcomer

Besides the overall average liquid circulation velocity ($U_{Lc}$), two other parameters known as superficial and linear liquid velocities in riser and downcomer can be defined. Continuity rule (Coulson and Robinson 1977, Chisti 1989) is used to express the relationship between superficial liquid velocities in the riser and downcomer:

$$U_{Lr} A_r = U_{Ld} A_d \qquad (2.6)$$

Superficial liquid velocity is defined based on the gas and liquid phases in either riser or downcomer. Since liquid fills only a part of the riser and downcomer and the rest is occupied by the gas, the true linear liquid velocity ($V_L$), also known as the interstitial velocity (Chisti 1989), is higher than the superficial liquid velocity ($U_L$) and they are related through the following formula:

$$V_{Lr} = \frac{U_{Lr}}{(1-\varepsilon_r)} \qquad (2.7)$$

and

$$V_{Ld} = \frac{U_{Ld}}{(1-\varepsilon_d)} \qquad (2.8)$$

Where $V_{Lr}$ is linear liquid velocity in riser and $V_{Ld}$ is linear liquid velocity in downcomer. "The velocity of liquid circulation, while itself being controlled by gas holdups in the riser and downcomer, in turn affects these gas holdups by either enhancing or reducing the velocity of bubble rise." (Chisti 1989)

The dependence of liquid velocity in the riser on superficial gas velocity was reported in the following form by several authors (El Gabbani 1977, Onken and Weiland 1983, Bello et al. 1984, Chisti 1989, Choi and Lee 1993):

$$U_{Lr} = \omega U_G{}^{v} \qquad (2.9)$$

Where the parameter ω is a function of reactor geometry and liquid properties inside the reactor and v is identified by the flow regime and the reactor geometry (Onken and Weiland 1983, Chisti 1989). Different values of exponent v have been reported in the literature, which depends on the design and geometry of reactors. El Gabbani (1977) reported the value of 0.237 for a concentric draught tube internal loop reactor using water or salt solution as a liquid phase, while Merchuk (1986) reported a value of 0.4 for this coefficient. Since the range of values reported in the literature for ω and v was too wide, several attempts were made to develop more reliable correlations. The application of Equation (2.9) is limited since too many geometrical and physical parameters were put into a coefficient and exponent.

This limitation was addressed by a number of investigators. For example, Bello et al. (1984) via an energy balance on the airlift loop suggested the following correlation for the prediction of linear liquid velocity in the riser:

$$V_{Lr} = \omega \left( \frac{A_d}{A_r} \right)^{\nu} U_G^{\frac{1}{3}} \qquad (2.10)$$

For the concentric draught-tube internal reactor the values of ω and v are equal to 0.66 and 0.78, respectively. This shows the dependence of the liquid velocity in the riser on the ratio of cross sectional area of the downcomer to riser ($A_d/A_r$). However, there is no general agreement on the effect of the term $A_d/A_r$ on liquid velocity, whereas Siegel at al. (1986) reported the value of almost 0.2 for the v exponent (Chisti 1989).

Chisti et al. (1988a) used an energy balance over an airlift loop to introduce a new equation for the prediction of liquid velocity applicable for all different type of internal airlift reactors within different ranges of geometry, including split cylinder and concentric internal loop reactor, as follows:

$$U_{Lr} = \left[ \frac{2gh_D(\varepsilon_r - \varepsilon_d)}{K_B \left( \frac{A_r}{A_d} \right)^2 \frac{1}{(1-\varepsilon_d)^2}} \right]^{0.5} \qquad (2.11)$$

In this equation, the parameters $\varepsilon_r$ and $\varepsilon_d$ are dependent on the superficial gas velocity and $K_B$ is dependent on the reactor geometry. $K_B$ is the friction loss coefficient for the

bottom of reactor and its value can be calculated from the following equation for most types of internal airlift reactors (Chisti et al. 1988a, Chisti et al. 1995):

$$K_B = 11.402\left(\frac{A_d}{A_b}\right)^{0.789} \qquad (2.12)$$

$A_b$ is the free area for the liquid flow between the riser and downcomer. The versatility and reliability of Equation (2.11) has been shown by several authors (Choi and Lee 1993, Garcia et al. 2000). The applicability of this correlation to the developed treatment system has been examined in the present work and will be discussed in the Results and Discussion chapter.

### 2.3.6 Overall volumetric oxygen transfer coefficient ($k_La_L$)

In airlift reactors designed for aerobic biological applications, oxygen transfer is an important parameter that controls the performance of the system. The entire resistance to the interfacial mass transfer of sparingly soluble gas is located in the liquid film in the interface (Chisti 1989). In fact, the liquid film controls the mass transfer of a sparingly soluble gas from the gas to the liquid phase and the transport rate is given by the following equation:

$$\frac{dC_L}{dt} = k_L a_L (C^* - C_L) \qquad (2.13)$$

Where $k_L$ is the true mass transfer coefficient, $a_L$ is the gas-liquid interfacial area per unit liquid volume, C* is the saturation concentration of oxygen in the liquid in contact with air and $C_L$ is the oxygen concentration in the liquid at any time t.

From the theoretical consideration performed by Chisti (1989), the gas-liquid interfacial area per unit liquid volume ($a_L$) can be calculated with the knowledge of gas hold up values as follows:

$$a_L = \frac{6\varepsilon}{d_B(1-\varepsilon)} \qquad (2.14)$$

Where $d_B$ is the Sauter mean bubble diameter.

By multiplying the right-hand side of Equation (2.14) by the true mass transfer coefficient, $k_L$, the following equation is obtained which is an important theoretical relationship developed by Chisti and Moo-Young (1988c):

$$k_L a_L = \frac{k_L 6\varepsilon}{d_B(1-\varepsilon)} \qquad (2.15)$$

Using the experimental values of $k_La_L$ and $\varepsilon$, the ratio of $k_L/d_B$, which is the slope of the line $k_La_L$ versus $6\varepsilon/(1-\varepsilon)$, can be obtained. This ratio is an important parameter in interpretation of mass transfer phenomena, as will be explained in section 5.4.3.

In order to obtain the true mass transfer coefficient ($k_L$) form Equation (2.13), the mass transfer interfacial area ($a_L$) needs to be calculated. However due to the difficulties

associated in the measurement of $a_L$, the calculation of overall volumetric mass transfer coefficient ($k_La_L$) is more favorable.

The integration of Equation (2.13) between the limits, $C_L = C_0$ at t = 0 and $C_L = C_L$ at t = t leads to the following equation:

$$\ln\frac{(C^* - C_0)}{(C^* - C_L)} = k_L a_L t \qquad (2.16)$$

Equation (2.16) is used for the determination of overall volumetric mass transfer coefficient ($k_La_L$) by employing the transient gassing-in method (Chisti and Moo –Young 1988a, Chisti 1989, Jamshidi et al. 2001). The oxygen transfer coefficient is measured by monitoring the changes in the concentration of dissolved oxygen when air is introduced to the reactor after the complete de-aeration of reactor. In this method, oxygen is completely depleted from a batch of liquid by either sparging nitrogen throughout the liquid or by adding sodium sulfite to the liquid. Following oxygen removal, aeration starts by introducing air to the reactor and continues until the DO electrode indicates saturated DO concentration. Meanwhile, the dissolved oxygen-time profile is obtained by monitoring the time-dependent variations of DO concentration in the reactor using DO probes located inside the reactor. The coefficient $k_La_L$ can be calculated as the slope of a semi-log plot of Ln $((C^*-C_0)/(C^*-C_L))$ vs. t. In this procedure it is assumed that liquid inside the reactor is fully mixed. Also, constant gas composition and negligible effect of the dynamics of dissolved oxygen electrodes are assumed (Benyahia and Jones 1997, Jin

et al. 2005). The $k_La_L$ can also be calculated using the modified sodium sulfite method as will be explained in section 4.2.4.

### 2.3.7 Residence time distribution (RTD)

The residence time distribution (RTD) of a reactor is the probability distribution function that describes the amount of time a fluid spends inside the reactor. The estimation of RTD enables the characterization of mixing and flow pattern inside reactors and facilitates the comparison of behavior of the real reactors to the ideal models.

The RTD of a reactor is defined by the function E(t) (Equation 2.17). The E(t) curve can be generated from a pulse-input tracer test by dividing the effluent concentration of tracer at any time, C(t), by the area under the concentration-time curve from the following equation (Bruce 2008):

$$E(t) = \frac{C(t)}{\int_0^\infty C(t)dt} \qquad (2.17)$$

The mean residence time of the tracer inside the reactor can be calculated by integrating the RTD as follows:

$$t_m = \int_0^\infty tE(t)dt \qquad (2.18)$$

By substituting Equation (2.17) in Equation (2.18), the mean residence time can be calculated from the following equation (Levenspiel 1972, Bruce 2008):

$$t_m = \frac{\int_0^\infty tC(t)dt}{\int_0^\infty C(t)dt} \quad (2.19)$$

The variance or square of the standard deviation of RTD is calculated using the following formula:

$$\sigma_t^2 = \int_0^\infty (t - t_m)^2 E(t)dt \quad (2.20)$$

The value of variance is an indication of the RTD spread which has a unit of time squared. The dimensionless variance can be obtained by dividing the variance ($\sigma^2_t$) by the square of mean residence time ($t_m$). This parameter measures the breadth of distribution in a way that is independent of the magnitude of $t_m$, according to the following equation:

$$\sigma^2 = \frac{\sigma_t^2}{t_m^2} \quad (2.21)$$

The value of $\sigma^2$ is helpful in the prediction of mixing behavior of reactors. For plug flow reactors (PFR) $\sigma^2=0$ and for continuous stirred tank reactors (CSTR) $\sigma^2=1$. The dimensionless variance of most reactors falls somewhere between these two limits of 0 and 1 (Bruce 2008).

## 2.4 Zone generation studies

The presence of different environmental conditions of aerobic, microaerophilic, anoxic and anaerobic is required in the treatment system in order to ensure an efficient removal of organic carbonaceous compounds as well as inorganic contaminants, notably

nitrogen and phosphorous, and suspended solids. The four zones are defined by their respective average concentrations of dissolved oxygen (DO) and oxidation-reduction or redox potential (ORP) in these zones. Table 1 presents the design conditions of dissolved oxygen (DO), pH and oxidation/reduction potential (ORP) in various zones of the treatment system.

Table 1. Design characteristics of each treatment zone in the reactors

| Parameter / Zone | DO (mg/L) | pH | ORP (mV) |
|---|---|---|---|
| Aerobic | 4-6 | 7-8.5 | > +200 |
| Microaerophilic | 0-1 | 7-8.5 | 0 to 200 |
| Anoxic | 0 | 6.5-7.5 | -100 to +100 |
| Anaerobic | 0 | 6-7 | < -100 |

Dissolved oxygen can be controlled by the air flow rate and velocity of liquid circulation between the aerobic and microaerophilic zones, controlled by the size and number of apertures between these zones to ensure that they are maintained in the required range. However, ORP values depend on several environmental factors including pH, the presence of oxidized or reduced species and their concentration and interactions. Therefore, the design values of ORP can only be developed in the system during actual treatment of wastewater. The methodology for creation of different biological zones based on DO concentration is explained in section 4.4.

# CHAPTER 3: THEORETICAL DEVELOPMENT

## 3.1 Theory and principles of liquid circulation between different zones of the reactor

### 3.1.1 Introduction

During the operation of treatment system, untreated wastewater is added to reactor I at a given flow rate from the top of aerobic zone on a continuous basis, as presented in Figure 1. The recycled liquid from the second reactor is also added to the top of aerobic zone. The upward flow of liquid in this zone carries the added wastewater towards the microaerophilic zone where it flows downward towards the anoxic zone. Since there is

no accumulation of liquid inside the reactor, a volume of liquid equal to the volume of influent wastewater (raw wastewater plus the recycled liquid from the second reactor) exits the reactor on a continuous basis while the rest of liquid flows towards the center of reactor where it is directed towards the aerobic zone. This flow pattern continues throughout the course of operation of first reactor, creating a continuously circulating liquid between the aerobic, microaerophilic and anoxic zones. The retention time of the circulating liquid in the aerobic zone is preset by adjusting the number of openings between the aerobic and microaerophilic zones which are the riser and downcomer of the airlift reactor, respectively, as well as the size of the openings (1" and ½") and the input power of the air compressor that introduces air through air diffusers into the aeration zone.

The following questions will be answered in next sections:

- What mathematical function can be used to model the passage of influent wastewater and its circulation through the aerobic, microaerophilic and anoxic zones?

- What is the time length of a single liquid cycle between the aerobic, microaerophilic and anoxic zones (instantaneous HRT)?

- What is the fraction of liquid that escapes circulation at every cycle of liquid circulation between the aerobic, microaerophilic and anoxic zones?

- What is the average time that a given quantity of wastewater circulates between the aerobic, microaerophilic and anoxic zones at any given operating condition before completely leaving the reactor?

- How long does it take to replace the content of the first reactor with the incoming wastewater?

### 3.1.2 Theoretical Considerations

The following analysis assumes that the first reactor, consisting of aerobic, microaerophilic and anoxic zones, is originally filled with mixed liquor that contains wastewater and microbial biomass at time zero. It also considers a gradual addition of influent wastewater (raw wastewater plus the recycled liquid from the second reactor) to the mixed liquor from the top of aeration zone.

In order to mathematically describe the passage of wastewater through the reactor, the volume of wastewater inside the reactor at any given time is defined as $Y_w$, while the volume of mixed liquor inside the reactor at any given time is defined as $Y_r$. It is understood that in reality, the wastewater and the mixed liquor are thoroughly mixed and cannot be considered as two separate streams. However, for the purpose of flow analysis and the development of mathematical models, it is helpful to consider the wastewater as a separate entity inside the reactor. Conceptually, it may be imagined that all the molecules of wastewater that enter the reactor are marked by a radioactive

marker or alternatively, they all "glow", making it possible to monitor the pattern of their movement through the reactor. This analysis does not address the biological treatment of wastewater and does not distinguish between the treated and untreated wastewater.

Assuming that the reactor volume ($V_R$) and the influent wastewater flow rate are constant, a constant percentage of the reactor's liquid content, i.e. mixture of wastewater and mixed liquor, leaves the reactor during any given period of time. Therefore, the change in time of mixed liquor's volume ($dY_r/dt$) is directly proportional to the volume of mixed liquor in the reactor. This relationship can be mathematically expressed as follows:

$$\frac{dY_r}{dt} = -kY_r \qquad (3.\ 1)$$

or

$$Y_r = Y_i e^{-kt} \qquad (3.\ 2)$$

Where $Y_r$ is the volume of mixed liquor at time (t) that is being gradually replaced by the added wastewater, $Y_i$ is the initial volume of mixed liquor that is equal to the overall reactor's volume ($V_R$), and k is a constant representing the specific rate of liquid discharge from the reactor. This constant defines the fraction of liquid discharged from the reactor per unit of time. The fraction of mixed liquor volume in the reactor at any given time (t) can be expressed by the following equation:

$$\%Y_r = \frac{Y_r 100}{Y_i} = e^{-kt} * 100 \qquad (3.3)$$

Since $Y_r+Y_w=Y_i$, the volume of wastewater inside the reactor at any given time may be expressed as follows:

$$Y_w = Y_i(1 - e^{-kt}) \qquad (3.4)$$

Where $Y_w$ is the volume of wastewater inside the reactor. The fraction of wastewater liquid based on the total content of the reactor is:

$$\%Y_W = \frac{Y_W 100}{Y_i} = (1 - e^{-kt}) * 100 \qquad (3.5)$$

Equations (3.1) to (3.5) demonstrate the following:

$t = 0 \Rightarrow Y_r = Y_i$ The initial volume of mixed liquor is equal to the reactor's overall volume.

$t = 0 \Rightarrow Y_w = 0$ There is no wastewater inside the reactor at time zero and the initial mixed liquor is the only liquid that occupies the reactor.

### 3.1.3 Dynamic changes in the volume of a discrete quantity of wastewater

A similar procedure may be used to determine the time-dependent changes in the volume of a discrete quantity of wastewater added to the reactor. The volume of the

added wastewater inside the reactor decreases in time because a fraction of this wastewater continuously exits the reactor as a part of the departing liquid. Again, it is assumed that a fraction of the reactor's liquid content, i.e. a mixture of wastewater and mixed liquor, continuously leaves the reactor since there is no liquid accumulation inside the reactor. The time-dependent changes in the volume of wastewater ($Y_w$) inside the reactor may be expressed by the following equation:

$$Y_W = Y_{Wi} e^{-kt} \qquad (3.6)$$

Where $Y_{wi}$ is the volume of the discrete quantity of wastewater added to the reactor at time zero.

The percentage of wastewater that has left the reactor at any given time (t) is expressed as follows:

$$\% \text{ wastewater volume that has left the reactor} = \frac{(Y_{Wi} - Y_W)100}{Y_{Wi}} \qquad (3.7)$$

Where $Y_w$ is the volume of wastewater (mixed liquor) inside the reactor at time (t).

Combining equations (3.6) and (3.7), the following relationship will result:

$$\% \text{ wastewater volume that has left the reactor} = (1 - e^{-kt}) * 100 \qquad (3.8)$$

The average time spent in the reactor for a given quantity of wastewater entering the reactor is estimated by rearranging Equation (3.6), as follows:

$$t = -\frac{1}{k}\ln\left(\frac{Y_W}{Y_{Wi}}\right) \quad (3.9)$$

$$\text{Average time} = t = -\frac{1}{k}\int \ln(Y_w)dY_w = \left[Y_w \ln(Y_w) - Y_w\right]_{(0-1)} \quad (3.10)$$

Average time = -1/k [-1-0] = 1/k (3. 11)

The average number of liquid circulations between the aerobic, microaerophilic and anoxic zones for a given quantity of wastewater before leaving the reactor is equal to:

Average number of circulations (N.O.C) = (1/k) / (time of one cycle of liquid between the three zones) (3.12)

The percentage of liquid that escapes circulation at each cycle is estimated by making a flow balance around the first reactor, as follows:

$$\%\ \text{liquid} = \frac{Q_e + Q_b}{Q_i + Q_r + Q_a} \quad (3.13)$$

Where:

$Q_a$ = Circulating liquid flow rate in the aerobic zone

$Q_i$ = Flow rate of raw wastewater

$Q_r$ = Flow rate of the recycled liquid between the second and first reactor. This flow rate can be fixed by the operator

$Q_e$ = Flow rate of liquid that exits the reactor through the clarifier

$Q_b$ = Flow rate of liquid that exits the reactor through the anoxic zone

The specific rate of liquid discharge from the reactor (k) is calculated from the following equation:

$$k = \frac{Q_e + Q_b}{V_a + V_m + V_x} \quad (3.14)$$

Where:

$V_a$ = Volume of aerobic zone

$V_m$ = Volume of microaerophilic zone

$V_x$ = Volume of anoxic zone.

The length of time of a single liquid cycle between the aerobic, microaerophilic and anoxic zones is equal to the sum of instantaneous hydraulic retention times in the three respective zones. This time is calculated as follows:

The length of time of a single liquid cycle between the zones = $HRT_a + HRT_m + HRT_x$ (3. 15)

Where:

$HRT_a = V_a/Q_a$ (3.16)

$HRT_m = V_m/Q_m = V_m/(Q_a + Q_i + Q_r)$ (3.17)

$HRT_x = V_x/Q_x = V_x/(Q_m - Q_e - Q_b)$ (3.18)

And:

$$Q_i + Q_r = Q_e + Q_b \quad (3.19)$$

$$Q_a = Q_m - Q_e - Q_b \quad (3.20)$$

$$Q_m = Q_i + Q_r + Q_a \quad (3.21)$$

$$Q_a = Q_x \quad (3.22)$$

Where:

$Q_a$ = Circulating liquid flow rate in the aerobic zone

$Q_m$ = Circulating liquid flow rate in the microaerophilic zone

$Q_x$ = Circulating liquid flow rate in the anoxic zone

Equations (3.1) to (3.22) along with the design parameters of the first reactor were used to estimate the process variables and to identify the developed mathematical models.

Once again, it should be emphasized that the developed mathematical equations only represent liquid displacement in the first reactor and do not discuss the treatment of wastewater, i.e. the question of whether or not the added wastewater is actually treated during its stay in the reactor is not addressed in this analysis. The mathematical equations simply define the number of liquid circulations through the zones of reactor and the overall time that is available for the treatment of wastewater in the first reactor.

A comparison between the results obtained from experimental work and theoretical model developed in this section will be presented in section 5.7.

## 3.2 Mathematical method for the calculation of linear liquid velocity in the downcomer and riser

### 3.2.1 Linear liquid velocity in the downcomer

Based on the law of continuity, the liquid flow rate passing through the riser is equal to that passing through the downcomer:

$$Q_{cir} = U_{Lr} A_r = U_{Ld} A_d \qquad (3.23)$$

In the studied treatment system, liquid circulates continuously between the riser and downcomer while passing through eight apertures between these two zones. Although the existence of these openings allows a better control over the oxygenation and circulation of mixed liquor between different zones of the reactor, it also restricts the passage of flow between the riser and downcomer. Therefore, the application of Equation (3.23), developed for conventional airlift reactors that do not have any restriction on liquid circulation between the riser and downcomer, will be limited for the reactor studied in the present work.

The volumetric flow rate of liquid circulating between the two zones of the reactor was estimated by measuring the liquid flow rate passing through one opening and

multiplying the obtained value by eight (number of openings). The volumetric flow rate of the circulating liquid ($Q_{cir}$) was measured for different air flow rates in the range of 10 to 70 L/min. The linear liquid velocity in the downcomer was calculated from the knowledge of the cross sectional area of the downcomer, $A_d$, as follows:

$$U_{Ld} = \frac{Q_{cir}}{A_d} \qquad (3.24)$$

Since the gas hold in the downcomer is negligible, superficial liquid velocity and linear liquid velocity can be assumed to be equal $V_{Ld}=U_{Ld}$.

### 3.2.2 Linear liquid velocity in the riser

A mathematical model was developed to express linear liquid velocity in the riser based on energy balances across the diffusers. Three diffusers at the bottom of the aerobic zone with air and water passing through them were employed in this study. The following assumptions were made in the development of mathematical model:

1) The system operates under steady- state and steady- flow mode.

2) There is no height difference between the points where air and water exchange the energy so potential energy changes are equal to zero. $\Delta E_P = 0$

3) The temperature is constant, thus heat exchange in the system is zero. $Q_{cv} = 0$

4) There is no external work done by / in to the system. $W_{cv} = 0$

5) The energy carried by air while exiting the diffusers, is totally transferred to the water, therefore:

$$\Delta E_{water} = \Delta E_{air} \qquad (3.25)$$

According to the above assumptions, the kinetic energy is the only form of energy that exists in the system. Therefore, Equation (3.25) can be written in the following form:

$$\frac{1}{2}\dot{m}_w(V_{2w}{}^2 - V_{1w}{}^2) = \frac{1}{2}\dot{m}_a(V_{2a}{}^2 - V_{1a}{}^2) \qquad (3.26)$$

Or:

$$V_{2w} = \left[\frac{\dot{m}_a}{\dot{m}_w}(V_{2a}{}^2 - V_{1a}{}^2) + V_{1w}{}^2\right]^{\frac{1}{2}} \qquad (3.27)$$

Where $V_{1W}$ and $V_{2W}$ are the velocities of water, and $V_{1a}$ and $V_{2a}$ are the velocities of air just before and after the diffusers, respectively. These parameters are estimated from the following equations:

$$V_{2a}A_2 = V_{1a}A_1 = Q_{air} \qquad (3.28)$$

Where $A_2$ is the total surface area of the holes of three air diffusers and $A_1$ is the surface area of inlet air pipe before diffusers.

The velocity of water just before the air diffusers, $V_{1W}$, can be calculated by dividing the volumetric flow rate of liquid flowing from the downcomer toward the riser, by the cross sectional area of the riser as follows:

$$V_{1w} = \frac{Q_{cir}}{A_r} \tag{3. 29}$$

$\dot{m}_a$ and $\dot{m}_w$ are mass flow rates of air and water which are related to the air and water volumetric flow rates by the following equations:

$$\dot{m}_a = \rho_a Q_{air} \tag{3. 30}$$

$$\dot{m}_w = \rho_w Q_{cir} \tag{3. 31}$$

The liquid flow velocity in the riser after passing through the diffusers can be obtained by substituting Equations (3.28), (3.30) and (3.31) in equation (3.27):

$$V_{2w} = \left[ \frac{\rho_a Q_{air}^{\ 3}}{\rho_w Q_{cir}} \left( \frac{1}{A_2^2} - \frac{1}{A_1^2} \right) + V_{1w}^{\ 2} \right]^{\frac{1}{2}} \tag{3. 32}$$

The value of $V_{2W}$ calculated from the theoretical method, as described, has been compared with empirical results obtained from acid tracer response technique used for the determination of linear liquid velocity in the riser.

# CHAPTER 4: DESIGN AND METHODOLOGY

## 4.1 Experimental setup

The first reactor contains three interactive zones of aerobic, microaerophilic and anoxic which are surrounded by a clarification unit (Figure 1). The aerobic and microaerophilic zones operate on the principles of concentric draught-tube airlift reactors. This reactor contains three air diffusers at the bottom of the aerobic zone for the introduction of air, providing high rate oxygenation and mixing while supporting the accumulation of a high concentration of biomass. Airlift reactors in general consist of two sections of riser and downcomer with diffusers at the bottom of riser to lift the liquid upward in the riser and

downward in the downcomer, thus facilitating the circulation of liquid between these two sections. In the examined system, aerobic and microaerophilic zones are the riser and downcomer of the airlift reactor, respectively. The placement of half cone at the bottom of downcomer (microaerophilic zone) facilitates the movement of liquid flow from the downcomer to riser while minimizing energy losses. The schematic diagram of the first reactor with essential details is presented in Figure 6.

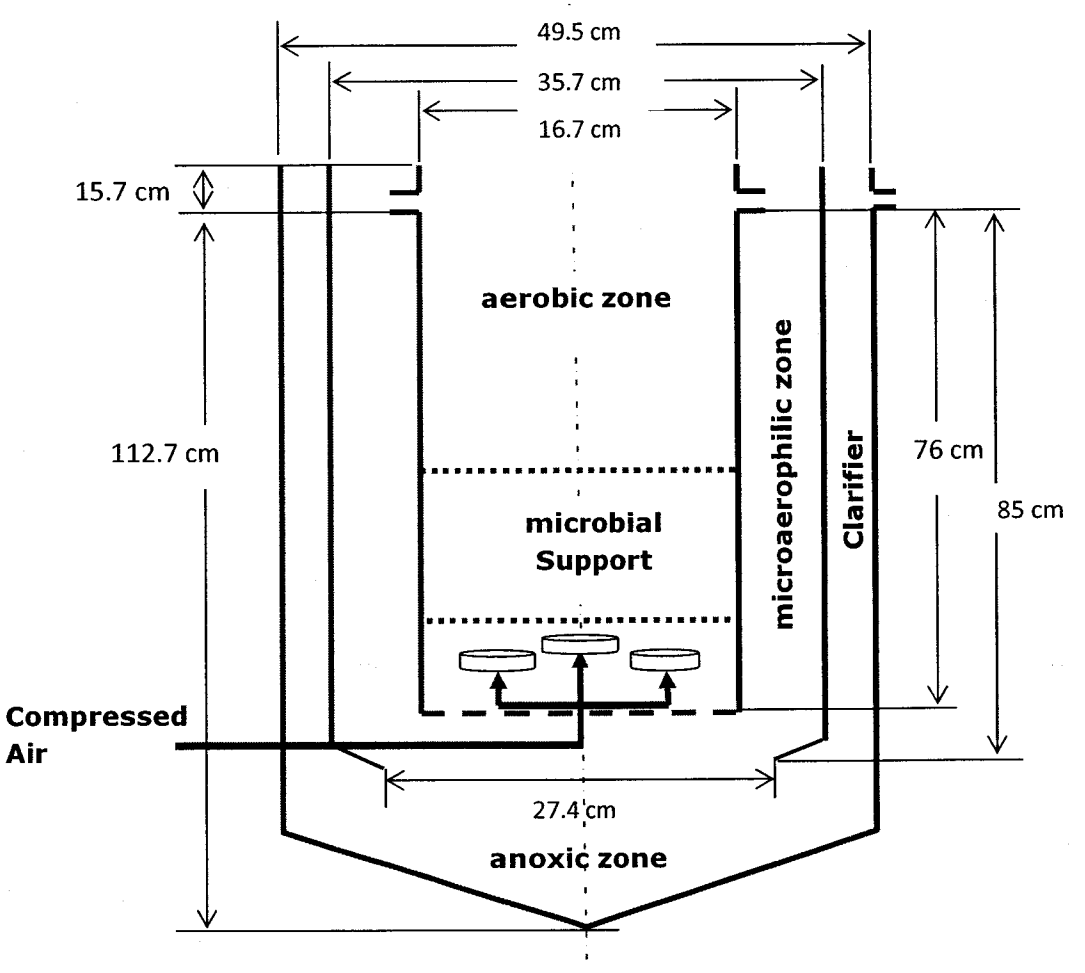


Figure 6: Dimensions of the first reactor

Three diffusers were installed 8 cm above the bottom of the draft tube. Each diffuser consists of 21 holes with the diameter of 1mm. This arrangement was satisfactory for aeration and liquid mixing inside the reactor.

The ratio of downcomer to riser cross sectional area ($A_d/A_r$) in most airlift reactors described in the literature is <1 but the treatment requirements of the examined system led to the design of a larger downcomer to riser cross sectional area ratio of about $A_d/A_r$=3.45.

## 4.2 Methodology for the evaluation of hydrodynamic characteristics

The employed methodologies for the evaluation of hydrodynamic parameters of the treatment system are extensively described in the following sections. The impact of operating conditions and process parameters on the examined hydrodynamic parameters of the system were also evaluated. The experiments were carried out at ambient temperature, using water as the liquid phase and air as the gas phase. Air was sparged in the draught tube (aerobic zone) from the bottom of reactor. All measurements were conducted under at least three operating conditions defined by three aeration power outputs. Selected experiments were repeated in the presence of a microbial support in the aerobic zone. The inlet air flow rate was measured by a flow meter and varied in the range of 10 to 70 L/min.

### 4.2.1 Measurement of gas hold-up (ε)

The overall gas holdup is commonly determined by using the volume expansion technique. In this method, the height of liquid in the reactor is measured when the reactor is not aerated ($h_L$) and when it is aerated ($h_D$). The overall gas hold up can then be calculated from the following equation: (Chisti 1989, Chisti et al. 1995, Choi et al. 1996, Hwang and Cheng 1997, Jamshidi et al. 2001, Jin and Lant 2004)

$$\varepsilon = \frac{h_D - h_L}{h_L} \qquad (4.1)$$

In the examined treatment system, due to the presence of openings between the riser and downcomer, most air dispersions occur in the riser. Therefore, the overall gas hold up can be calculated by using the definition of gas hold (Equation (2.3)), as follows:

$$\varepsilon = \frac{V_G}{V_G + V_{Li}} = \frac{A_r(h_D - h_L)}{A_r(h_D - h_L) + h_L(A_r + A_d)} \qquad (4.2)$$

If $h_D$-$h_L$=$h_{dis}$,

$$\varepsilon = \frac{h_{dis}}{h_{dis} + h_L(1 + \frac{A_d}{A_r})} \qquad (4.3)$$

Where $A_d$ and $A_r$ are the cross sectional areas of the downcomer and riser, respectively.

If the specific gas hold ups in the riser ($\varepsilon_r$) and downcomer ($\varepsilon_d$) of an airlift reactor are needed to be estimated, the manometric technique is applied. In this method, a U-tube

or an inverted U-tube manometer is used. The U-tube monometer is filled with water-immiscible fluid while the inverted U-tube monometer is filled with the same fluid that is used inside the reactor. In both cases, two sampling ports of the monometer are connected to two pressure taps located at two different axial positions either in the riser or in the downcomer of reactors for the measurement of $\varepsilon_r$ and $\varepsilon_d$ , respectively. Depending on the type of manometer set up employed, the gas hold up can be obtained by the following equations (Chisti1989, Chisti et al. 1995):

$$\varepsilon = \frac{\rho_M - \rho_L}{\rho_L - \rho_G}\frac{dh_M}{dz} \qquad \text{for the U-tube manometer} \qquad (4.4)$$

$$\varepsilon = \frac{\rho_L}{\rho_L - \rho_G}\frac{dh_M}{dz} \qquad \text{for the inverted U-tube manometer} \qquad (4.5)$$

Where $\rho_G$, $\rho_L$, $\rho_M$ are the densities of gas, liquid and manometer fluid, respectively. dz is the vertical distance of pressure taps in the riser or downcomer and $dh_M$ is the manometer reading. As mentioned earlier, in the system examined in this work the majority of gas hold up occurs in the riser. Therefore, only gas hold up in the riser was measured. The inverted U-type manometer technique was used by inserting two pipes with different lengths, connected by plastic tubing at the top, inside the riser (Figure 7).

The gas hold up in the riser was determined by monitoring $dh_M$ in the presence of aeration from the difference of fluid rise inside the pipes and knowledge of dz which represents the difference in the length of pipes. Equation (4.5) expresses the observed relationship.

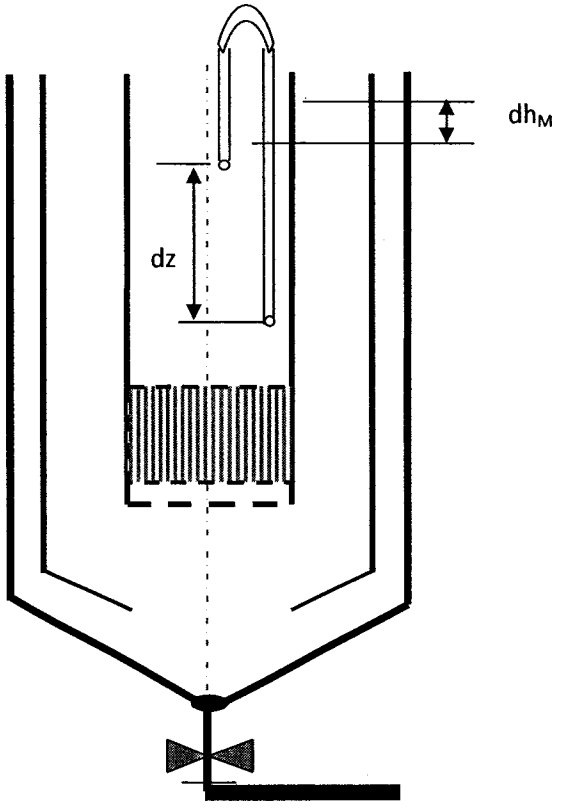


Figure 7: Experimental set up for determination of gas holdup in the riser

The estimation of gas hold up was carried out by sparging air in the aerobic zone of reactor at different flow rates in the range of 10 to 70 L/min. The overall gas hold up and the gas hold up in the riser (aerobic zone) for two sizes of the openings of 1" and ½" were calculated using Equation (4.3) and (4.5). In order to evaluate the impact of microbial support on the gas hold up in the riser, same set of the experiments were repeated by placing the microbial support inside the aerobic zone and above the diffusers. The results are reported in section 5.1.

### 4.2.2 Measurement of mean circulation time ($t_C$) and mean liquid circulation velocity ($U_{LC}$)

The acid tracer response technique was used to estimate the mean liquid circulation time ($t_c$) and the mean liquid circulation velocity ($U_{LC}$). In this technique, a pulse injection of 25 ml hydrochloric acid (HCl) was made at the top of aerobic zone to allow the tracer disperse in a radial plane. A pH probe (Cole Parmer- 3 ft, 100Ω RTD Submersible), placed 15 cm below the water level in the microaerophilic zone and connected to a pH/ORP meter (Oakton-Model PD650), was used to detect the pulse and to transmit the data to a computer every 3 seconds using a USB IrDA converter (SWEEX-Model KB200010). The tracer injections were made 15 seconds after the initiation of data logging in order to ensure the consistency of results. The circulation time was estimated from the average time between the two minima in the recorded chart. Hydrochloric acid at three different concentrations of 2N, 5N and 10N were used to ensure the validity of results. The most reliable results in terms of creating more clear curves were obtained with 5N HCl. The Experiments were carried out with air flow rates in the range of 10 to 70 L/min and with two different sizes of openings between the riser and downcomer. Each set of the experiment was carried out twice using eight openings of 1" and ½" diameter between the riser and downcomer.

The mean liquid circulation velocity was estimated from the ratio of liquid circulation path to the liquid circulation time according to Equation (2.5).

It should be noted that the locations of the tracer injection and measurement points must be carefully controlled since they affect the estimated values of liquid circulation time and mean circulation velocity. The trend of pH variations inside the microaerophilic zone after releasing the tracer is shown in Figure 8.

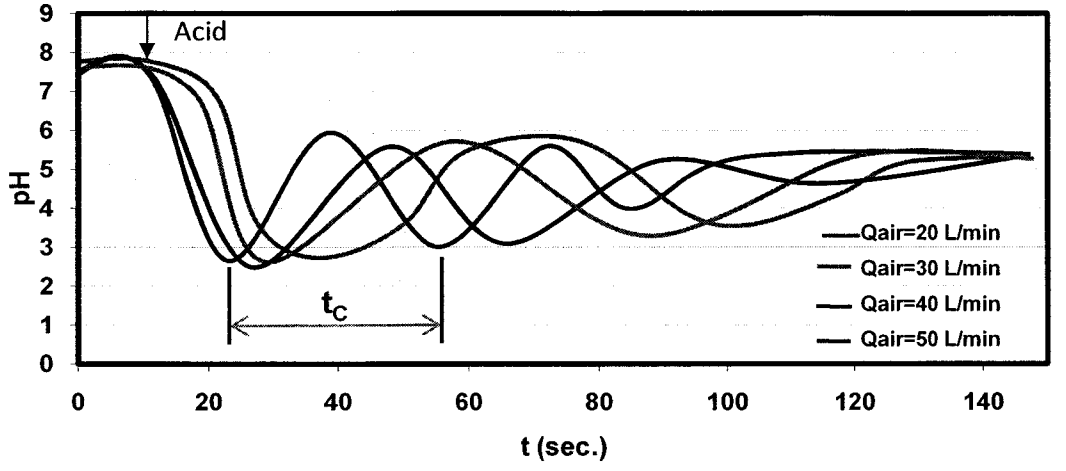


Figure 8. pH variations in the microaerophilic zone after acid injection at different air flow rates

The curves, each having two peaks, correspond to the different air flow rates examined. Two methods of calculation were used to estimate the mean circulation time. In the first method, the horizontal distance between two minima on each curve was estimated as the time of one complete liquid circulation between the zones.

In the second method, pH values were converted to hydrogen ion concentration using the following formula. The typical resulting curves are shown in Figure 9:

$$[H^+]=10^{-pH} \qquad (4.6)$$

The corresponding time for the occurrence of peaks on each curve was estimated from the first moment of the hydrogen ion concentration curve versus time, from the following formula:

$$t_p = \frac{\int_0^\infty tC(t)dt}{\int_0^\infty C(t)dt} \qquad (4.7)$$

The mean liquid circulation time at each examined air flow rate was calculated from the difference between the first moment of the first and second peak of each curve (Merchuk et al. 1996). The obtained results from the two employed techniques, i.e. pH graphs and $[H^+]$ graphs were compared as reported in section 5.2. The mean liquid circulation velocity was further estimated from the knowledge of liquid circulation path ($x_c$).

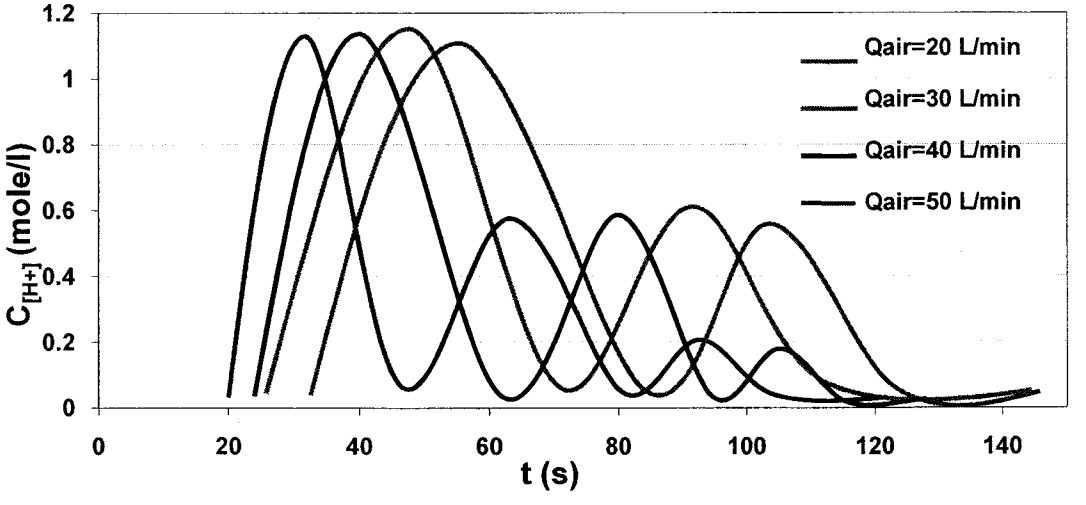


Figure 9. Typical variations of hydrogen ion concentration after acid injection for different air flow rates

The experiments were repeated at different air flow rates while maintaining the size of apertures between the riser and downcomer. Two different aperture sizes of 1" and ½" were used in this study in order to determine the dependence of mean liquid circulation time and liquid circulation velocity on the size of openings, as discussed in section 5.2. Moreover, by installing the microbial support just above the diffusers at the bottom of draught tube, the same set of experiments was repeated, hence the impact of microbial support on the mean circulation time for different superficial gas velocities was evaluated.

### 4.2.3 Measurement of linear liquid velocity in the riser and downcomer

The independent values of linear liquid velocity in the riser and downcomer were estimated by using the tracer technique as described before (Chisti 1989, Lu and Hwang 1995, Hwang and Cheng 1997, Gourich et al. 2005). However, in this estimation pH was monitored by two identical pH probes placed at two different locations in the microaerophilic zone as shown in Figure 10. The pH probe 1 was placed 15 cm below the water level in order to have a fully developed flow and the pH probe 2 was located at the bottom of downcomer where the water flows toward the riser.

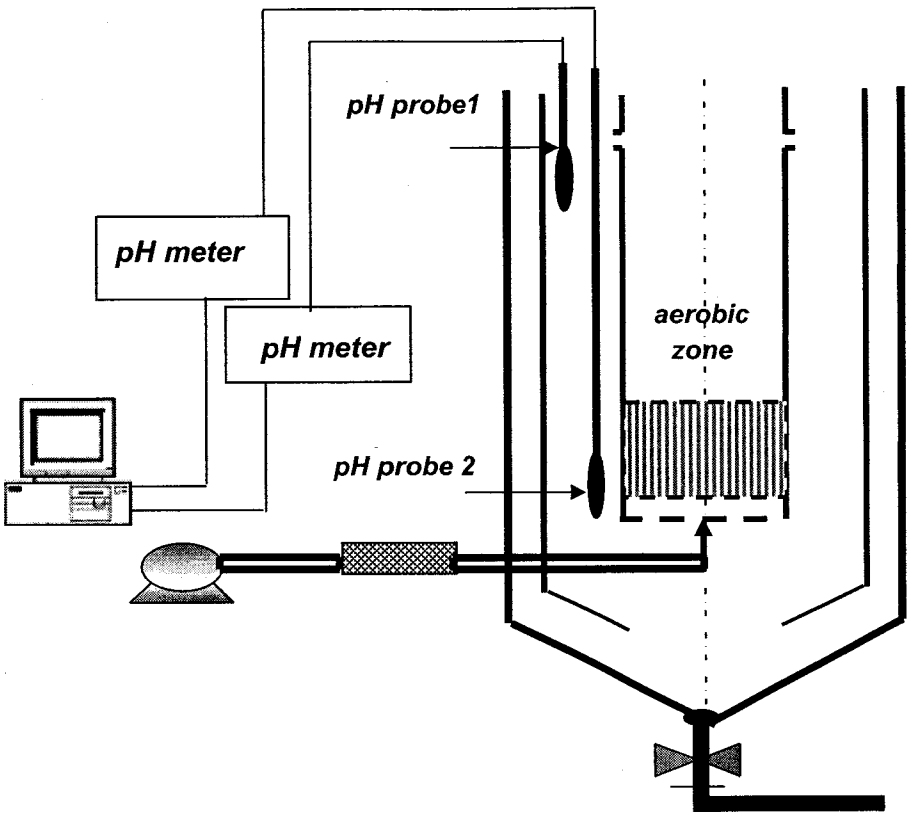


Figure 10. Schematic diagram of experimental set up for measurement of linear liquid circulation velocity in the downcomer

The pH probes were connected to two separate pH meters (Oakton-Model PD650). The obtained data from pH meters were transmitted to the computer by the USB IrDA converter. A typical response curve illustrating changes in the liquid pH inside the reactor after the release of tracer from the top of aerobic zone is presented in Figure 11.

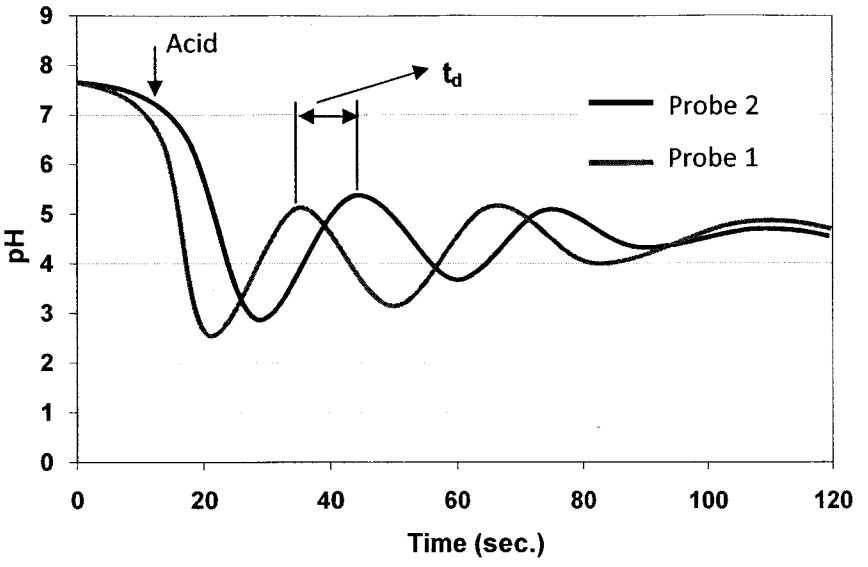


Figure 11. Typical response curves from two pH electrodes placed at two locations inside the microaerophilic zone

The estimation of liquid velocities in the riser and downcomer is schematically presented in Figure 12.

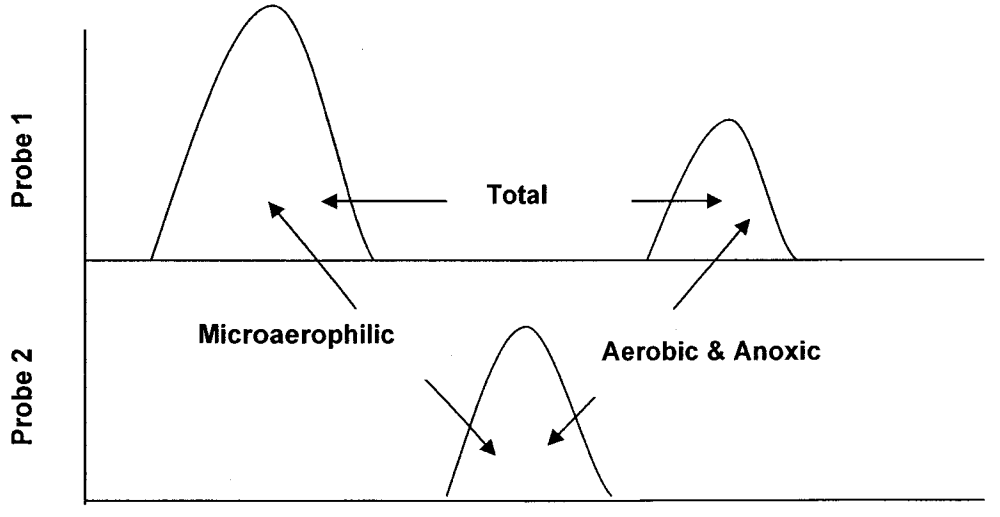


Figure 12. Typical peaks resulting from two pH electrods inside the microaerophilic zone

The travel time of tracer between the two pH electrodes was estimated from the difference between the first moments of the first response peak of pH probe 1 and 2, which is almost equal to the overall length of the downcomer.

The linear liquid velocity in the downcomer (microaerophilic zone) was calculated from the following equation:

$$V_{Ld} = \frac{L_d}{t_d} \qquad (4.8)$$

$L_d$ is the distance between two pH electrodes in the microaerophilic zone and $t_d$ is the difference in the response time of the first peaks, corresponding to the response curves of the two pH probes in the microaerophilic zone, respectively (Lu and Hwang 1995). The residence time and the corresponding linear liquid velocity in the riser were estimated by deducting the residence time of the liquid in downcomer ($t_d$) from mean liquid circulation time ($t_C$).

### 4.2.4 Measurement of the overall volumetric oxygen transfer coefficient ($k_La_L$)

The modified sulfite method was used for the determination of overall volumetric mass transfer coefficient ($k_La_L$). This method has been applied earlier by other investigators (Imai et al. 1987, Ghosh et al. 1993, Vilaça et al. 2000, Gouveia et al. 2003). The experiments were carried out with a solution of sodium sulfite as the liquid phase and

air as the gas phase. Air was sparged through the diffusers while its flow rate was measured by a mass flow meter (AALBORG- Model GFM 47, 0-100 Std L/min) installed in the air line just before air enters the reactor. All experiments were carried out at room temperature and at atmospheric pressure.

Initially the reactor was filled with tap water. Anhydrous sodium sulfite (Fisher Scientific) was added to the rector's content and mixed thoroughly, providing a concentration of 0.5 g/L. The solution remained for almost 2 hours until sulfite sodium consumed all the dissolved oxygen in the reactor. The reaction between sodium sulfite and dissolved oxygen is given in the following stoichiometric equation:

$$Na_2SO_3 + 1/2\,O_2 \longrightarrow Na_2SO_4 \qquad (4.9)$$

The concentration of dissolved oxygen inside the reactor was monitored during the experiment by a DO probe (Cole Parmer, 0-20 ppm, 10') placed inside the riser, which was connected to a DO transmitter/controller (EUTECH INSTRUMENT-Model alpha, DO2000 W). Using a data logger (Dickson- Model ES120) the data were transferred from the DO transmitter/controller to the computer. The DO probe was calibrated before each experiment, alternatively using oxygen-saturated and oxygen-depleted water samples. The former water sample was prepared by bubbling air through the liquid for about an hour, and the latter was prepared by adding an adequate amount of sodium sulfite to water. The DO electrode and controller were automatically temperature compensated in order to eliminate the possible effect of temperature variations on dissolved oxygen measurements.

The DO transmitter was turned on with the onset of aeration. A fraction of the added sodium sulfite was used to deplete the dissolved oxygen inside the reactor before aeration started and the rest was enough to maintain the dissolved oxygen concentration around zero during a long period after aeration. The time ($\Delta t$) required for the complete consumption of dissolved sodium sulfite was measured. This time corresponds to the initial rise of dissolved oxygen concentration in the liquid, as presented typically in Figure 13, where different curves correspond to different air flow rates.

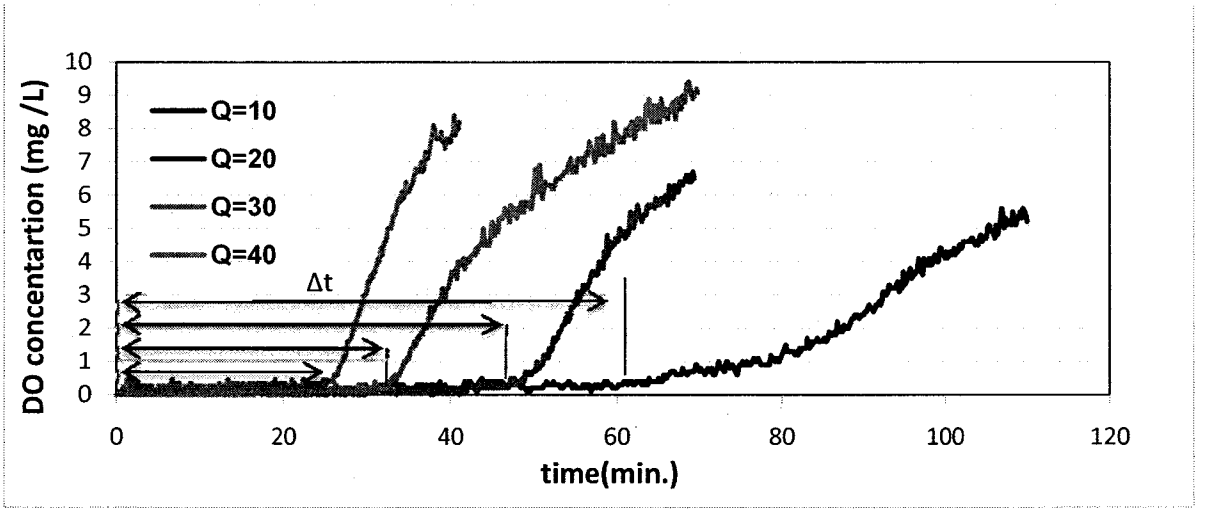


Figure 13. Typical dissolved oxygen concentration profiles versus time at different air flow rates

According to the stoichiometric Equation (4.9), the consumption rate of dissolved oxygen is equal to half of the sodium sulfite consumption rate. Therefore, the volumetric oxygen transfer rate and the volumetric oxygen transfer coefficient ($K_La_L$) can be determined from the following equations:

$$r(O_2) = \frac{1}{2} r(Na_2SO_3) \quad (4.10)$$

$$\frac{dC(O_2)}{dt} = \frac{1}{2}\frac{dC(Na_2SO_3)}{dt} = k_L a_L (C^* - C) \quad (4.11)$$

$$k_L a_L = \frac{1}{2}\frac{C_0(Na_2SO_3)}{(C^* - C)}\frac{1}{\Delta t} \quad (4.12)$$

Where

$k_L$ = mass transfer coefficient (m/s)

$a_L$ = interfacial area between gas and liquid per unit volume ($m^2/m^3$)

C = dissolved oxygen concentration at time t (mmole/L)

$C^*$ = saturation oxygen concentration (mmole/L)

$C_0$ ($Na_2SO_3$) = initial concentration of sodium sulfite in the reactor (mmole/L)

It should be noted that the amount of sodium sulfite consumed initially in order to deplete the dissolved oxygen in the liquid before aeration, should be subtracted from the total amount of sodium sulfite added to the reactor.

In order to evaluate the effect of superficial gas velocity ($U_G$) on the overall volumetric mass transfer coefficient ($K_La_L$), the experiments were repeated at different air flow rates in the range of 10 to 50 L/min. For each measurement, the reactor was filled with fresh water and the procedure was repeated. The same set of experiments was also repeated in the presence of microbial support.

### 4.2.5 Measurement of residence time distribution

The residence time distribution (RTD) of liquid inside the reactor is determined experimentally by pulse-input tracer technique (Levenspiel 1972, Gavrilescu & Tudose 1996, 1999, Choi et al. 2004). In the examined treatment system, the liquid is circulated in a closed loop through the aerobic, microaerophilic and anoxic zones, while air continuously diffuses into the system. It is anticipated that a pulse of a tracer injected in the aerobic zone will be evenly distributed throughout the system after a short period of time.

During the experiments, the reactor was filled with tap water. Aeration through the diffusers located at bottom of aerobic zone started. Tap water at a constant flow rate ($Q_i$) started to be added to the system from the top of aerobic zone. Since the system operated at steady state and there was no liquid accumulation inside the reactor, a flow equal to the water flow rate, continuously left the reactor ($Q_e$).

Water-soluble Quinoline-Yellow (QY) 95%, (Fisher Scientific) was used as a tracer or used independently to qualitatively observe the turbulence of fluid through the transparent material used in the construction of the reactor.

1.5 g QY, dissolved in 10 ml of tap water to make a highly concentrated tracer solution, was instantaneously injected into the system from the top of aerobic zone at time zero. A small amount of tracer was used in comparison to the total volume of reactor and injection was made as quickly and as smoothly as possible. Samples were taken from the reactor's exit where the liquid leaves the reactor toward the clarifier. The concentration

of samples was analyzed using a spectrometer (HACH-Model DR2800). Immediately after the release of tracer from the top of aerobic zone, samples were taken every 1 minute for half an hour and continued to be taken with time intervals of 5 minutes for an additional hour. After this time, the changes in tracer's concentration were less variable and sampling was carried out every half an hour until the tracer's concentration inside the reactor approached zero, implying that the entire volume of reactor was replaced by the fresh water added to the system.

Using the values of tracer (QY) concentration in the effluent at any time, C(t), and Equation (2.17), RTD curves were obtained. Equation (2.19) was then used to calculate the average residence time of the tracer in the reactor.

The experiments were carried out at various operating conditions in order to evaluate the effect of different air flow rates and different influent water flow rates on RTD of the first reactor. The experiments were performed at three different influent water flow rates ($Q_i$) of 720, 1030 and 1450 L/d and three air flow rates ($Q_{air}$) of 15, 30 and 45 L/min, making a total of 9 experiments. In order to ensure the ratability of results, each experiment was repeated at least three times. RTD results are presented in section 5.5. All experiments were carried out using eight openings of 1" size between the riser and downcomer.

### 4.2.6 Evaluation of time-dependent changes in the volume of mixed liquor ($Y_r$) and the volume of wastewater ($Y_w$) in the first reactor

Experimental verification of the theoretical model developed in sections (3.1.2) and (3.1.3) was accomplished by using the following method:

The reactor was filled with tap water and 1.5 g of water-soluble Quinoline-Yellow (QY) 95%, (Fisher Scientific) used as the tracer, was dissolved in the entire volume of the reactor. The resulting solution defined the initial volume of mixed liquor ($Y_i$) that is equal to the overall volume of the reactor ($V_R$). Following the mixing of solution for half an hour, samples were taken from different zones of the reactor and the concentration of QY in each sample was measured using a spectrometer (HACH-Model DR2800) in order to ensure the homogeneity of the solution inside the reactor. The initial concentration of QY was considered as $C_{max}$. Aeration through the diffusers located at the bottom of aerobic zone started while tap water at a constant flow rate ($Q_i$) started to be added to the system from the top of aerobic zone. Since the system was operating at steady state with no liquid accumulation inside the reactor, liquid at a flow rate equal to that of water, should continuously leave the reactor ($Q_e$). Samples were collected every 15 minutes from the reactor's exit. The optical density of samples was estimated by spectrometric methods using the spectrophotometer. The relative concentration of each sample ($C/C_{max}$) was determined and was multiplied by 100 in order to estimate the time-dependent changes in the percentage of mixed liquor inside the reactor ($Y_r$). The sampling measurements continued until the percentage of mixed liquor inside the

reactor approached zero, implying that the entire volume of mixed liquor inside the reactor was gradually replaced by the added water ($Y_w$). In fact, the initial QY solution prepared at the beginning of the test resembled the initial volume of mixed liquor ($Y_i$) and the continuous flow rate of tap water to the top of the aerobic zone was considered as the influent flow rate of wastewater as explained in section 3.1.2.

The experiments were performed at various operating conditions in order to evaluate the effect of different air flow rates and different influent water flow rates on liquid displacement in the first reactor. The experiments were carried out at four different influent water flow rates ($Q_i$) of 500, 720, 1000 and 1450 L/d and three air flow rates of 15, 30 and 45 L/min, making a total of 12 experiments. Results are presented in section 5.6. All experiments were carried out using the openings of 1" size between the riser and downcomer.

## 4.3 Design and development of the monitoring and control system

A monitoring and control system was developed for the measurement and control of the pertinent operating and process parameters including dissolve oxygen (DO) concentration in the aerobic zone, oxidation-reduction potential (ORP) in the microaerophilic and anoxic zones, and air flow rate in the aerobic zone. The required dissolved oxygen concentration in the aerobic zone is in the range of 2 to 4 mg/L. This

parameter is controlled by a DO probe (Cole Parmer, 0-20 pp, 10') connected to a DO controller/transmitter (EUTECH INSTRUMENT-Model alpha, DO2000 W), a shut-off valve (ASCO-Red Hat, 3/8") and a gas flow meter (AALBORG- Model GFM 47, 0-100 Std L/min ) as presented in Figure 14.

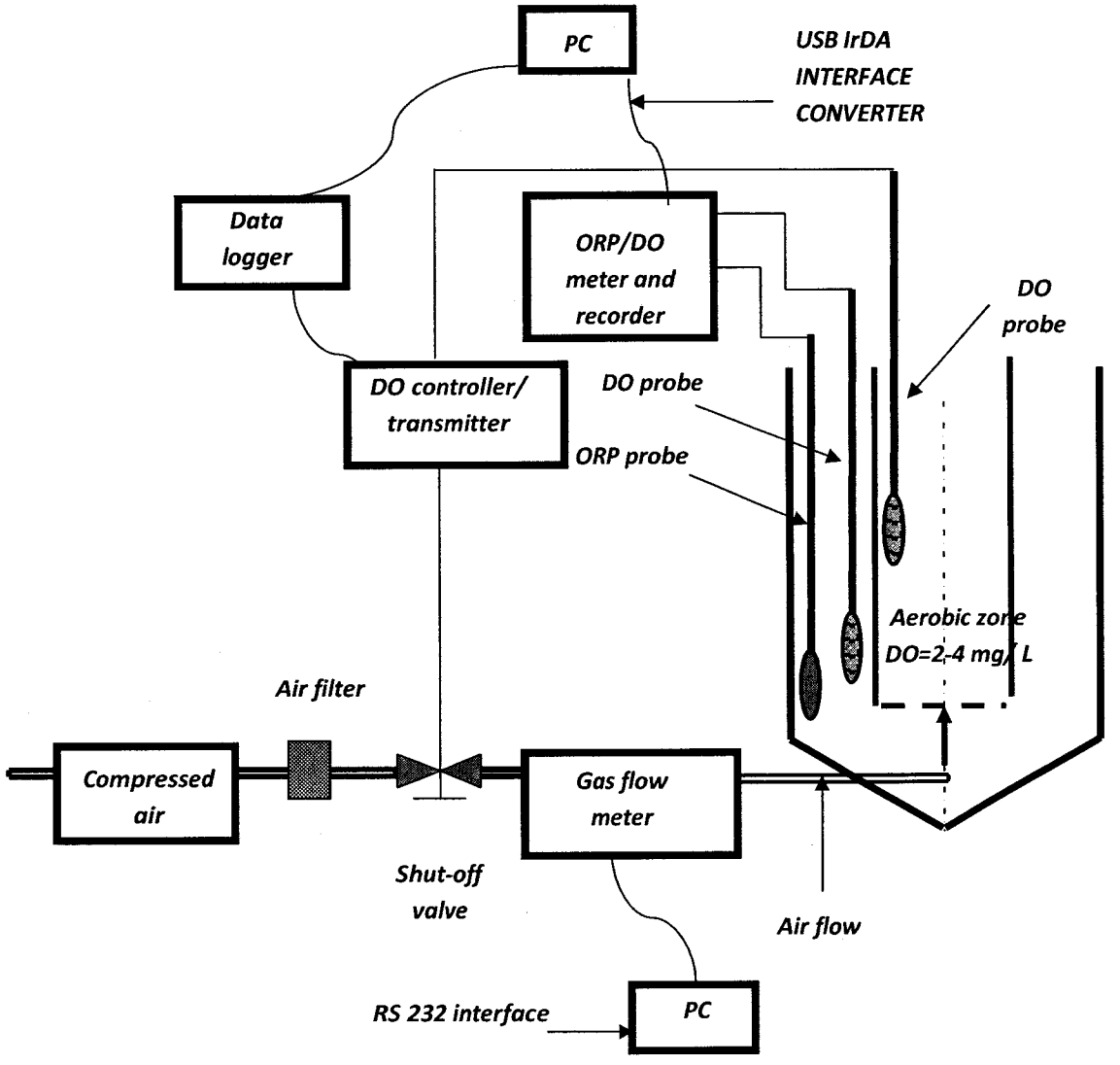


Figure 14: Flow chart diagram of the control loop around the first reactor

The DO controller/transmitter has two set points corresponding to the minimum and maximum DO concentrations required. The DO probe transmits electronic signals corresponding to the DO concentration in the liquid to the DO controller/transmitter. The controller will send appropriate signals to the shut-off valve for adjusting the amount of air that needs to be transferred to the aerobic zone. The electronic signals will also be transmitted from the DO controller/transmitter to a data logger and acquisition system (Dickson-Model ES120) connected to a computer. Variations of air flow rate were monitored by transmitting the data from the gas flow meter to the computer using the RS 232 interface cable.

The dissolved oxygen (DO) concentration and redox potential (ORP) can also be monitored inside the microaerophilic and anoxic zones using the DO probe (Cole Parmer-10' cable) and ORP electrode (Cole Parmer, Submersible) connected to the pH/ORP meter (Oakton-Model PD650).

## 4.4 Zone generation

The aerobic, microaerophilic, anoxic and anaerobic zones of the treatment system are defined by the different dissolved oxygen (DO) concentrations and oxidation-reduction or redox potential (ORP) in these zones.

In order to create different environmental conditions of aerobic, microaerophilic, and anoxic inside the first reactor of the treatment system based on DO concentration (table

1), the reactor was initially filled with tap water. An adequate amount of anhydrous sodium sulfite (100 g for the entire volume of the reactor) was added to the rector's content and mixed thoroughly. The solution remained for almost 2 hours until sodium sulfite completely consumed the dissolved oxygen in the reactor. Aeration started from the bottom of aerobic zone. The DO concentration and redox potential in the aerobic, microaerophilic, and anoxic zones were monitored during the entire duration of the test under all different conditions using appropriate probes and electrodes connected to recorders. The inlet air flow rate varied in the range of 15 to 50 L/min. Also, different sizes of the apertures in the range of ½" to 1" were examined in order to establish the required level of dissolved oxygen concentration in each zone. The right combination of the inlet air flow rate, determined by the gas flow meter, and the number and size of apertures between the aerobic and microaerophilic zones were determined for the establishment of required environmental conditions for the creation of different biological zones. The redox potential in the aerobic zone is not controlled and it is a strong function of the dissolved oxygen (DO) concentration. The results of this experiment are presented in section 5.7.

# CHAPTER 5: RESULTS AND DISCUSSION

## 5.1 Gas hold up

### 5.1.1 Overall gas hold up

The overall gas hold up in the treatment system was estimated by using the volume expansion method explained in section 4.2.1. The unaerated liquid height in the reactor was estimated to be 0.82m and the liquid height in the presence of air flow rate in the range of 10 to 70 L/min was measured and the value of $h_{dis}$ was calculated. The ratio of cross sectional area of downcomer to riser was $A_d/A_r = 3.45$. This information along with

Equation (4.3), was used to estimate the overall gas hold up for different air flow rates in the range of 10 to 70 L/min and two different sizes of openings, i.e. 1" and ½" as presented in Table 2:

Table 2. Overall gas hold ups for air flow rates in the range of 10 to70 L/min

| $Q_{air}$ (L/min) | $U_G$ (m/s) | Opening 1" | | Opening ½" | |
|---|---|---|---|---|---|
| | | $h_{dis}$ (cm) | ε | $h_{dis}$ (cm) | ε |
| 10 | 0.008 | 1 | 0.00274 | 1.5 | 0.0041 |
| 20 | 0.015 | 3 | 0.00817 | 3.5 | 0.0095 |
| 30 | 0.023 | 5 | 0.01355 | 5.5 | 0.0149 |
| 40 | 0.030 | 6 | 0.01621 | 8 | 0.0215 |
| 50 | 0.038 | 7 | 0.01886 | 10 | 0.0267 |
| 60 | 0.045 | 8 | 0.0215 | 12 | 0.0319 |
| 70 | 0.053 | 9 | 0.02412 | 13 | 0.0345 |

A typical correlation between gas hold up and superficial gas velocity can be written as:

$$\varepsilon = \alpha U_G^{\beta} \qquad (5.1)$$

Where $\alpha$ is a function of geometrical dimensions of the reactor, especially the ratio of downcomer to riser cross sectional area, and liquid phase properties of the system, while the coefficient $\beta$ is more dependent on the flow regime (Chisti and Moo-Young 1988b, Chisti 1989, Garcia et al. 2000, Jin et al. 2006).

The variations in the overall gas hold up with the change of superficial gas velocity for the opening sizes of 1"and ½" between the riser and downcomer are plotted in Figure 15.

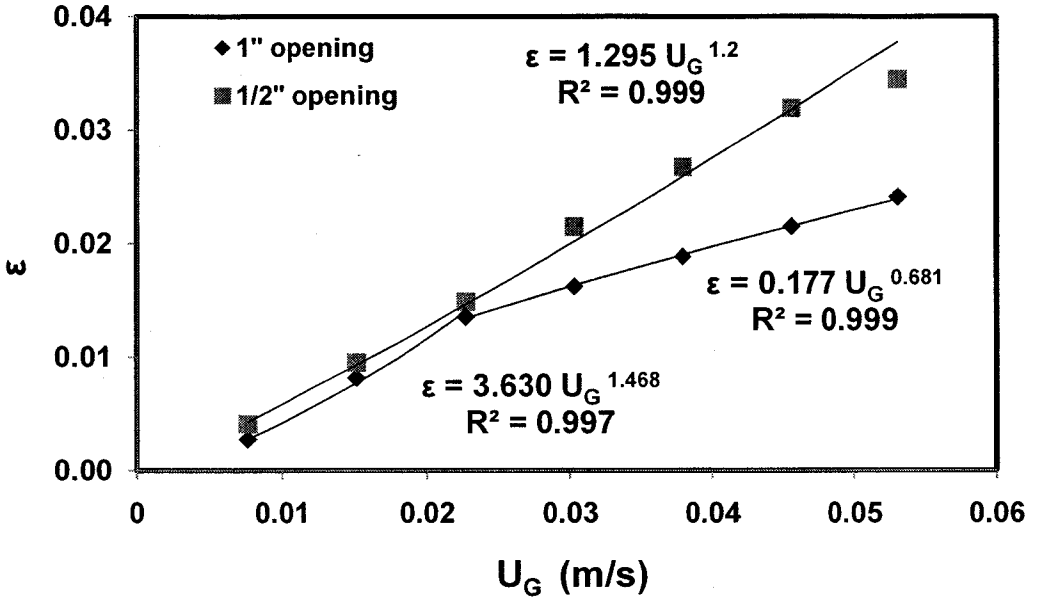


Figure 15. Gas hold up profile vs. superficial gas velocity

It can be observed that for both sizes of openings, the gas hold up increases with the increase of superficial gas velocity. However, for opening size of 1" the initial rapid increase of gas hold up is followed by a gradual increase when it approaches the superficial gas velocity of 0.023 m/s. This can be due to the bubble coalescence originating from higher bubble collision frequency at greater air flow rates (Chisti and Moo-Young 1988c, Jin et al. 2005). The relationship between gas hold up and superficial gas velocity for the opening size of 1"exhibits two different trends. Based on Equation (5.1), the value of $\alpha$ and $\beta$ for superficial gas velocities ($U_G$) less than 0.023 m/s are equal

to 3.63 and 1.468, respectively, while these values reduce dramatically to 0.177 and 0.68 for superficial gas velocities above 0.023 m/s. This shows that the dependence of gas hold up on superficial gas velocity decreases for superficial gas velocities above 0.023 m/s.

### 5.1.2 Gas hold up in the riser (aerobic zone)

The inverted U-tube manometer technique was used to estimate the magnitude of gas hold up in the riser as explained in section 4.2.1. The results of gas hold up estimation in the riser using Equation (4.5) for two different opening sizes of 1" and ½"and air flow rates in the range of 10 to 70 L/min are presented in Table 3.

$\rho_L$ =1000 kg/m$^3$ , $\rho_G$ =1.2041 kg/ m$^3$

$$\frac{\rho_L}{\rho_L - \rho_G} = 1.0012 \qquad (5.2)$$

Table 3. Gas hold up in the riser for air flow rates of 10 to70 L/min

| $Q_{air}$ (L/min) | $U_G$(m/s) | Opening 1" | | Opening ½" | |
|---|---|---|---|---|---|
| | | $dh_M$(cm) | $\varepsilon_r$ | $dh_M$ (cm) | $\varepsilon_r$ |
| 10 | 0.008 | 1.3 | 0.024 | 1.8 | 0.033 |
| 20 | 0.015 | 2.2 | 0.041 | 2.5 | 0.046 |
| 30 | 0.023 | 3.2 | 0.059 | 4.1 | 0.076 |
| 40 | 0.03 | 4.1 | 0.076 | 5.7 | 0.106 |
| 50 | 0.038 | 4.9 | 0.091 | 6.1 | 0.113 |
| 60 | 0.045 | 5.7 | 0.106 | 7.1 | 0.132 |
| 70 | 0.053 | 6.2 | 0.115 | 8 | 0.148 |

The variations of gas hold up with superficial gas velocity in this zone are illustrated in Figure 16. The impact of microbial support, placed above the diffuser in the riser, on gas hold up is also shown in this figure.

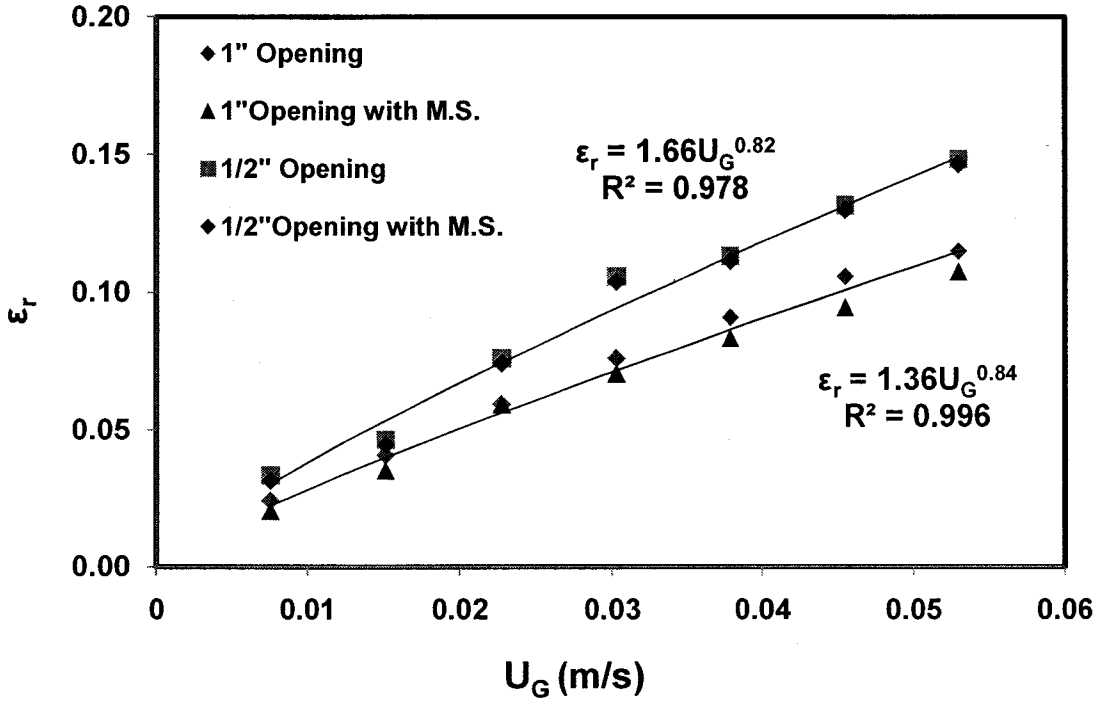


Figure 16. Gas Hold up variations in the riser ($\varepsilon_r$) as a function of superficial gas velocity ($U_G$)

M.S. = microbial support

Similar trends were observed for the variations of gas hold up in the riser with superficial gas velocity for both sizes of openings, as was observed for the overall gas hold up (Figure 15). Here again, gas hold up increases with the increasing air flow rate. However, in the riser, the same linear relationship was valid for the entire range of superficial gas velocities examined as illustrated in Figure 16.

### 5.1.3 Comparison with previous work

Figure 17 presents the comparison of experimental data obtained in the present work with the predictions using the empirical correlations in airlift reactors reported in the literature (Chisti 1989, Bello et al. 1985a, Hill 1976). The correlations are presented in Table 4.

Table 4. Empirical correlations for gas holdup

| Author | Correlation |
|---|---|
| Chisti 1989 | $\varepsilon = 0.65(1 + A_d / A_r)^{-0.258} U_G^{\ 0.0603}$ |
| Bello et al. 1985a | $\varepsilon = 0.16(1 + A_d / A_r)(U_G / U_{Lr})^{0.57}$ |
| Hills 1976 | $\varepsilon = \frac{U_G}{(0.243 + 1.35(U_G + U_{Lr})^{0.93})}$ |

As observed in Figure 17, the correlations proposed by Chisti (1989) and Bello et al. (1985a) overestimated the gas hold up in comparison with the values estimated in this work, while the relationship proposed by Hill (1976) produced an excellent agreement at low air flow rates while slightly underestimating the gas hold up with the increase of air flow rate. Moreover, using the relationships proposed by Chisti (1989) and Bello et al. (1985a) resulted in a slight increase in gas hold up in the range of superficial gas velocities examined in this work. The correlation reported by Hills (1976) considered a strong dependence of gas hold up on the superficial gas velocity without incorporating the geometrical properties such as $A_d/A_r$.

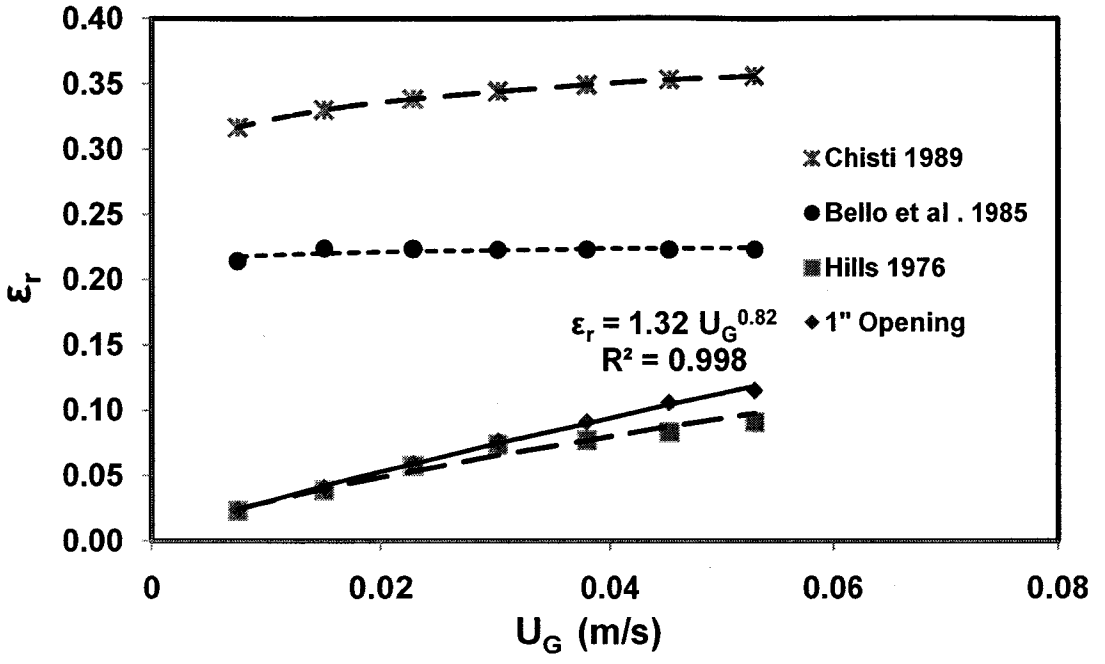


Figure 17. Correlations of gas hold up in the riser ($\varepsilon_r$) as a function of superficial gas velocity in comparison with some correlations from the literature

## 5.2 Mean circulation time ($t_C$ ) and liquid circulation velocity ($U_{LC}$)

The acid tracer response technique, explained in section 4.2.2, was used to measure the mean circulation time and liquid circulation velocity in the system. Figure 18 displays the variations of mean circulation time with superficial gas velocity for both sizes of openings of 1"and ½" between the riser and downcomer. The obtained values from the two calculation methods used, i.e. the distance between the peaks and the first moment analysis have been compared in Figure 18. It can be seen that an excellent agreement between the two methods of calculation was obtained. These values are also presented in Table 5.

Table 5. Mean circulation time for air flow rates of 10 to70 L/min

| $U_G$ (m/s) | Opening 1" | | Opening ½" | |
|---|---|---|---|---|
| | $t_C$ (Peak) (s) | $t_C$ (first moment ) (s) | $t_C$ (Peak) (s) | $t_C$ (first moment ) (s) |
| 0.008 | 66 | 67.3 | 186 | 184.1 |
| 0.015 | 54 | 51.4 | 139.5 | 139.9 |
| 0.023 | 33 | 32.7 | 124.5 | 126.2 |
| 0.03 | 31.5 | 30.6 | 111 | 109.1 |
| 0.038 | 28.2 | 28.5 | 97.5 | 99.7 |
| 0.045 | 25.5 | 27.9 | 84 | 84.8 |
| 0.053 | 25.5 | 26.4 | 82.5 | 80.2 |

Figure 18 shows that the mean circulation time is higher for the smaller size of openings since under this condition liquid circulates more slowly in the reactor because of flow restrictions. This figure also shows that although the mean circulation time ($t_C$) decreased with the increase of superficial gas velocity for both sizes of openings, it exhibited a stronger dependence on the superficial gas velocity ($U_G$) for smaller openings (1/2 "). For larger opening size of 1", the mean circulation time ($t_C$) is almost independent of $U_G$ at $U_G$>0.023 m/s. The correlation between the mean circulation time ($t_C$) and superficial gas velocity ($U_G$) for both sizes of openings are as follows:

$t_C = 24.57 \times U_G^{-0.42}$ Opening ½" (5. 3)

$t_C = 5.69 \times U_G^{-0.5}$ Opening 1" (5. 4)

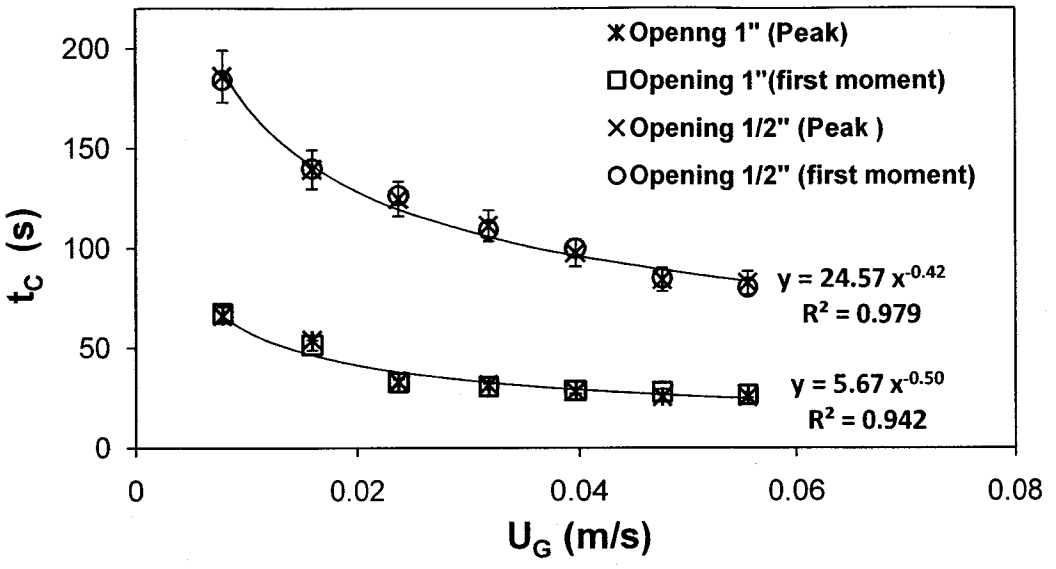


Figure 18. Circulation time of liquid ($t_C$) as a function of superficial gas velocity ($U_G$) estimated by two different techniques

The mean liquid circulation velocity ($U_{LC}$) can be calculated from the estimated values of mean circulation time ($t_C$) and circulation path ($x_C$) by using Equation (2.5). The impact of superficial gas velocity, $U_G$, on mean liquid circulation velocity, $U_{LC}$, as a function of opening sizes between the riser and downcomer is shown in Figure 19.

For the opening size of 1", a rapid increase of liquid circulation velocity at low air flow rates was followed by a smooth increase at relatively higher air flow rates. This trend is consistent with the changes of overall gas hold up with superficial gas velocity for opening size of 1"as presented in Figure 15. This means that at air flow rates less than 30 L/min corresponding to superficial gas velocity ($U_G$) less than 0.023 m/s, the increase of superficial gas velocity increases the gas hold up in the riser as well as liquid circulation velocity in the entire reactor due to the greater difference in bulk density of

riser and downcomer. However at relatively higher air flow rates above 30 L/min, corresponding to the superficial gas velocity ($U_G$) more than 0.023 m/s, the increasing effect of gas hold diminishes due to the restrictions on liquid flow caused by the presence of apertures (openings) between the riser and downcomer. Under this condition, the increased gas hold at higher air flow rates only creates a greater water head above the openings without having much effect on increasing the circulation velocity.

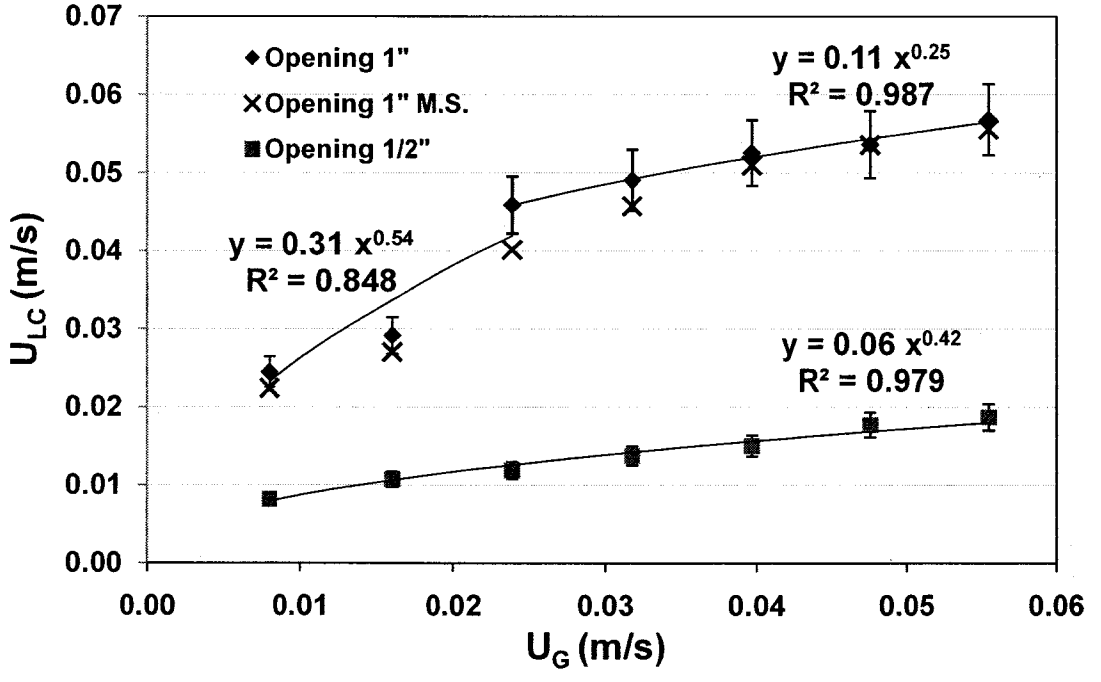


Figure 19. Effect of superficial gas velocity ($U_G$) on the mean liquid circulation velocity ($\bar{U}_{LC}$) as a function of opening size between the riser and downcomer, M.S. = microbial support

Similar trends for the variation of liquid circulation velocity with superficial gas velocity were previously observed by other investigators (Weiland 1984, Choi and Lee 1993,

Merchuk et al. 1996). The smooth increase of $V_L$ with the superficial gas velocity at higher air flow rates was explained by Merchuk et al. (1996) as follows: Initially, the increasing rate of gas hold up in the riser ($\varepsilon_r$) with the increase of superficial gas velocity is greater than that in the downcomer ($\varepsilon_d$) which leads to a rapid increase in liquid circulation velocity. With continued aeration, the increase of superficial gas velocity, due to the recirculation and bubble entrainment in downcomer, leads to higher values of gas hold up in downcomer. Consequently, gas hold up differences in the riser and downcomer, which is the driving force for liquid circulation, decreases and cancels the increasing effect of superficial gas velocity. As a result, the variations in liquid circulation velocity are relatively smooth at higher air flow rates. However, this reasoning does not apply to the system examined in this study because of different design for the passage of the liquid flow from the riser to downcomer; in the examined experimental system, gas hold up in the downcomer under any condition is negligible ($\varepsilon_d \sim 0$), therefore with increasing the superficial gas velocity that leads to the increase of gas hold up in the riser ($\varepsilon_r$), the difference between bulk density of riser and downcomer increases. This increase is expected to induce a higher liquid circulation velocity; however, due to the existence of openings between the riser and downcomer, the large difference in the gas hold up of riser and downcomer does not lead to higher liquid circulation velocities in the system.

Additionally, Figure 19 demonstrates the impact of microbial support on liquid circulation velocity for different air flow rates for the opening sizes of 1". Microbial

support causes a slight decrease in liquid circulation velocities at superficial gas velocities ($U_G$) less than 0.04 m/s while at superficial gas velocities above 0.04 m/s, the flow regime inside the riser is turbulent and the impact of microbial support is negligible.

As presented in Figure 19, the mean liquid circulation velocity ($U_{LC}$) increases constantly with the increase of superficial gas velocity ($U_G$) for the opening size of ½" and exhibits a lower rate compared to the larger opening size of 1 ". The magnitude of mean liquid circulation velocities ($U_{LC}$) for the opening size of ½" is also smaller. This is directly related to higher mean circulation times ($t_C$) for the opening ½" as observed in Figure 18.

## 5.3 Linear liquid velocity in the downcomer and riser

The linear liquid velocity in the riser and downcomer were estimated independently using the acid tracer response technique and the first moment equation as explained in section 4.2.3. The estimated values of linear liquid velocities in the riser and downcomer as a function of superficial gas velocity using the opening sizes of 1" between the riser and downcomer are presented in Figure 20.

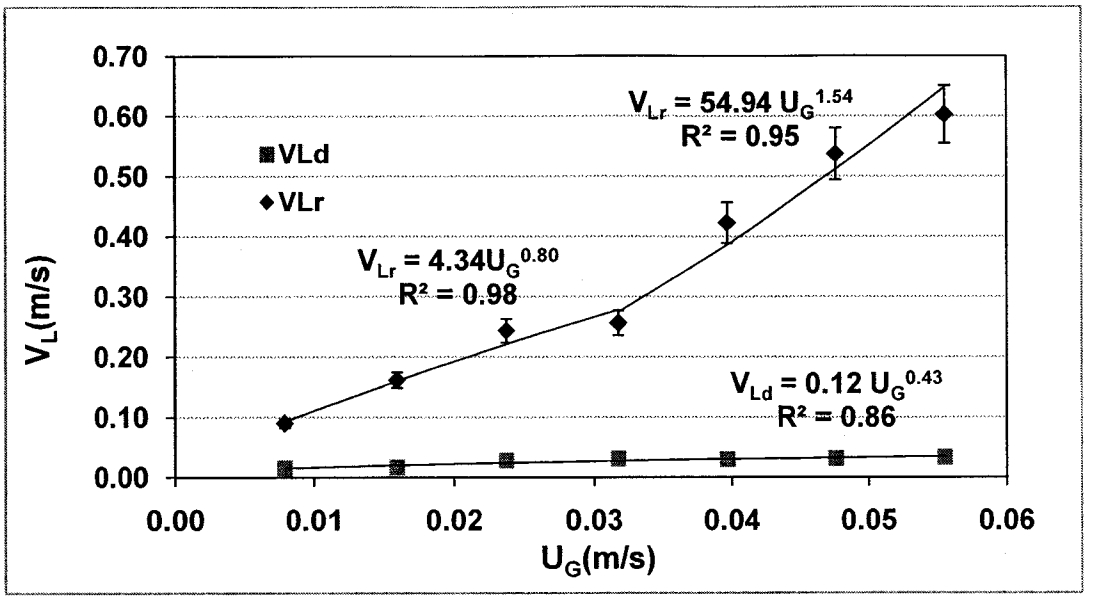


Figure 20. Linear liquid velocity in the riser and downcomer as a function of superficial gas velocity ($U_G$) using openings with the size of 1" (m/s)

In the downcomer, the liquid velocity ($V_{Ld}$) showed a small increase with the increase of air flow rate. It eventually leveled off and reached a stable value of about 0.03 m/s at superficial gas velocities > 0.032 (m/s). However, in the riser, liquid velocity ($V_{Lr}$) increased gradually with the increase of superficial gas velocity ($U_G$) and showed a strong dependence on $U_G$ at higher air flow rates ($U_G$>0.032m/s). This dependence was shown in Equation (3.32). In this equation the liquid velocity in the riser ($V_{2W}$) is proportional to the exponent 3/2 of the air flow rate. This dependence causes the liquid velocity in the riser to dramatically increase at higher air flow rates.

However, in the examined system, higher liquid velocities in the riser did not lead to higher liquid velocities in the downcomer. Since the passage of liquid flow from the riser to downcomer is controlled by the area of eight openings and there is a maximum

circulation flow that can pass through the openings regardless of the magnitude of air flow rate, the increase of air flow rate at superficial gas velocities>0.032 (m/s) simply caused a water head above the openings in the riser.

### 5.3.1 Analytical estimation of linear liquid velocity in the downcomer

The values of liner liquid velocity in the downcomer ($V_{Ld}$) can also be calculated analytically by using Equation (3.24) and by dividing the volumetric flow rate of liquid circulation ($Q_{cir}$) by the downcomer cross sectional area ($A_d$). The theoretical values of linear liquid velocity in downcomer are tabulated in Table 6.

Table 6. Analytical estimation of liquid velocity in downcomer for air flow rates of 10 to70 L/min

| $Q_{air}$ (L/min) | $U_G$ (m/s) | Opening 1" | | Opening ½" | |
|---|---|---|---|---|---|
| | | $Q_{cir}$ (L/min) | $V_{Ld}$ (m/s) | $Q_{cir}$ (L/min) | $V_{Ld}$ (m/s) |
| 10 | 0.008 | 62 | 0.0137 | 17.5 | 0.0039 |
| 20 | 0.015 | 83 | 0.0183 | 27 | 0.0060 |
| 30 | 0.023 | 108 | 0.0238 | 32 | 0.0071 |
| 40 | 0.03 | 128 | 0.0283 | 37 | 0.0082 |
| 50 | 0.038 | 142 | 0.0313 | 41 | 0.0091 |
| 60 | 0.045 | 156 | 0.0344 | 45 | 0.0099 |
| 70 | 0.053 | 163 | 0.0360 | 49 | 0.0108 |

Figure 21 shows the comparison between the analytical and experimental values of linear liquid velocity in the downcomer for two sizes of the openings between the riser and downcomer.

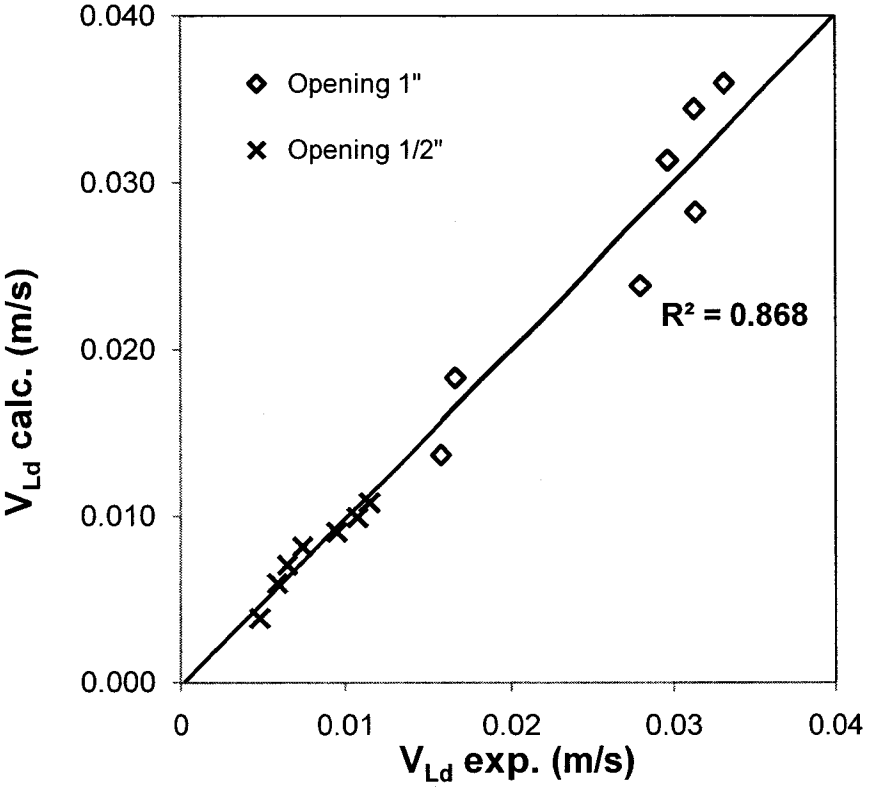


Figure 21. Comparison of experimental and analytical values of linear liquid velocity in downcomer

A good agreement was observed between the experimental and the calculated liquid velocity in the downcomer. In the analytical calculation, an empirical value was used for the volumetric liquid circulation flow rate ($Q_{cir}$).

### 5.3.2 Analytical estimation of linear liquid velocity in the riser

The analytical values of linear liquid velocities in the riser ($V_{Lr}$) were calculated by using Equation (3.32). This equation was modified by substituting the values of total surface area of three air diffuser's holes ($A_2$) and the surface area of inlet air pipe ($A_1$), and using water and air physical properties as follows:

$$V_{Lr} = V_{2W} = \left[ 0.0361 \frac{P}{T} \frac{Q_{air}^{\ 3}}{Q_{cir}} + V_{1w}^{\ 2} \right]^{0.5} \qquad (5.5)$$

The velocity of liquid just before the diffusers ($V_{1w}$) can be obtained using Equation (3.29). The values of linear liquid velocity in the riser ($V_{Lr}$), which are equal to the values of liquid velocity just after the diffusers inside the aerobic zone ($V_{2w}$) are presented in Table 7.

Table 7. Analytical values of liquid velocity just before and after the diffusers in the riser for the openings of 1"and air flow rates of 10 to70 L/min

| $Q_{air}$ (L/min) | $Q_{cir}$ (L/min) | $V_{1w}$ (m/s) | $P$ (atm) | $T$ (K) | $V_{2w}$ (m/s) |
|---|---|---|---|---|---|
| 10 | 62 | 0.047 | 1.1 | 293 | 0.066 |
| 20 | 83 | 0.063 | 1.2 | 293 | 0.135 |
| 30 | 108 | 0.082 | 1.3 | 293 | 0.216 |
| 40 | 128 | 0.097 | 1.4 | 293 | 0.309 |
| 50 | 142 | 0.108 | 1.5 | 293 | 0.417 |
| 60 | 156 | 0.118 | 1.6 | 293 | 0.536 |
| 70 | 163 | 0.123 | 1.7 | 293 | 0.675 |

Figure 22 presents the close agreement between the analytical values of linear liquid velocity in the riser ($V_{Lr}$) and the experimental data.

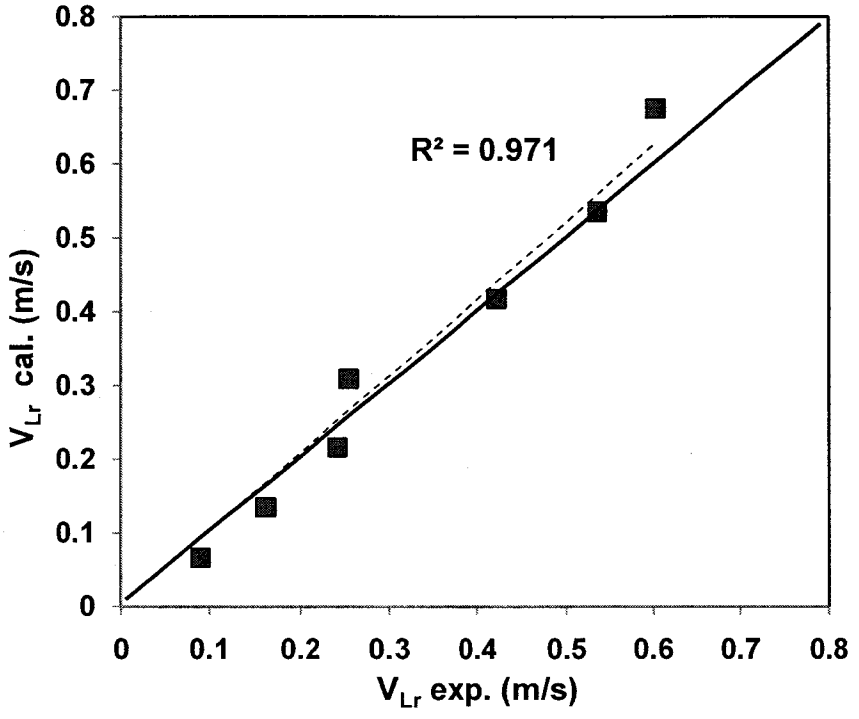


Figure 22. Comparison of experimental and analytical values of the linear liquid velocity in the riser

### 5.3.3 Comparison with previous work

The agreement between the experimentally-measured linear liquid velocity in the riser ($V_{Lr}$) and the empirical correlations suggested by Bello et al. (1984), and Chisti et al. (1988a) (Table 8) was examined.

Table 8. Empirical correlations for liquid velocity in the riser

| Author | Correlation | |
|---|---|---|
| Bello et al. 1984 | $V_{Lr} = 0.66 \left(\frac{A_d}{A_r}\right)^{0.78} U_G^{\frac{1}{3}}$ | (2.10) |
| Chisti et al. 1988a | $U_{Lr} = \left[\frac{2gh_D(\varepsilon_r - \varepsilon_d)}{K_B\left(\frac{A_r}{A_d}\right)^2 \frac{1}{(1-\varepsilon_d)^2}}\right]^{0.5}$ | (2.11) |

Equation (2.11) proposed by Chisti et al. (1988a) for all different types of internal airlift reactors can be simplified to Equation (5.6) for the current system since gas hold up in the downcomer is almost zero ($\varepsilon_d$~0):

$$U_{Lr} = \left[\frac{2 \cdot g \cdot h_D \cdot \varepsilon_r}{K_B\left(\frac{A_r}{A_d}\right)^2}\right]^{0.5} \qquad (5.6)$$

As shown in Figure 23, there is an excellent agreement between the experimental values and theoretical predictions using the equations developed for the examined system. However, the predictions by Bello et al. (1984) (Equation 2.10), are considerably higher than those obtained in this work, especially at lower air flow rates, while the model developed by Chisti et al. (1988a) (Equation 2.11) predicted lower values of liquid velocities. The experimental results of this work presented a better agreement at lower air flow rates with the correlation developed by Chisti et al. (1988a) compared to that

developed by Bello et al. (1984). This is due to the fact that the relationship developed by Bello et al. (1984) is primarily based on geometrical and operational parameters whereas hydrodynamic characteristics were also incorporated in the relationship developed by Chisti et al. (1988a).

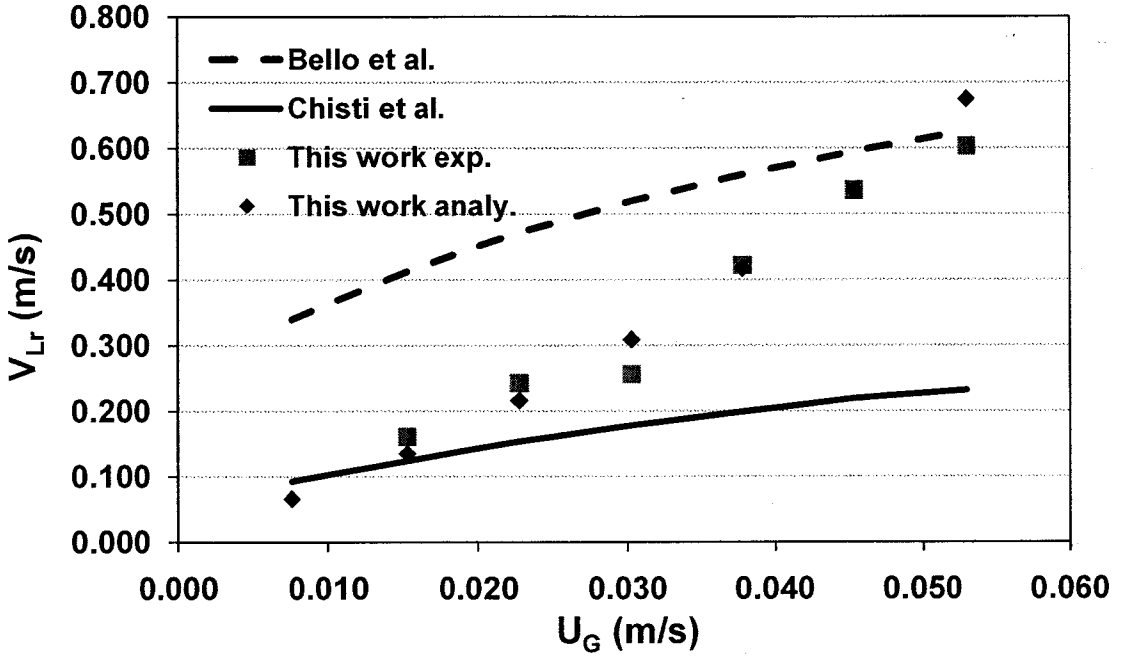


Figure 23. Comparison of experimental and analytical values of linear liquid velocity in the riser and the predictions by Bello et al. (1984) and Chisti et al. (1988a).

The lack of agreement between the experimental results of the present study and the literature-predicted values is due to the differences between the design and operations strategies of reactors employed in these studies. The reactor examined in this study contains apertures between the riser and downcomer that exert resistance on the movement of flow and circulation of liquid between the zones.

## 5.4 Overall volumetric mass transfer coefficient ($k_La_L$)

The overall volumetric oxygen transfer coefficient ($k_La_L$) was estimated using modified sulfite method explained in section 4.2.4. The values of $k_La_L$ for five different air flow rates in the range of 10 to 50 L/min and for two different opening sizes of 1" and ½" between the riser and downcomer were obtained and results are presented in Figure 24. $k_La_L$ varied in the range of 0.0015 1/s to 0.0140 1/s as the superficial gas velocity increased from 0.008 to 0.040 m/s. As demonstrated in Figure 24, $k_La_L$ increased with the increase of $U_G$ for both sizes of openings. However, the magnitude of $K_La_L$ is remarkably higher for the opening size of ½". This behavior is directly related to the higher values of gas hold for the opening size of ½" compared to the opening size of 1" as shown in Figure 15.

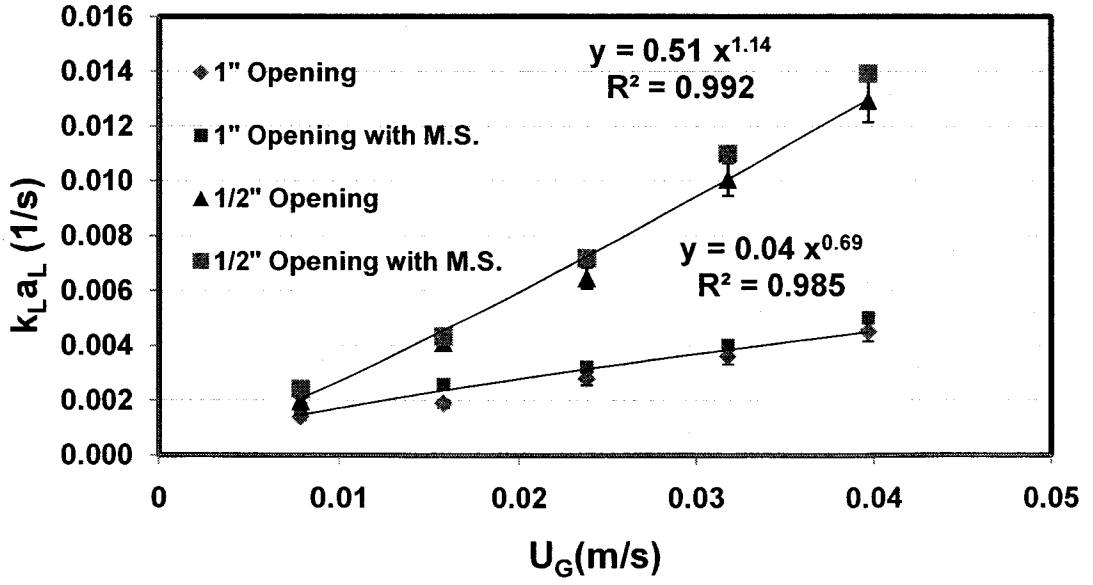


Figure 24. The dependence of overall volumetric mass transfer coefficient ($k_La_L$) on the superficial gas velocity ($U_G$), MS= Microbial Support

The use of smaller sizes of openings between the riser and downcomer exert resistance on the passage of liquid from the riser to downcomer, and consequently increases the mean residence time of the gas inside the riser, leading to higher values of volumetric mass transfer coefficient in the riser for the opening size of ½". Experiments for estimation of $k_La_L$ were repeated in the presence of microbial support and no remarkable changes were observed in the results, as presented in Figure 24.

### 5.4.1 Comparison with previous work

The experimental values of $K_La_L$ obtained in the present study using the opening size of 1" were compared with the correlations developed in the literature. The relationships suggested by Bello et al. (1985) and Chisti (1989), presented in Table 9, correlate the $k_La_L$ with the operating variable of superficial gas velocity ($U_G$) and the geometrical parameter of $A_d/A_r$ in airlift reactors.

Table 9. Empirical correlations for overall volumetric mass transfer coefficient

| Author | Correlation |
|---|---|
| Bello et al. 1985 | $K_La_L = 0.76U_G^{0.8}(1+\frac{A_d}{A_r})^{-2}$ |
| Chisti 1989 | $K_La_L = 0.349U_G^{0.837}(1+\frac{A_d}{A_r})^{-1}$ |

As exhibited in Figure 25, the experimental data obtained in this work was close to the values estimated by Chisti (1989) correlation.

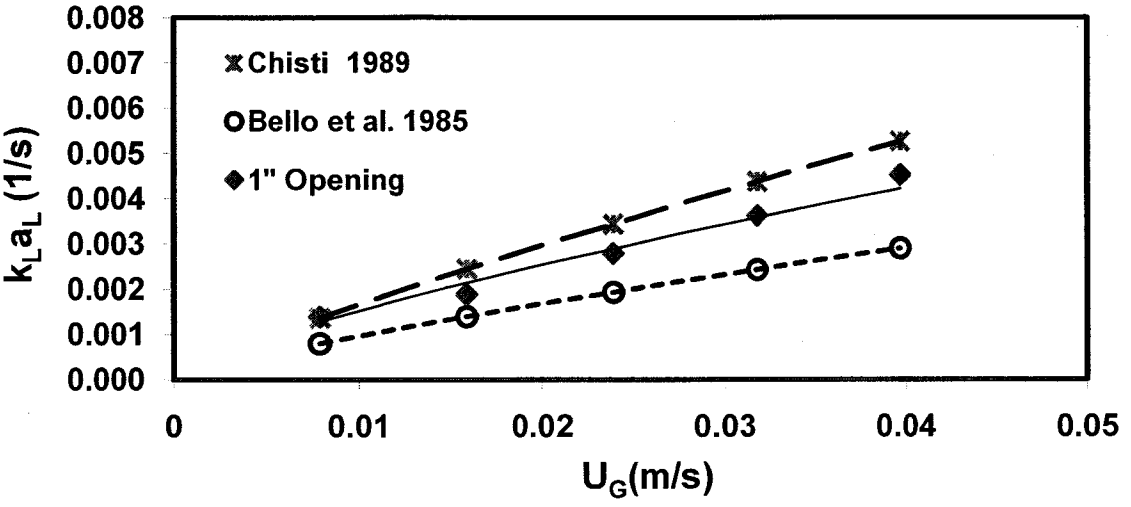


Figure 25. Comparison of experimental values of the overall volumetric mass transfer coefficient and the predictions by Bello et al. (1985) and Chisti (1989)

### 5.4.2 Relationship between volumetric mass transfer coefficient and gas hold up

The relationship between $k_La_L$ and $\varepsilon$ has been studied by several investigators. It has been found that in airlift reactors the volumetric mass transfer coefficient is a strong function of gas hold up. Nicolella et al. (1998) found a linear correlation between $k_La_L$ and $\varepsilon$ while Jin et al. (2006) reported an exponential correlation between these two parameters.

Figure 26 presents the values of $k_La_L$ estimated in the present work as a function of $\varepsilon$ for two different opening sizes of 1" and ½". A linear relationship is obtained between $k_La_L$

and ε for the openings of 1", implying that the increase of superficial gas velocity ($U_G$) affects the gas hold up by increasing the total area of gas bubbles ($a_L$) while the mass transfer coefficient ($k_L$) remains constant. For the apertures with the size of ½", there is an exponential correlation between $k_La_L$ and ε, which means that increasing the superficial gas velocity ($U_G$) not only increases gas hold up which enhances the effective mass transfer interfacial area, but also increases the mass transfer coefficient ($k_L$). The latter possibly happens because of the increased turbulence of the flow regime that occurs inside the riser due to the existence of smaller size of openings between the riser and downcomer.

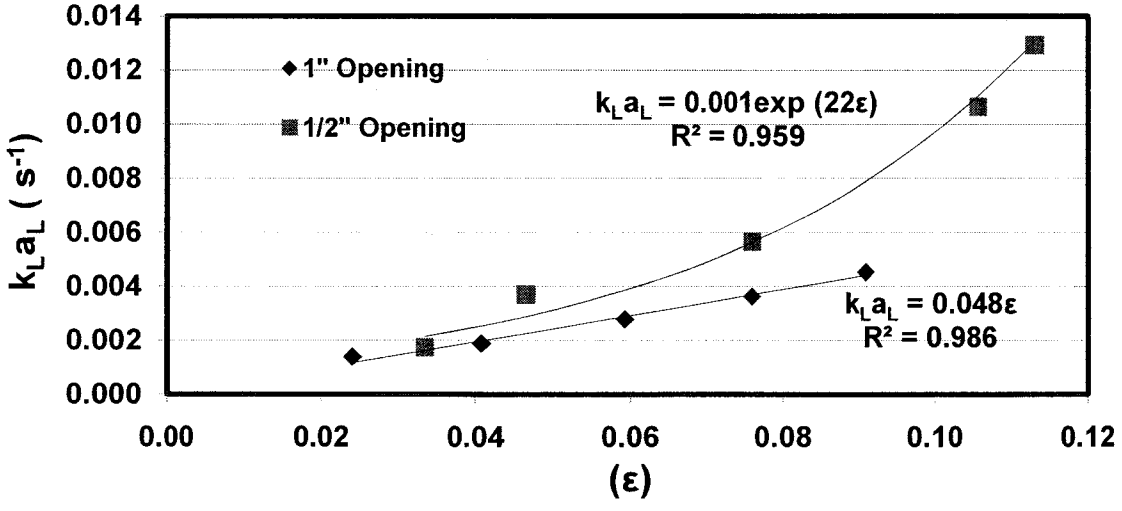


Figure 26. Overall volumetric mass transfer coefficient ($K_La_L$) as a function of gas hold up (ε) for two different sizes of the openings

### 5.4.3 Relationship between mass transfer coefficient ($k_L$) and bubble diameter ($d_B$)

The ratio of mass transfer coefficient to the bubble diameter, $k_L/d_B$, can be obtained by rearrangement of Equation (2.15) as follows:

$$\frac{k_L}{d_B} = k_L a_L \frac{(1-\varepsilon)}{6\varepsilon} \qquad (5.7)$$

Using the experimental values of $k_La_L$, $\varepsilon$, and Equation (5.7), the ratio of $k_L/d_B$ was calculated for two different opening sizes of 1"and ½".

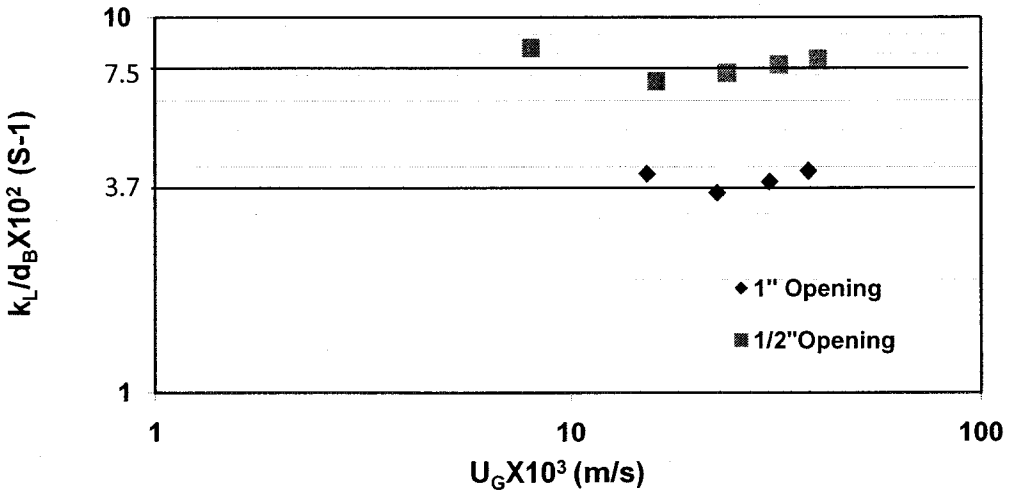


Figure 27. Mass transfer coefficient to bubble diameter ratio ($k_L/d_B$) as a function of superficial gas velocity ($U_G$) for two different sizes of openings between the riser and downcomer

The results presented in Figure 27 show that this ratio ($k_L/d_B$) remains constant for a given size of openings and it is independent of $U_G$. However, with the change of the

opening size between the riser and downcomer, this ratio changes and exhibits higher values for the smaller size of openings. Assuming equal sizes of bubbles under both experimental conditions, it can be concluded that the true mass transfer coefficient ($k_L$) increased for the smaller size of openings.

The relationship between $k_La_L$ and 6 $\varepsilon/(1-\varepsilon)$ (Figure 28) is almost linear for both sizes of openings, indicating that the $K_L/d_B$ ratio, which is the slope of the curves, was almost constant and equal to 0.037 ($R^2$=0.882) for the opening size of 1"and 0.075 ($R^2$=0.993) for the opening size of ½" which is consistent with the results obtained from Figure 27 for $K_L/d_B$ ratio.

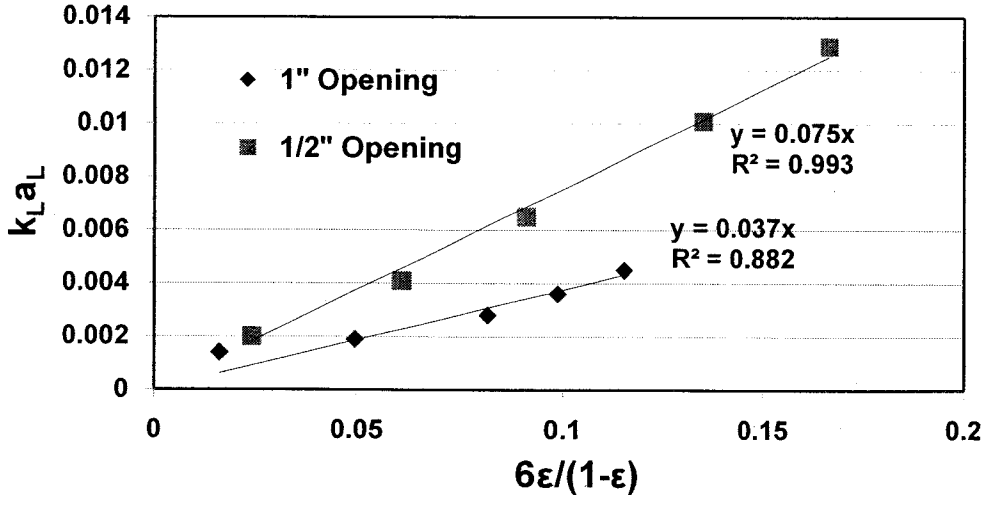


Figure 28.Correlation between measured overall volumetric mass transfer coefficient ($K_La_L$) and gas hold up ($\varepsilon$) values for two different sizes of openings

## 5.5 Residence time distribution

The residence time distribution in the first reactor of the examined system was evaluated by the pulse-input tracer technique as explained in section 4.2.5. Figure 29-31 illustrate the experimental values of residence time distribution of tracer QY inside the first reactor for three influent water flow rates of 720, 1030 and 1450 L/d, respectively. The impact of different air flow rates of 15, 30 and 45 L/min on each influent water flow rate was presented by different curves in Figures 29-31. All curves exhibit a sharp initial increase during the first few minutes followed by an exponential decrease, a behavior consistent with the RTD in completely mixed reactors. However, the curves slightly deviate from the trends in ideal mixed reactors where residence time distribution should increase abruptly at time zero and decrease exponentially in a very smooth manner. In the examined treatment system, residence time distribution exhibited a small delay at time zero in the initial increase in all experimental curves, as presented in Figure 29-31.

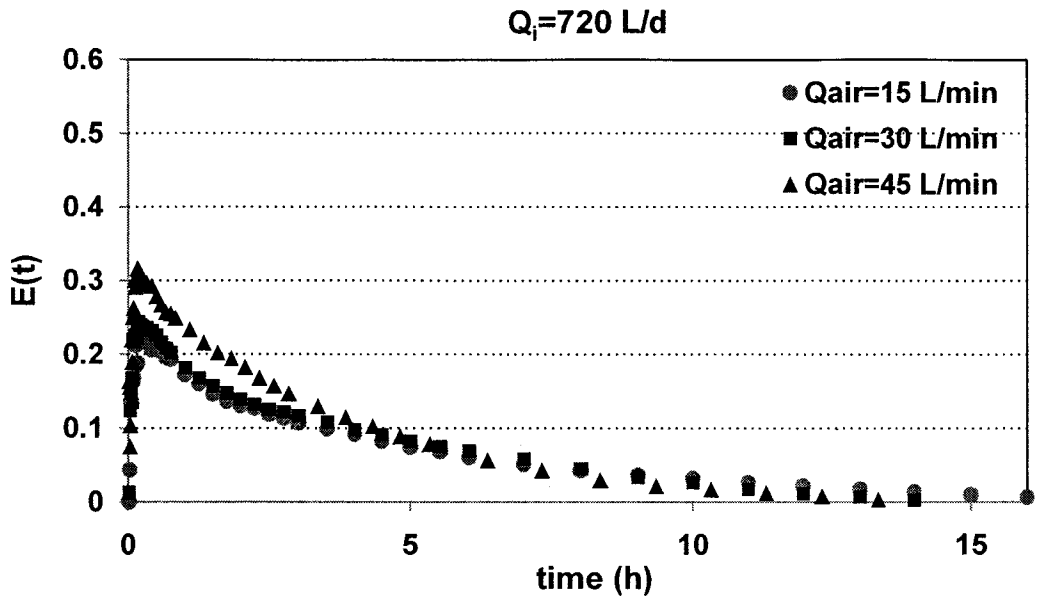


Figure 29. RTD measured in the first reactor at the influent flow rate $Q_i$=720 L/d at three air flow rates of 15, 30 and 45 L/min

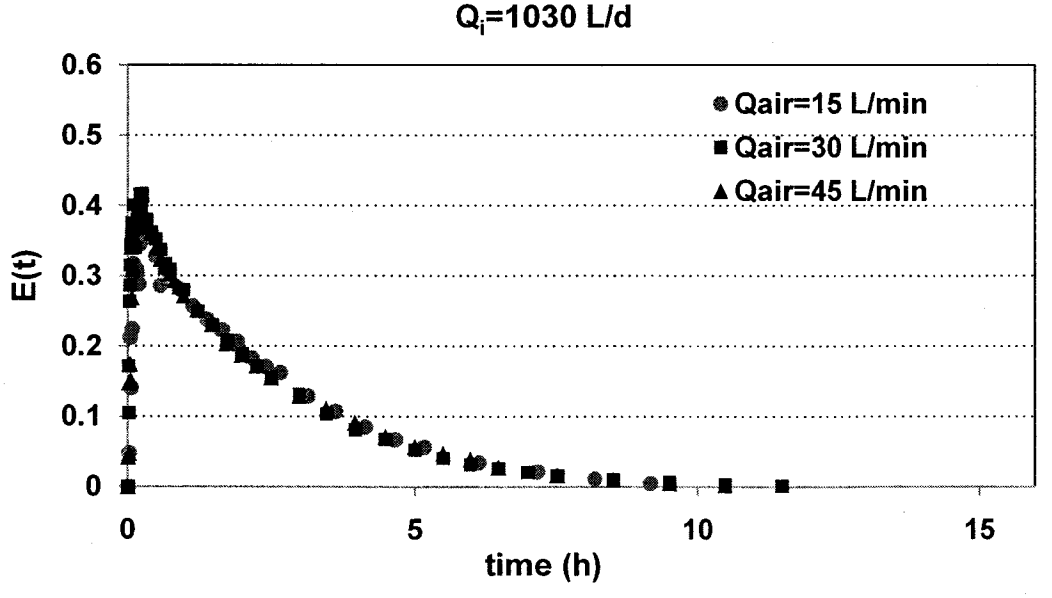


Figure 30. RTD measured in the first reactor at the influent flow rate $Q_i$=1030 L/d at three air flow rates of 15, 30 and 45 L/min

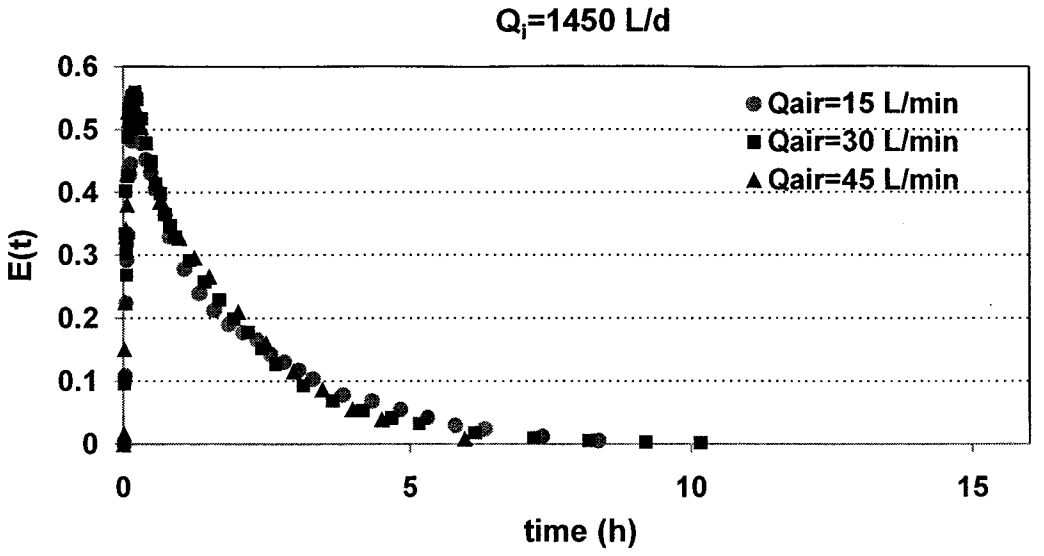


Figure 31. RTD measured in the first reactor at the influent flow rate $Q_i$=1450 L/d at three air flow rates of 15, 30 and 45 L/min

The above figures demonstrate that the effect of air flow rate on RTD for a given influent flow rate is negligible. Alternatively, Figure 32-34 illustrate the changes of RTD in the first reactor at three air flow rates of 15, 30 and 45 L/min, respectively. These figures emphasize the impact of influent flow rates of 720, 1030 and 1450 L/d on RTD at a constant air flow rate. Comparison of Figure 29-31 with Figure 32-34, shows that RTD variations are more sensitive to the influent flow rate compared to the air flow rate.

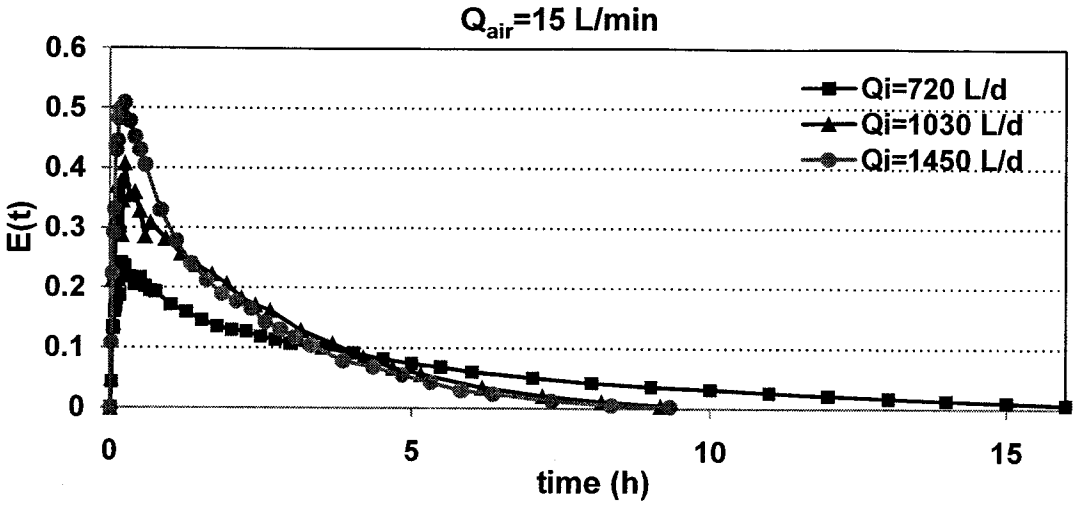


Figure 32. RTD measured in the first reactor at an air flow rate of $Q_{air}$=15 L/min as a function of different influent flow rates

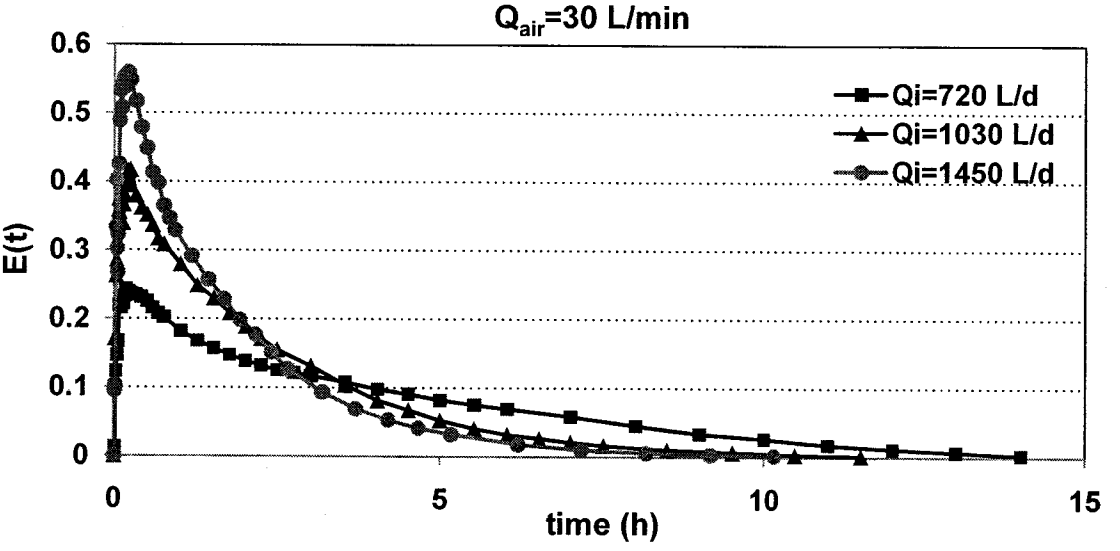


Figure 33. RTD measured in the first reactor at an air flow rate of $Q_{air}$=30 L/min as a function of different influent flow rates

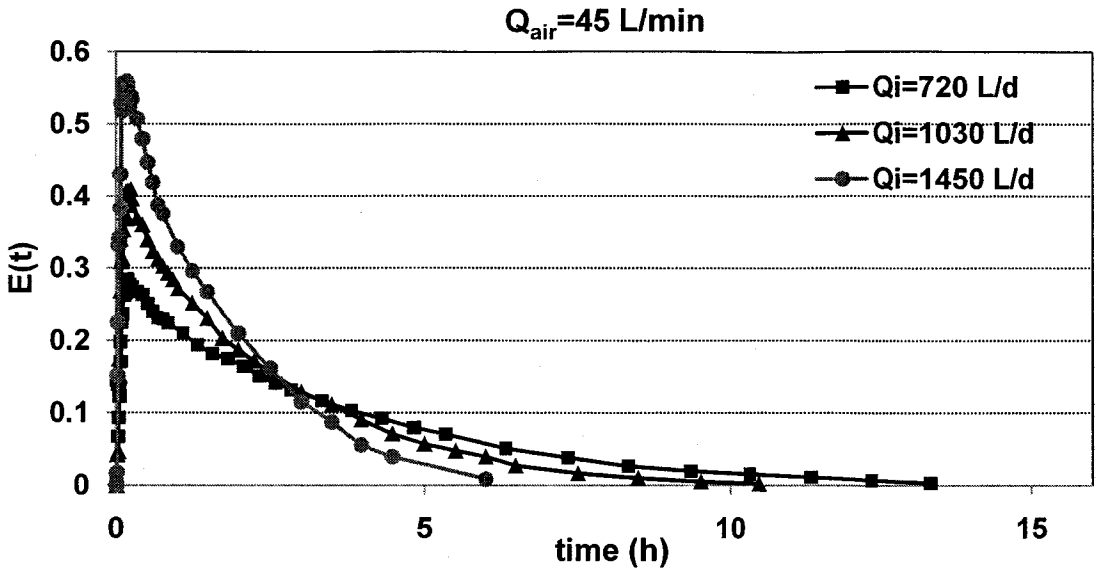


Figure 34. RTD measured in the first reactor at an air flow rate of $Q_{air}$=45 L/min as a function of different influent flow rates

The mean residence time of the tracer in the first reactor was calculated for different operating conditions using Equation (2.19) and the results are presented in Table 10. The overall HRT or space-time of the reactor can be calculated by dividing the volume of liquid inside the reactor by the influent flow rate using the following equation:

$$Overall\ HRT = \frac{V_{Li}}{Q_i} \qquad (5.\ 8)$$

Table 10. Experimental conditions for RTD measurements in the first reactor

| Influent flow rate $Q_i$ (L/d) | Air flow rate $Q_{air}$ (L/min) | Overall HRT=V/Q (h) | Mean residence time $t_m$(h) | $t_m$ /HRT |
|---|---|---|---|---|
| 720 | 15 | 3.52 | 4.52 | 1.29 |
| | 30 | 3.52 | 3.82 | 1.09 |
| | 45 | 3.52 | 3.26 | 0.93 |
| 1030 | 15 | 2.46 | 2.31 | 0.94 |
| | 30 | 2.46 | 2.26 | 0.92 |
| | 45 | 2.46 | 2.32 | 0.94 |
| 1450 | 15 | 1.75 | 1.99 | 1.14 |
| | 30 | 1.75 | 1.77 | 1.01 |
| | 45 | 1.75 | 1.58 | 0.90 |

The quotient of mean residence time ($t_m$) and the overall HRT, shown in Table 10, is plotted as a function of air flow rate for various influent flow rates of 720, 1030 and 1450 L/d (Figure 35). It can be seen that the mean residence time decreases with the increase of air flow rate and approaches unity, implying that mean residence time is almost equal to the overall HRT at higher air flow rates.

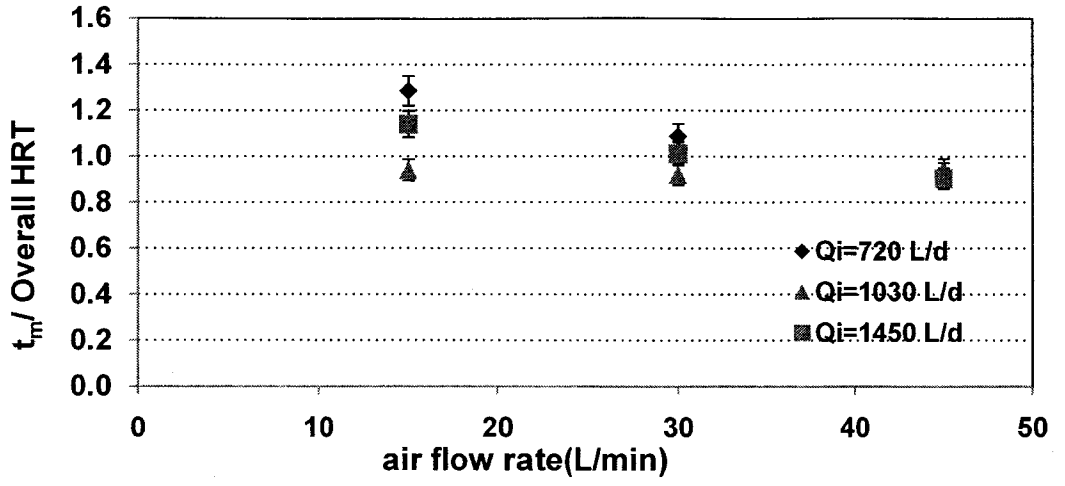


Figure 35. $t_m$/(Overall HRT) as a function of air flow rate at different influent flow rate

The values of variance ($\sigma^2_t$) and dimensionless variance ($\sigma^2$) were calculated using Equations (2.20) and (2.21) for various operating conditions and the results are presented in Table 11.

Table 11. Values of variance and dimensionless variance at different operating conditions

| Influent flow rate $Q_i$ (L/d) | Air flow rate $Q_{air}$ (L/min) | Variance ($\sigma^2_t$) ($h^2$) | Dimensionless variance ($\sigma^2$) |
|---|---|---|---|
| 720 | 15 | 14.85 | 0.73 |
| | 30 | 9.53 | 0.65 |
| | 45 | 6.49 | 0.61 |
| 1030 | 15 | 3.54 | 0.66 |
| | 30 | 4.14 | 0.81 |
| | 45 | 3.96 | 0.74 |
| 1450 | 15 | 3.16 | 0.80 |
| | 30 | 2.83 | 0.91 |
| | 45 | 1.69 | 0.68 |

The values of dimensionless variance ($\sigma^2$) of RTD (Table 11) as a function of air flow rate are presented in Figure 36 for different influent flow rates of 720, 1030 and 1450 L/d. The ideal values of this parameter for continuous stirred tank reactors (CSTRs) and plug flow reactors (PFRs) are equal to 1 and 0, respectively.

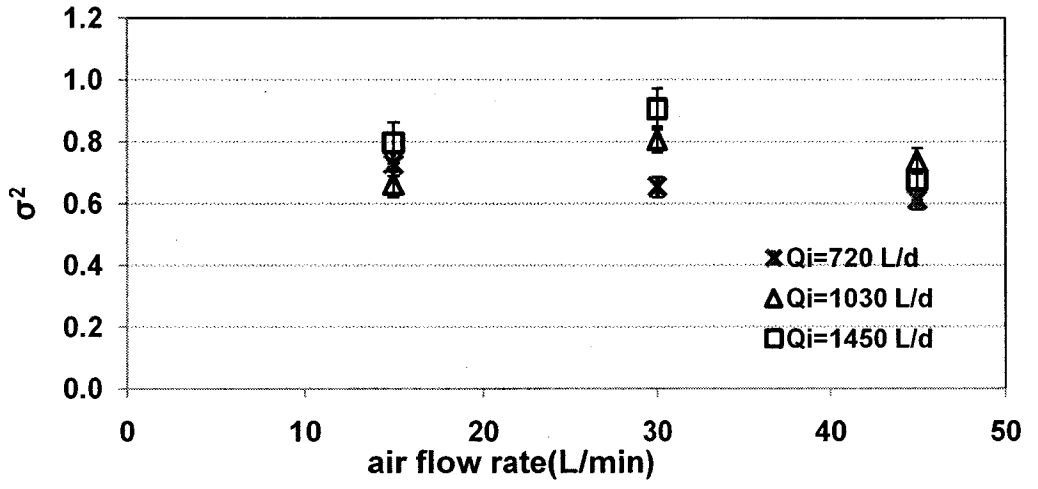


Figure 36. Values of dimensionless variance ($\sigma^2$) as a function of air flow rate at different influent flow rates

As presented in Table 11 and Figure 36, the value of this parameter is close to unity, implying that RTD of the first reactor of the examined system is consistent with the RTD in CSTRs, especially at influent flow rate of 1450 L/d and air flow rate of 30 L/min.

## 5.6 Liquid displacement in the first reactor

### 5.6.1 Specific rate of liquid discharge from the reactor (k)

The dimensions of the first reactor used in this analysis and their corresponding operating conditions are presented in Table 12.

Table 12. Dimensions and operating conditions of the first reactor

| Parameter | First reactor of the examined system |
|---|---|
| Volume of the aerobic zone (L) | 16.455 |
| Volume of the microaerophilic zone (L) | 62.05 |
| Volume of the anoxic zone (L) | 27 |
| Overall volume of the reactor (L) | 105.5 |
| Influent flow rate, $Q_i$ (L/d) | 500, 720, 1000, 1450 |
| Air flow rate, $Q_{air}$ (L/min) | 15, 30, 45 |

Using the volumes of aerobic zone ($V_a$), microaerophilic zone ($V_m$) and anoxic zones ($V_x$) from Table 12, and the circulating liquid flow rates in the aerobic ($Q_a$), microaerophilic ($Q_m$) and anoxic ($Q_x$) zones, obtained by the method explained in section 3.2.1, the instantaneous hydraulic retention times (Ins. HRT) of the circulating liquid in the three zones as well as the overall instantaneous HRT can be calculated using Equation (3.15) through (3.18). The overall instantaneous HRT which is equal to the time length of a single liquid cycle between the three zones for three air flow rates of 15, 30 and 45 L/min are presented in Table 13. In the calculation of instantaneous HRT at each zone, the value of recycled liquid flow rate between the second and first reactors ($Q_r$) and the

value of influent flow rate ($Q_i$) are negligible compared to the value of $Q_a$. Therefore Equations (3.19) to (3.22) will yield the following equation:

$$Q_a = Q_m = Q_x \qquad (5.9)$$

Table 13. Overall instantaneous HRT for three air flow rates of 15, 30 and 45 L/min

| $Q_i$(L/d) | $Q_{air}$ (L/min) | $Q_{cir}=Q_a$ (L/min) | Overall Ins. HRT (s) |
|---|---|---|---|
| 500, 720, 1000, 1450 | 15 | 73 | 86 |
| 500, 720, 1000, 1450 | 30 | 108 | 58 |
| 500, 720, 1000, 1450 | 45 | 135 | 47 |

As discussed in section 3.1.1, the instantaneous HRT can be controlled by changing the air flow rate in the aerobic zone and the size and number of openings between the aerobic and microaerophilic zones. Since in these set of experiments, eight openings of 1" size were used, the instantaneous HRT can only be controlled by changing the air flow rate as it is shown in Table 13. This table also shows that the value of instantaneous HRT is constant for a given air flow rate regardless of the influent flow rate ($Q_i$), as explained earlier.

Using the methodology explained in section 4.2.6, the validity of mathematical model developed in section 3.1 for the passage of wastewater through the reactor was examined. Figure 37-39 present the experimental values obtained for the decrease of the mixed liquor volume inside the reactor using three air flow rates of 15, 30 and 45

L/min, respectively. The curves in the following figures correspond to the influent flow rates of 500, 720, 1000 and 1450 L/d.

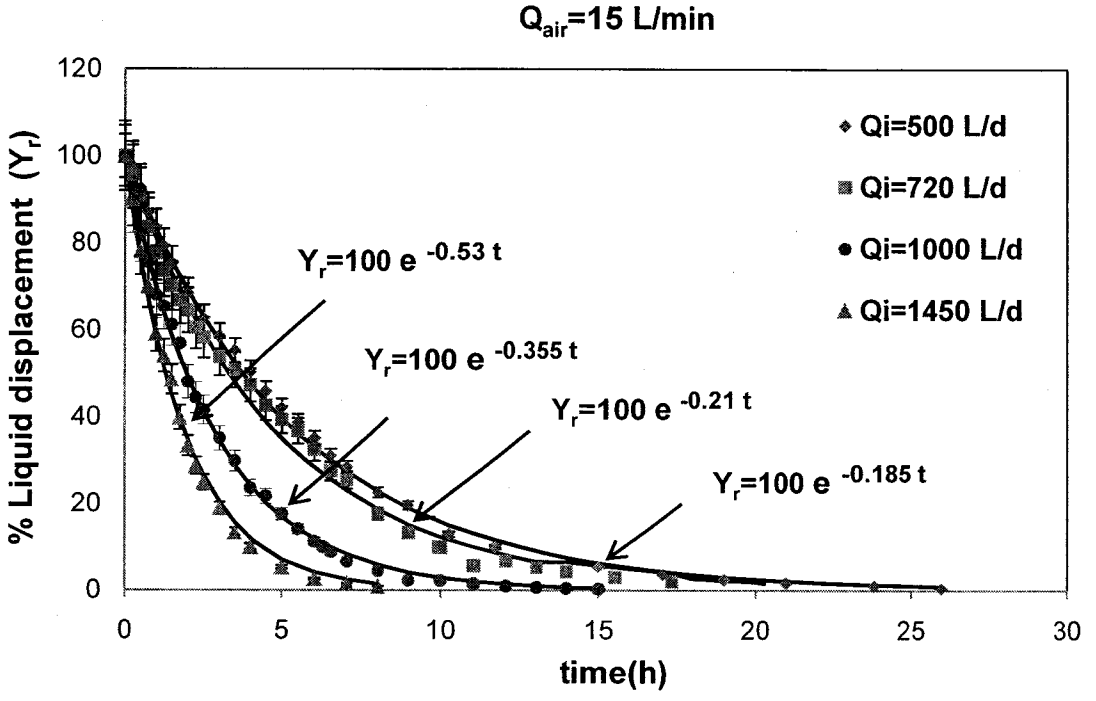


Figure 37. Time dependent changes in the volume of mixed liquor ($Y_r$) for $Q_{air}$=15 L/min

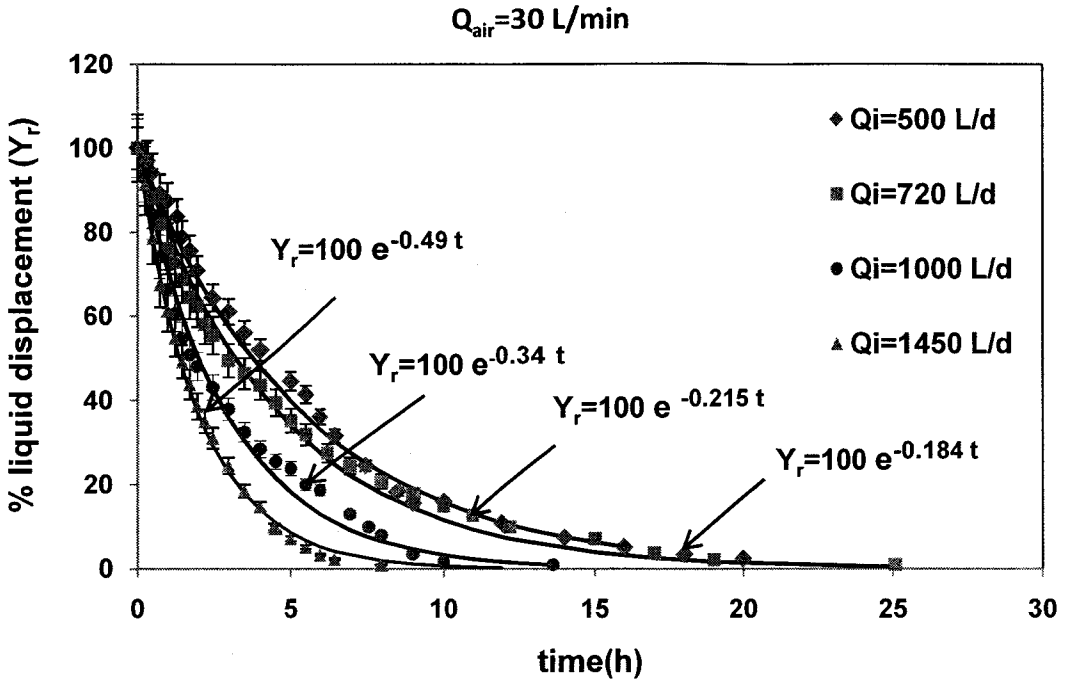


Figure 38. Time dependent changes in the volume of mixed liquor ($Y_r$) for $Q_{air}$=30 L/min

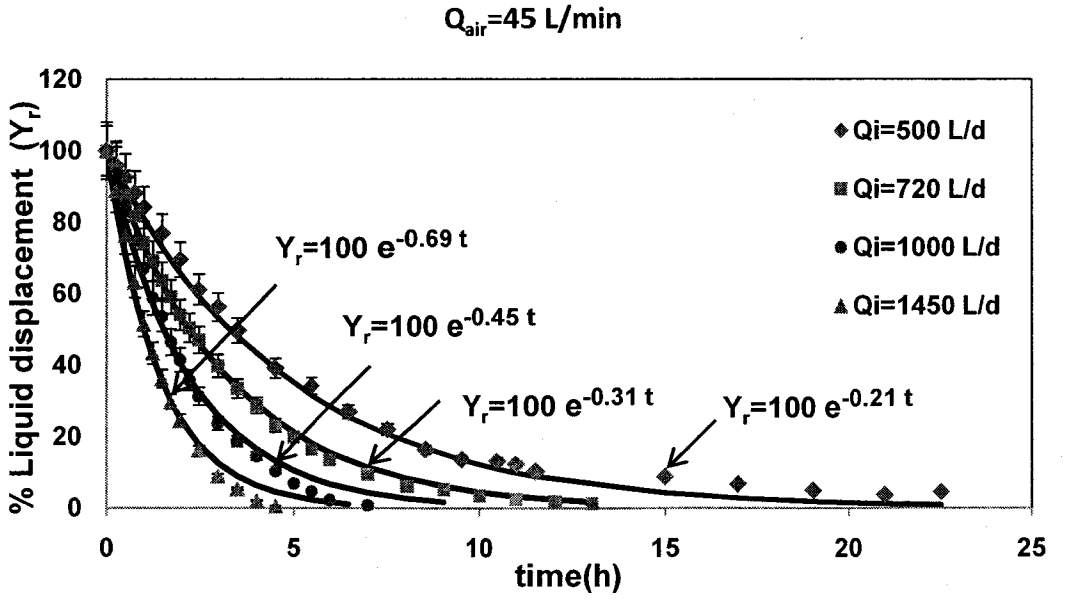


Figure 39. Time dependent changes in the volume of mixed liquor ($Y_r$) for $Q_{air}$=45 L/min

The specific rate of liquid discharge from the reactor (k) at each operating condition was obtained by using Equation (3.2) and the experimental values presented in Figure 37-39, as shown in Table 14. As expected, the value of k increased by the increasing influent flow rate. It can be seen from Figure 37-39 that under the examined operating conditions, the time–dependent changes in the volume of mixed liquor ($Y_r$) followed an exponential trend as it was predicted earlier by the mathematical model developed in section 3.1.

Table 14. Specific rate of liquid discharge from the reactor, k, (1/h) at different operating conditions

| $Q_i$ (L/d) | $Q_{air}$ =15 (L/min) | $Q_{air}$ =30(L/min) | $Q_{air}$ =45 (L/min) |
|---|---|---|---|
| 500 | 0.185 | 0.184 | 0.21 |
| 720 | 0.21 | 0.215 | 0.31 |
| 1000 | 0.355 | 0.34 | 0.45 |
| 1450 | 0.53 | 0.49 | 0.69 |

### 5.6.2 Average number of liquid circulations between the zones and percentage of liquid escape in each circulation

The average number of liquid circulations between the three zones (aerobic, microaerophilic and anoxic) for a discrete quantity of wastewater entering the system before it completely leaves the reactor was estimated from Equation (3.12) at different operating conditions, as presented in Table 15. This table also presents the percentage of liquid (mixture of mixed liquor and wastewater) that escapes circulation at each cycle under different operating conditions, as estimated from Equation (3.13).

Table 15. Average number of liquid circulations (N.O.C) and liquid escape % at different operating conditions

| $Q_{air}$ (L/min)=15 | | | |
|---|---|---|---|
| Overall Ins. HRT (s)=86 | | | |
| $Q_{cir}=Q_a$(L/min)=73 | | | |
| $Q_i$ (L/d) | k(1/h) | Average N.O.C | Liquid escape % |
| 500 | 0.185 | 226 | 0.47 |
| 720 | 0.21 | 199 | 0.67 |
| 1000 | 0.355 | 118 | 0.94 |
| 1450 | 0.53 | 79 | 1.34 |
| $Q_{air}$ (L/min)=30 | | | |
| Overall Ins. HRT (s)=58 | | | |
| $Q_{cir}=Q_a$(L/min)=108 | | | |
| $Q_i$ (L/d) | k(1/h) | Average N.O.C | Liquid escape % |
| 500 | 0.184 | 336 | 0.32 |
| 720 | 0.215 | 288 | 0.46 |
| 1000 | 0.34 | 182 | 0.64 |
| 1450 | 0.49 | 126 | 0.92 |
| $Q_{air}$ (L/min)=45 | | | |
| Overall Ins. HRT (s)=46 | | | |
| $Q_{cir}=Q_a$(L/min)=135 | | | |
| $Q_i$ (L/d) | k(1/h) | Average N.O.C | Liquid escape % |
| 500 | 0.21 | 366 | 0.25 |
| 720 | 0.31 | 248 | 0.37 |
| 1000 | 0.45 | 171 | 0.51 |
| 1450 | 0.69 | 111 | 0.74 |

From the data presented in Table 15, it can be concluded that less than 1.5% of liquid (mixture of mixed liquor and wastewater) escapes circulation at each cycle. Moreover, the percentage of escaped liquid increases with the increasing influent flow rate at a given air flow rate. However, at a constant influent flow rate ($Q_i$) the percentage of escaped liquid decreases with the increasing air flow rate.

### 5.6.3 Time and number of liquid circulations for 90% and 99% liquid displacement

The time required for the replacement of 90% and 99% of the reactor's content by the added wastewater was calculated by rearranging Equation (3.3) and by using the experimental values of k obtained under different operating conditions (Table 14), as presented below:

$$time\ for\ 90\%\ of\ liquid\ displacement(LD) = \frac{\ln(0.1)}{-k} \qquad (5.10)$$

$$time\ for\ 99\%\ of\ liquid\ displacement(LD) = \frac{\ln(0.01)}{-k} \qquad (5.11)$$

The number of liquid circulations (N.O.C) between the three zones before 90 % and 99% of the reactor's volume was replaced by the added wastewater was obtained from the following equations:

$$N.O.C.\ for\ 90\%\ of\ LD = \frac{time\ for\ 90\%\ of\ LD}{Ins.\ HRT} \qquad (5.12)$$

$$N.O.C.\ for\ 99\%\ of\ LD = \frac{time\ for\ 99\%\ of\ LD}{Ins.\ HRT} \qquad (5.13)$$

The results of the estimation of the time and number of liquid circulations for 90% and 99% of liquid displacement at different operating conditions are shown in Table 16.

Table 16. Time and number of liquid circulations (N.O.C) for 90 % and 99% of liquid displacement at different operating conditions

| $Q_{air}$ (L/min)=15 | | | | | |
|---|---|---|---|---|---|
| Overall Ins. HRT (s)=86 | | | | | |
| $Q_i$ (L/d) | k (1/h) | Time for 90% LD (h) | Time for 99% LD (h) | N.O.C. for 90% LD (h) | N.O.C. for 99% LD (h) |
| 500 | 0.185 | 12.44 | 24.890 | 520 | 1040 |
| 720 | 0.21 | 10.96 | 21.920 | 458 | 916 |
| 1000 | 0.355 | 6.48 | 12.970 | 271 | 542 |
| 1450 | 0.53 | 4.34 | 8.680 | 181 | 362 |
| $Q_{air}$ (L/min)=30 | | | | | |
| Overall Ins. HRT (s)=58 | | | | | |
| $Q_i$ (L/d) | k (1/h) | Time for 90% LD (h) | Time for 99% LD (h) | N.O.C. for 90% LD (h) | N.O.C. for 99% LD (h) |
| 500 | 0.184 | 12.51 | 25.02 | 774 | 1548 |
| 720 | 0.215 | 10.71 | 21.41 | 662 | 1324 |
| 1000 | 0.34 | 6.77 | 13.54 | 419 | 838 |
| 1450 | 0.49 | 4.69 | 9.39 | 290 | 580 |
| $Q_{air}$ (L/min)=45 | | | | | |
| Overall Ins. HRT (s)=46 | | | | | |
| $Q_i$ (L/d) | k (1/h) | Time for 90% LD (h) | Time for 99% LD (h) | N.O.C. for 90% LD (h) | N.O.C. for 99% LD (h) |
| 500 | 0.21 | 10.96 | 21.92 | 843 | 1686 |
| 720 | 0.31 | 7.42 | 14.85 | 571 | 1142 |
| 1000 | 0.45 | 5.11 | 10.23 | 393 | 787 |
| 1450 | 0.69 | 3.33 | 6.67 | 256 | 513 |
| LD=liquid displacement | | | | | |

It should be noted that according to the exponential function used to express liquid displacement, it will theoretically take an infinite number of circulations for a complete (100%) liquid replacement in the first reactor.

The dependence of the number of liquid circulations between the aerobic, microaerophilic and anoxic zones on the influent flow rate for 90% and 99% liquid displacement in the reactor are graphically presented in Figure 40-42 for three different air flow rates of 15, 30 and 45 L/min, respectively.

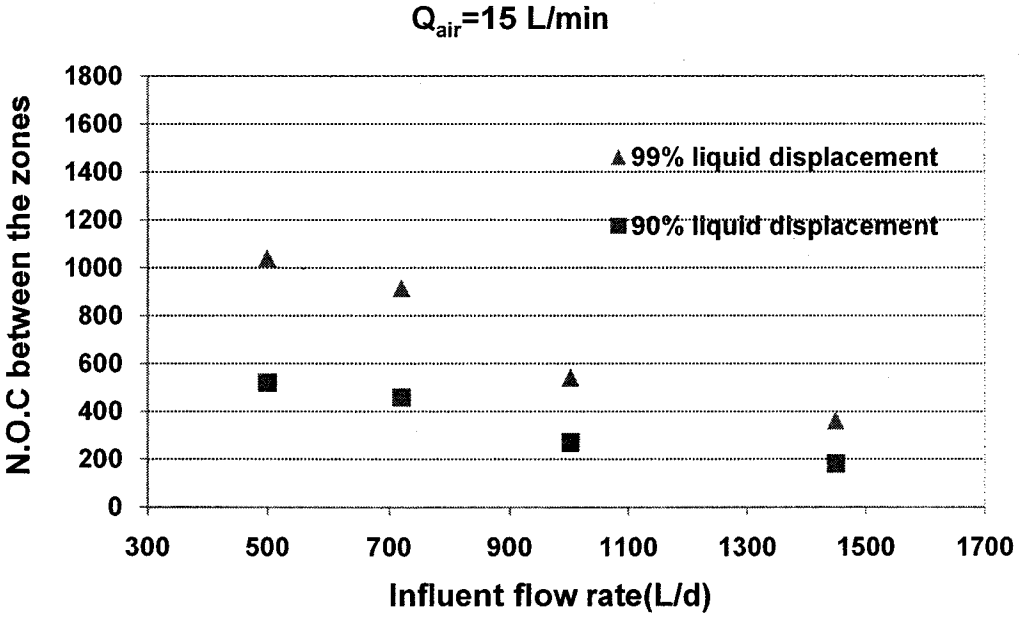


Figure 40. Dependence of the number of liquid circulations between the three zones of reactor on the influent flow rate for 90% and 99% liquid displacement ($Q_{air}$=15 L/min)

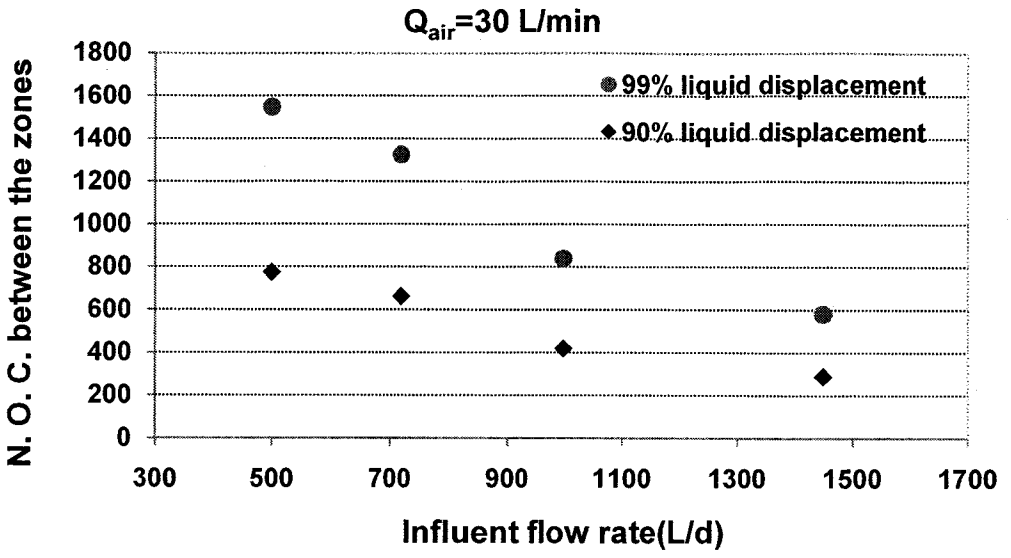


Figure 41. Dependence of the number of liquid circulations between the three zones of reactor on the influent flow rate for 90% and 99% liquid displacement ($Q_{air}$=30 L/min)

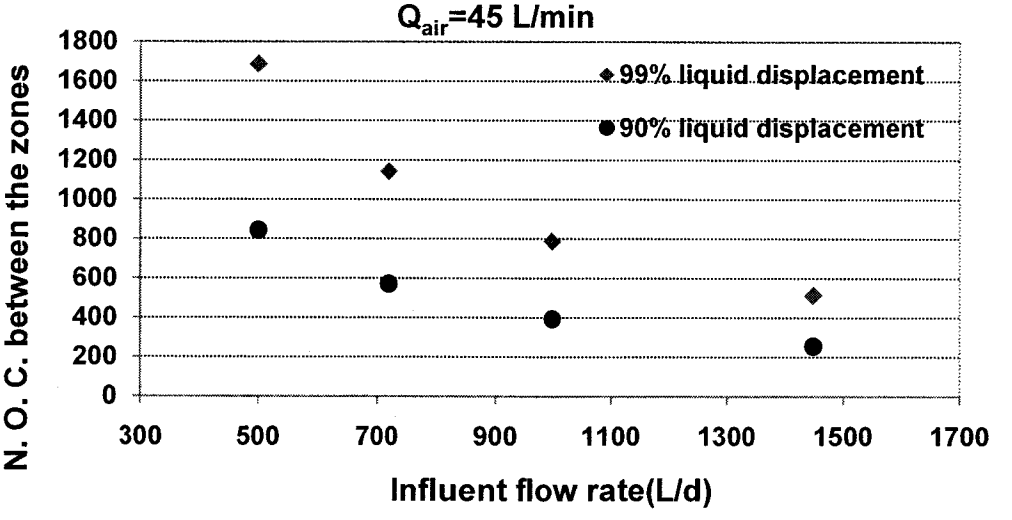


Figure 42. Dependence of the number of liquid circulations between the three zones of reactor on the influent flow rate for 90% and 99% liquid displacement ($Q_{air}$=45 L/min)

As presented in the above figures, the number of liquid circulations between the zones for 90% and 99% liquid displacement decreases with the increasing influent flow rate of wastewater at a given air flow rate. This is directly related to the time required for 90 % and 99% of liquid displacement. It can be noticed from Table 16 that at a constant air flow rate, the time required for 90% and 99% of liquid displacement decreases with the increasing influent flow rate. Since the overall instantaneous hydraulic retention time is constant, this leads to the decreasing number of liquid circulation for 90% and 99% of liquid displacement.

At the range of examined influent flow rates of 500 to 1450 L/d and air flow rates of 15 to 45 L/min, mixed liquid circulates between 181 to 843 times between the aerobic, microaerophilic and anoxic zones of the reactor before 90% of reactor's volume is replaced by the added wastewater. Similarly, for the replacement of 99% of reactor's volume, mixed liquor circulations of 363 to 1686 times between the three zones are required.

## 5.7 Zone generation

The methodology explained in section 4.4 was applied in order to create different zones of aerobic, microaerophilic and anoxic in the examined treatment system. By adjusting the air flow rate in the range of 15 to 30 L/min, and by installation of eight openings of ½" size between the aerobic and microaerophilic zones, the required values of dissolved oxygen concentration for the development of each zone were established. These values

are in the range of 2 to 4 mg/L in the aerobic zone, less than 1 mg/L in the microaerophilic zone and zero in the anoxic zone. This demonstrated the successful generation of zones in the examined treatment system. The ORP values in various zones did not correspond to the predicted values (Table 1) due to the absence of biological treatment that facilitates the establishment of the required ORP.

## 5.8 Overall summary of the results

In general, the evaluation of hydrodynamic characteristics of the integrated multi-environment treatment system as a function of operating parameters demonstrated similar trends to conventional airlift reactors. However, certain differences were observed mainly due to the different geometrical design of the examined treatment system compared to conventional airlift reactors.

The aerobic zone in the examined technology was designed based on the concept of concentric–tube airlift reactors while incorporating the following design modifications:

- The presence of eight openings with an adjustable size between the aerobic (riser) and microaerophilic (downcomer) zones of the first reactor. This design, while being essential for zone generation and operation strategy of the examined multi-environment treatment technology, exerts restrictions on the passage of liquid flow between the riser and downcomer. This restriction does not exist in conventional airlift reactors.

- The ratio of cross sectional area of microaerophilic to aerobic zones (downcomer to riser) ($A_d/A_r$) is greater than 1. Again, this design characteristic is essential for treatment purposes. The value of this ratio is commonly less than 1 in most conventional airlift reactors.

- In concentric-tube airlift, the distance from the reactor base to the bottom of draft tube (bottom clearance) is in the range of few centimeters (less than 10 cm) (Merchuk 1994, Gouveia et al. 2003) while in the examined system, the placement of a cone at the bottom of reactor creates a 30 cm bottom clearance which makes a difference in the liquid flow pattern in this area.

The hydrodynamic characterization showed that the optimized operating conditions during the treatment operation would be the use of openings with the size of ½"and air flow rate in the range of 15 to 30 L/min, due to the following reasons:

- Establishment of a higher volumetric mass transfer coefficient which is an essential parameter in biological treatment systems.

- Establishment of different environmental conditions of aerobic, microaerophilic and anoxic in the first reactor based on DO concentration in the examined range of operating conditions.

# CHAPTER 6: CONCLUSIONS AND RECOMMENDATIONS

## 6.1 Conclusions

The following conclusions have been made during the hydrodynamic evaluation of the integrated multi-environment treatment system:

1- The aerobic zone of the treatment system exhibits properties of airlift reactors.

The analysis of experimental results showed that air flow rates greater than 15 L/min, corresponding to superficial gas velocity of 0.011 m/s, satisfy the needs of the treatment system in terms of:

-Maintenance of continuous circulation of liquid between the three zones of aerobic, microaerophilic and anoxic.

-Supply of an adequate amount of oxygen to support aerobic biological processes in the aerobic zone.

-Mixing of liquid and solids in the aerobic zone in order to provide a homogenous medium.

2- The evaluation of the impact of operating and process parameters on hydrodynamic characteristics of the first reactor of the examined treatment system revealed that:

-The mean liquid circulation velocity and gas hold-up increase with the increase of superficial gas velocity for both opening sizes of 1"and ½" between the aerobic and microaerophilic zones, while the mean circulation time decreases with the increase of air flow rate under the same condition. The mean circulation time is a stronger function of the air flow rate for smaller openings (1/2") while at air flow rates greater than 30 L/min, the mean circulation time is almost independent of air flow rate for the opening size of 1".

- The overall volumetric mass transfer coefficient ($k_La_L$) increases with the increase of superficial gas velocity ($U_G$). However, application of the smaller size of openings (1/2") between the aerobic and microaerophilic zones leads to higher values of $k_La_L$ which is directly related to higher values of gas hold for the smaller size of openings.

- Within the range of examined influent flow rates of 700 to 1450 L/d and air flow rates of 15 to 45 L/min, the residence time distribution in the first reactor resembles the patterns observed in a continuous stirred tank reactor (CSTR), specifically at the air flow rate of 30 L/min and influent flow rate of 1450 L/d.

- The presence of a stationary support material (microbial support) for the development of biofilm in the aerobic zone does not cause any restriction of liquid circulation inside the reactor due to the design and non-clogging nature of the microbial support, implying that its impact on the examined hydrodynamic parameters is negligible.

3- The time-dependent changes in the volume of mixed liquor inside the treatment system were mathematically expressed and the dependence of the number of liquid circulations between the aerobic, anoxic and microaerophilic zones on the influent flow rate ($Q_i$) and air flow rate ($Q_{air}$) was determined. This analysis showed that:

-At a constant air flow rate, the number of liquid circulations between the three zones for 90% and 99% liquid displacement decreases with the increasing influent flow rate of wastewater which is directly related to higher specific rate of liquid discharge from the reactor (k) for higher influent flow rates. In the range of the examined influent flow rates of 500 to 1450 L/day and air flow rates of 15 to 45 L/min, mixed liquid circulates between 181 to 843 times between the three zones of aerobic, microaerophilic and anoxic before 90% of bioreactor's volume is replaced by the added wastewater. Under

the same condition, liquid circulates between 363 to 1686 times for 99% liquid displacement.

- The three different zones of aerobic, microaerophilic and anoxic in the first reactor are successfully generated by installing eight openings with the size of ½" between the aerobic and microaerophilic zones and by applying air at the flow rate of 15 to 30 L/min.

## 6.2 Recommendations

**Scale-up**

The new multi-environment wastewater treatment system can be scaled up to a semi-industrial scale. For this purpose, the hydrodynamic properties evaluated in this work such as gas hold up and mass transfer coefficient and their corresponding operational ranges can be used to develop empirical correlations. The effect of reactor geometry and various dimensionless groups such as the ratio of downcomer-to-riser areas on hydrodynamic characteristics of the system can be investigated to determine the optimum range of these parameters and their impact on the performance of the system.

**Computational flow dynamic (CFD) study and modeling**

A more elaborate study such as CFD analysis can be performed to better evaluate the hydrodynamic behavior of the system and different hydrodynamic aspects such as two-

phase characteristics and axial dispersion. This analysis can lead to the development of a mathematical model to simulate the hydrodynamic behavior of the examined treatment system.

# REFERENCES


- Ahn K.H., Park K.Y., Maeng S.K., Hwang J.H, Lee J.W, Song K. G. & Choi S., Ozonation of wastewater sludge for reduction and recycling, Water and Science Technology, Sludge Management, Regulation, Treatment, Utilization and Disposal. *IWA*, 2002, 46(10), 71-77

- Bakker W.A.M., Kers P., Beefting H.H., Tamper J., and de Gooijer C. D., Nitrite Conversion by Immobilized Nitrobacter agilis in an Airlift Loop Bioreactor Cascade: Effects of Combined Substrate and Product Inhibition, *J Ferm. Bioeng.*, 1996, 81, 390–393

- Bello R.A., Robinson C.W., and Moo-Young M., Liquid circulation and mixing characteristics of airlift contactors. *Canadian Journal of Chemical Engineering*, 1984, 62, 573-577

- Bello R.A., Robinson C.W., Moo-Young M., Gas holdup and overall volumetric oxygen transfer coefficient in airlift contactors, *Biotechnology and Bioengineering*, 1985a, 27, 369–381

- Bello R.A., Robinson C.W., Moo-Young M., Prediction of the volumetric mass transfer coefficient in pneumatic contactors, *Chem. Eng. Sci.*, 1985b, 40, 53-58

- Benyahia F., Jones L. Scale effects on hydrodynamic and mass transfer characteristics of external loop airlift reactors. *J. Chem Tech Biotechnol,* 1997, 69, 301-308

- Blenke H., Loop reactors, Advances in Biochemical Engineering,1979, 13, 121-124

- Bruce N.E., Chemical Reactor Design, Optimization, and Scale up, Second Edition, John Wiley & Sons, Hoboken, New Jersey, 2008

- Chisti M.Y., Airlift Bioreactors, Elsevier Applied Biotechnology Series. Elsevier, New York, 1989

- Chisti M.Y., Halard B., and Moo-Young M., Liquid circulation in airlift reactors, *Chem. Eng. Sci.*, 1988a, 43, 451-457

- Chisti M.Y. and Moo-Young M., Gas holdup in pneumatic reactors, *Chem. Eng. J.*, 1988b, 38(3), 149-152

- Chisti M.Y. and Moo-Young M., Hydrodynamics and Oxygen mass transfer in pneumatic bioreactor devices, *Biotechnical. Bioeng.*, 1988c, 31, 487-494

- Chisti Y., Wenge F. and Moo-Young M., Relationship between riser and downcomer gas hold-up in internal-loop airlift reactors without gas-liquid separators, *The Chemical Engineering Journal*, 1995, 57(1), b7-b13

- Choi B.S., Wan B., Philyaw S., Dhanasekharan K., and Ring T.A., Residence Time Distributions in a Stirred Tank – Comparison of CFD predictions with Experiment, *Industrial & Engineering Chemistry Research*, 2004, 43(20), 6548–6556

- Choi E., Kim D., Eum Y., Yun Z. and Min K., Full-scale experience for nitrogen removal from piggery waste, *Water Environ. Res.* 2005, 77, 381–389

- Choi K.H., Chisti Y., Moo-Young M., Comparative evaluation of hydrodynamic and gas–liquid mass transfer characteristics in bubble column and airlift slurry reactors, *Chem. Eng. J*, 1996, 62, 223–229

- Choi K.H., Lee W.K., Circulation liquid velocity, gas hold up and volumetric oxygen transfer coefficient in external-loop airlift reactors, *J. Chemical Technology and Biotechnology*, 1993, 56, 51-58

- Coulson J.M. and Richardson J. F., Chemical Engineering 1, 3rd edition, Pergamon Press oxford, 1977

- de-Bashan L.E. & Bashan Y., Recent advances in removing phosphorus from wastewater and its future use as fertilizer. *Water Res.*, 2004, 38(19), 4222–4246

- de Nevers N., Bubble driven fluid circulations, *AICHE J.* 1968, 14, 222-226

- El-Gabbani, D.H., Hydrodynamic and mass transfer characteristics of an airlift contactor, MASc. Thesis University of Waterloo, Ontario, 1977

- Freedman W., Davidson J.F., Hold–up and liquid circulation in bubble columns, *Trans. Inst. Chem. Eng.*, 1969, 47, T251-T262

- Frijters C. T. M. J., Eikelboom D. H., Mulder A. and Mulder R., Treatment of municipal wastewater in a CIRCOX® airlift reactor with integrated denitrification, *Water Science and Technology, IWA*, 1997, 36(1), 173–181

- Garcia J. C., Lavin A. G. and Diaz M., High liquid holdup airlift tower loop reactor: I. Riser hydrodynamic characteristics. *J Chem. Technol. Biotechnol.*, 2000, 75, 369-377

- Gavrilescu M., Tudose R.Z., Residence time distribution of liquid phase in an external-loop airlift bioreactor, *Bioprocess Engineering*, 1996, 14, 183-193

- Gavrilescu M., Tudose R.Z., Residence time distribution of the liquid phase in a concentric-tube airlift reactor, *Chemical Engineering and Processing*, 1999, 38, 225 – 238

- Ghosh, T.K., Maiti B.R., and Bhattacharyya B.C., Studies on mass transfer characteristics of a modified airlift fermenter, *Bioprocess and Biosystems Engineering*, 1993, 9, 239-244

- Gourich B., EL Azher N., Soulami Bellhaj M., Delmas H., Bouzidi A., Ziyad M., Contribution to the study of hydrodynamics and gas–liquid mass transfer in a two- and three-phase split-rectangular airlift reactor, *Chemical Engineering and*

*Processing*, 2005, 44, 1047-1053

- Gouveia E.R., Hokka C.O., Badino-Jr A.C., The effects of geometry and operational conditions on gas holdup, liquid circulation and mass transfer in an airlift reactor, *Brazilian Journal of Chemical Engineering*, 2003, 20(4), 363-374

- Hills J.H., The operation of a bubble column at high throughputs I. Gas holdup measurements. *Chemical Engineering J.*, 1976, 12, 89-99

- Hwang S.J., Cheng Y.L., Gas holdup and liquid velocity in three-phase internal-loop airlift reactors, *Chemical Engineering Science*, 1997, 52(21-22), 3949-3960

- Im J.H., Woo H.J., Choi M.W., Han K.B., and Kim C.W., Simultaneous organic and nitrogen removal from municipal landfill leachate using an anaerobic–aerobic system, *Water Res.* 2001, 35, 2403–2410

- Imai Y., Takei H., and Matsumura M., A simple $Na_2SO_3$ feeding method for $K_La$ measurement in large-scale fermentors, *Biotechnol. Bioeng.*, 1987, 29, 982-993

- Jamshidi A, Sohrabi A, Vahabzadeh F, and Bonakdarpour B. Hydrodynamic and mass transfer characterization of a down flow jet loop bioreactor, *Biochem Eng J,* 2001, 8, 241–250

- Jin B., Lant P., Flow regime, hydrodynamics, floc size distribution and sludge properties in activated sludge bubble column, air-lift and aerated stirred reactors, *Chemical Engineering. Science*, 2004, 59, 2379–2388

- Jin B., Lant P. and Ge X., Hydrodynamics and mass transfer coefficient in activated sludge aerated stirred column reactor: Experimental analysis and modeling. *Biotechnology And Bioengineering*, 2005, 91(4), 406-417

- Jin B., Yin P., and Lant P., Hydrodynamics and mass transfer coefficient in three-phase air-lift reactors containing activated sludge, *Chemical Engineering and*

*Processing,* 2006, 45(7), 608-617

- Kreuk M.K., Heijnen J.J., van Loosdrecht M.C.M., Simultaneous COD, nitrogen, and phosphate removal by aerobic granular sludge. *Biotechnology and Bioengineering*, 2005, 90(6), 761-769

- Levenspiel O., Chemical Reaction Engineering, John Wiley and Sons, New York, 1972

- Liu, Y., Chemically reduced excess sludge production in the activated sludge process. *Chemosphere*, 2003, 50(1), 1-7

- Lu W.J. and Hwang S.J., Liquid velocity and gas holdup in three-phase internal loop airlift reactors with low-density particles *Chemical Engineering Science*, 1995, 50(8), 1301-1310

- Merchuk J.C., Gas hold-up and liquid velocity in a two dimensional air lift reactor, *Chemical Engineering science*, 1986, 41, 11-16

- Merchuk J.C., Concentric-tube airlift reactors: effects of geometrical design on performance, *AICHE Journal,* 1994, 40(7), 1105-1117

- Merchuk J.C., Ladwa N., Cameron A., Bulmer M., Berzin I., Pickett A.M., Liquid flow and mixing in concentric tube air-lift reactors, *J. Chemical Technology and Biotechnology*, 1996, 66, 174-182

- Nicolella C., van Loosdrecht M.C., van der Lans R.G., Heijnen J.J., Hydrodynamic characteristics and gas–liquid mass transfer in a biofilm airlift suspension reactor, *Biotechnol.* Bioeng. 1998, 60(5), 627–635

- Onken U., and Weiland P., Airlift fermenters: Construction behavior and uses, Advances in biotechnological Processes, 1, (Mizrahi, A., and Van Wezel, L., editors) Alan R. Liss, Inc. (New York), 1983, 67-95

- Siegel M.H., Merchuk J.C., Schugerl K., Air-lift reactor analysis: Interrelationships between riser, downcomer, and gas-liquid separator behavior, including gas recirculation effects, *AIChE,* 1986, 32(10), 1585-1596

- van Benthum, W.A.J., van der Lans R.G.J.M., van Loosdrecht, M.C.M. and Heijnen J.J., Bubble Recirculation Regimes in an Internal-Loop Airlift Reactor, *Chem. Eng. Sci.*, 1999a, 54, 3995–4006

- van Benthum, W.A.J., van der Lans R.G.J.M., van Loosdrecht, M.C.M. and Heijnen J.J. The biofilm airlift suspension extension reactor. Part II: Three-phase hydrodynamics, *Chem. Eng. Sci.*, 1999b, 54, 1909–1924

- Vilaça P.R., Badino A.C., Facciotti M.C.R. and Schmidell W., Determination of Power Consumption and Volumetric Oxygen Transfer Coefficient in Bioreactors. *Bioprocess Engineering*, 2000, 22(3), 261-265

- Water Environment Federation (WEF), Biological Nutrient Removal (BNR) Operation in Wastewater Treatment Plants. McGraw-Hill, VA, USA, 2006

- Wei Y.S., Van Houten R.T., Borger A.R., Eikelboom D.H. & Fan Y.B. , Minimization of excess sludge production for biological wastewater treatment, *Water Res.*, 2003, 37(18), 4453–4467

- Weiland P., Influence of draft tube diameter on operation behavior of airlift loop reactors, *Ger. Chem. Eng.*, 1984, 7, 374-385

- Zhang X., Zhou j., Guo H., Qu Y., i Liu G., Zhao L., Nitrogen removal performance in a novel combined biofilm reactor, Process Biochemistry, 2007, 42, 620–626